USE OF HYDRATED GLASS FOR SYNTHESIS OF WASTE-BASED FOAMED GLASS

Uroš Hribar

Doctoral Dissertation
Jožef Stefan International Postgraduate School
Ljubljana, Slovenia

Supervisor: Dr. Jakob König, Jožef Stefan Institute, Ljubljana, Slovenia

Evaluation Board:
Prof. Dr. Srečo Davor Škapin, Chair, Jožef Stefan International Postgraduate School and Jožef Stefan Institute, Ljubljana, Slovenia
Dr. Vilma Ducman, Member, Slovenian National Building and Civil Engineering Institute, Ljubljana, Slovenia
Prof. Dr. Yuanzheng Yue, Member, Aalborg University, Aalborg, Denmark

MEDNARODNA PODIPLOMSKA ŠOLA JOŽEFA STEFANA
JOŽEF STEFAN INTERNATIONAL POSTGRADUATE SCHOOL

Uroš Hribar

USE OF HYDRATED GLASS FOR SYNTHESIS OF WASTE-BASED FOAMED GLASS

Doctoral Dissertation

UPORABA HIDRIRANEGA STEKLA ZA SINTEZO PENJENEGA STEKLA IZ ODPADNIH MATERIALOV

Doktorska disertacija

Supervisor: Dr. Jakob König

Ljubljana, Slovenia, February 2023

Acknowledgments

The first one I would like to thank is my supervisor Jakob who is an excellent researcher and always knows how to ask the right questions. Thank you for your guidance, suggestions, discussions and honesty. Second, I wish to thank Sonja Smiljanić, who was at the time working as a Post Doc in our thermal insulation group, for her time, advice and friendly discussions.

Another thank you goes to the head of the Advanced Materials Department, Matjaž, for his openness, availability for advice, and the way of management that made the workplace very pleasant.

I wish to also thank all my fellow Young Researchers from the Advanced Materials Department: Blaž Jaklič, Jan Žuntar, Petruša Borštnar, Nina Kuzmič, Alja Čontala, Lea Gazvoda, Tjaša Parkelj-Potočnik and Urška Gabor. Thank you all for contributing to the relaxed and friendly atmosphere. Special thanks to Urška, Nina and Petruša for the help with the XRD measurements and Lea for the help with IR spectroscopy.

Also, thank you to all the co-workers from the Advanced Materials Department, who are always ready to give advice, many of which helped me during my research. I am positive that each of you has contributed to this thesis. Another big thank you to the creative trio: David Fabijan, Damjan Vengust and Mario Kurtjak. Thank you for always taking your time to discuss even seemingly least relevant topics and also directly helping me with my research by measuring the thermal conductivity (David), FTIR measurements (Mario) and helping me with the SEM (Damjan).

I appreciate all the help from Martin Bonderup Østergaard; performing the gas chromatography analysis and his willingness to help during my visit at the Department of Chemistry and Bioscience in Aalborg.

Finally, a thank you to my family, and a special thank you to my girlfriend Teja for her endless patience during the course of my PhD.

I would like to acknowledge that this research was funded by the Slovenian Research Agency (grant numbers PR-08980 and P2-0091).

Abstract

Thermal insulation materials have a strong impact on energy efficiency of buildings which are one of the main energy consumers in the EU. Thermal insulation materials are widely used and improving their properties or improving their production can therefore have a rapid impact on the efficient use of energy in buildings. Foamed glass is an interesting thermal insulation material since it can be produced from a cullet, i.e. crushed glass from the production or postconsumer source. Here, the use of carbonaceous foaming agents allows the synthesis of best quality foamed glass, while at the same time requires the implementation of the process in the inert atmosphere, which is a less environmentally friendly option in comparison to the air atmosphere.

In this thesis, different types of waste glass cullets, with the emphasis on cathode ray tube panel glass, were investigated for their expansion ability either by hydrothermal treatment or by mixing them with water glass. Chemical and crystallographic changes in the glass powder mixtures were followed by X-ray diffraction and infrared spectroscopy. Mass loss and evolution of gases during the heating were analyzed with thermogravimetry coupled with mass spectrometry. Porosity of the obtained foams was analyzed with Archimedes method in water and with He-pycnometer, while the structural characteristics were analyzed using scanning electron microscope. Atmosphere within the closed pores of the foamed glass was analyzed with gas chromatography.

In the first part of the research, foaming of cathode ray tube panel glass with the addition of water glass in air was investigated. Chemical and crystallographic changes in the glass powder mixtures suggest that a new carbonate phase is formed after glass powder is mixed with water glass. Analysis of the atmosphere from within the closed pores of the foamed glass has revealed that it is mostly composed of carbon dioxide. A new carbonate-based foaming mechanism is proposed as an alternative to the water-dominated mechanism.

In the second part of the research, glass powders were hydrothermally treated to different water content and investigated for their ability to foam in the air atmosphere. Newly obtained glass powders foam in the air atmosphere, however, this ability does not change significantly with their water content.

In the last part of the research, both possibilities of foaming with hydrosilicates were utilized for foaming with the addition of carbonaceous foaming agent in air atmosphere. Use of carbonaceous foaming agent in combination with the hydrothermally treated glass powder leads to slightly improved foaming ability in the air atmosphere. However, the use of water glass in combination with the waste glass powder results in significantly enhanced foaming ability, leading to high-porosity foamed glass. Furthermore, as-obtained foams exhibit a homogeneous porous structure and low thermal conductivity. Both cases of hydrosilicate use protect the carbon from the premature burning and allow implementation of the foaming process in the air atmosphere.

This research explains a novel foaming mechanism for the foaming with water glass, which emphasizes the importance of the foaming mixture reactivity with the carbon dioxide from the surrounding atmosphere. Furthermore, the research demonstrates the

applicability of hydrosilicates for the implementation of the glass foaming with the use of carbonaceous foaming agent in the air atmosphere. The dissertation consists of two articles published in scientific journals.

Povzetek

Toplotno-izolacijski materiali močno vplivajo na energetsko učinkovitost stavb, ki so en izmed glavnih porabnikov energije v EU. Toplotno-izolacijski materiali so zelo razširjeni in izboljšanje njihovih lastnosti oziroma izboljšanje njihove proizvodnje lahko zato hitro vpliva na učinkovitejšo rabo energije v stavbah. Penjeno steklo je zanimiv toplotno-izolacijski material, saj ga je mogoče izdelati iz odpadnega drobljenega stekla. Pri tem uporaba ogljikovih penilnih sredstev omogoča sintezo najkakovostnejšega penjenega stekla, hkrati pa onemogoča proizvajanje penjenega stekla v okolju bolj prijazni zračni atmosferi.

V okviru doktorske disertacije sem testiral sposobnost ekspanzije različnih vrst odpadnega stekla, s poudarkom na steklu iz katodnih cevi – bodisi s hidrotermalno obdelavo stekla bodisi dodajanjem vodnega stekla. Kemijske in kristalografske spremembe v mešanicah sem spremljal preko rentgenske difrakcije in infrardeče spektroskopije z analizo vzorcev po obdelavi pri izbranih temperaturah. Izgubo mase in razvoj plinov med segrevanjem sem analiziral s termogravimetrijo, sklopljeno z masno spektrometrijo. Poroznost dobljenih pen sem spremljal z Arhimedovo metodo v vodi ali He piknometrom, strukturne značilnosti pa z vrstičnim elektronskim mikroskopom. Atmosfero znotraj zaprtih por penjenega stekla sem analiziral s plinsko kromatografijo.

V prvem delu raziskave sem se osredotočil na penjenje katodnega stekla na zraku z dodatkom vodnega stekla. Rezultati so pokazali, da po mešanju praškastega stekla in vodnega stekla nastane nova karbonatna faza. Analiza atmosfere iz notranjosti zaprtih por penjenega stekla je pokazala večinsko sestavo iz ogljikovega dioksida. Na podlagi dobljenih rezultatov sem predlagal nov mehanizem penjenja, ki temelji na novonastali karbonatni fazi, kot alternativno razlago penjenju zaradi izparevanja vode.

V drugem delu raziskave sem raziskal sposobnost penjenja hidrotermalno obdelanega stekla. Novo pridobljeni steklasti prahovi se v zračni atmosferi penijo in ta sposobnost se z vsebnostjo vode ne spreminja bistveno.

V zadnjem delu raziskave sem raziskal uporabo obeh vrst hidrosilikatov za penjenje z dodatkom ogljika v zračni atmosferi. Uporaba ogljika v kombinaciji s hidrotermalno obdelanim steklom vodi do nekoliko izboljšane sposobnosti penjenja v zračni atmosferi. Vendar pa uporaba vodnega stekla povzroči znatno izboljšano sposobnost penjenja in vodi do visoko poroznega penjenega stekla. Poleg tega ima tako pridobljeno penjeno steklo homogeno strukturo in nizko toplotno prevodnost. Oba primera uporabe hidrosilikatov tako ščitita ogljik pred prezgodnjim izgorevanjem in omogočata izvedbo procesa v zračni atmosferi.

Doktorska disertacija se direktno navezuje na članka številka 1 in 2 v poglavju Bibliografija in indirektno na članek s številko 3. V tej raziskavi predlagam nov mehanizem penjenja za penjenje z vodnim steklom, ki poudarja pomen reaktivnosti penilne mešanice z ogljikovim dioksidom iz okoliške atmosfere. V nadaljevanju raziskava prikazuje uporabnost hidrosilikatov za penjenje stekla z dodatkom ogljika v zračni atmosferi. Dizertacija je sestavljena iz dveh člankov, objavljenih v znanstvenih revijah.

Contents

List of Figures

List of Tables

Chapter 1

Introduction

Glass is deeply embedded in our everyday environment even though we often fail to appreciate its existence. Modern renewable energy devices, packaging, buildings, furniture, electronics, transportation, etc., would not be the same without glass, being humanity's companion from the beginning of the first civilizations. Natural or artificial, glass is commonly attractive because of its visual appearance (transparency, brilliance), creating an illusion of structural perfection. The structure of glass and its effect on glass properties have been an intriguing matter of scientific research since the 19th century with Faradays' thoughts "*...there is scarcely any artificial substance in which it is so difficult to unite what is required to satisfy the wants of science.*"[1] remaining true to the present day.

The widely spread presence of glass products through everyday appliances suggests the presence of enormous quantities of glass which will eventually reach the end of its current application life. The fact that glass is practically infinitely recyclable is a good guide for its sustainable use where the development of new glass or glass-containing materials requires the development of new recycling strategies. A typical example is cathode ray tube (CRT) glass which was recycled in a closed loop for many years. With the appearance of new technologies, CRT-containing screens became obsolete, recycling was discontinued, and the disposal or re-use of CRT glass remains a challenge.

Glass is a fascinating research subject not only to feed our curiosity about its mysterious nature but also to satisfy our need for technical solutions. Efficiency improvement in the production of materials and energy consumption is one of the most demanding challenges of our time. Progress in materials and their synthesis is essential for accomplishing this goal, especially in light of increasing population size and global energy consumption trends. Recent projections regarding the CO_2 emissions, temperature increase, and their effect on the environment further confirm that the efforts to improve our energy consumption efficiency and sustainability should become one of our top concerns.

The construction sector is one of the largest energy consumers and should significantly reduce its energy consumption. A large amount of that energy provides thermal comfort in buildings and the reduction of sectors' energy consumption could be achieved by improving the buildings' energy efficiency and production processes of related materials. The use of a material with high thermal resistance decreases the heat flow rate and the exchange of heat with the environment is standard practice and a legal requirement for buildings in the EU. However, due to the recent trends in energy demand, the requirements for building energy efficiency are already high. Despite several advances towards low thermal conductivity materials, the energy cost of their production is commonly extremely high which diminishes their attractiveness as a construction thermal insulation. On the other hand, insulation material that can be produced by a less energy-intensive process can contribute to a decrease in total energy consumption. Additionally, efficiently produced thermal insulation materials with good performance can result in a significantly positive net energy balance

by saving a larger amount of energy in comparison to the energy needed for their production. In this aspect, the use of waste materials can be especially beneficial and the material discussed in this work, i.e. foamed glass, is a promising candidate for further improvement of properties as well as production efficiency.

In this doctoral thesis, I explore the applicability of silicate hydrates for the foaming of glass, intending to achieve high-performance thermal insulation material based on waste glass via an energy efficient process.

Chapter 2

Theory and Literature Review

2.1 Foamed Glass

Foamed glass is a glass-based, highly-porous material (> 85 %), most commonly used as a lightweight construction element. Homogeneously distributed gas bubbles represent the majority of the foamed glass volume, contributing to its lightweight nature and good insulation properties. Additionally, foamed glass does not contain volatile organic compounds, has good dimensional stability and mechanical properties, does not burn, is vapor-proof, resistant to the majority of industrial reagents, microbes, and vermin. Because of these properties, foamed glass can be used as a thermal insulation material for various industrial or domestic applications.

In terms of thermal conductivity, the performance of foamed glass is similar in comparison to stone/glass wool and organic foams as expanded polystyrene (XPS) (30 – 40 mW $m^{-1}K^{-1}$) and worse in comparison to the state-of-the-art thermal insulators as vacuum insulation panels (VIP) (4 – 9 mW $m^{-1}K^{-1}$) [2]. While the use of some state-of-the-art materials can be profitable over traditional insulators in terms of cost per thermal resistance, their durability, service life, embedded energy, and challenges related to their installation remain a problem, resulting in significantly higher lifecycle costs [3]. From the sustainability aspect, foamed glass offers an additional advantage since it can be produced from waste glass, which is one of the focus points of this thesis.

2.1.1 Important properties

A short review of the properties important for the performance of foamed glass as a thermal insulation material.

2.1.1.1 Porosity and pore structure

Foams are defined as three-dimensional cellular materials, meaning they consist of void cells, and of a solid which is surrounding them. Porosity is the single most important characteristic of foams and therefore also significantly affects the majority of the properties of foamed glass. It is normally expressed as a volumetric fraction represented by the void space present within a solid material. In the case of foamed glass, the "void" phase is normally a mixture of gases with CO_2 and air being the most common ones. The definition above more precisely describes the total porosity (ε_{tot}) which is the counterpart of the other often reported foam characteristic called relative density (ρ_{re}), where: $\rho_{re} = 1 - \varepsilon_{tot}$. However, foam properties are not affected only by the total fraction of the gas phase, but also by its distribution throughout the material.

Foamed glass as a typical foam material consists of cells, which are bound by the solid (glass). The solid surrounding the cells is located in the cell edges and faces, also termed struts and walls, respectively. The distribution of the solid between the struts and walls determines the amount of open and closed porosity (ε_{op} and ε_{cl}. respectively). When the solid is mainly located in the struts, the foam has a high amount of ε_{op} and is said to be open-celled. If the solid is present in the walls, the cells are sealed, the amount of ε_{op} is low, and the foam is said to be closed-celled. The type of porosity and its effect on the foam's visual appearance is shown for two extreme examples in Figure 2.1.

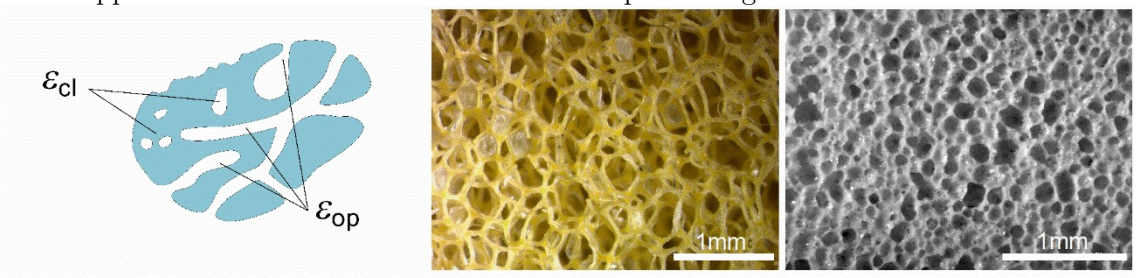

Figure 2.1: Void phase distribution within the solid (left) and two extreme examples of solid phase distribution: open-celled structure of a cleaning sponge (middle) and closed-celled structure of foamed glass (right).

ε_{cl} and ε_{op} can therefore reveal more about the distribution of the gas phase and detrimentally affect the range of foam's properties. For example, large ε_{cl} can result in the material's improved thermal insulation properties [4] and, more importantly, vapor non-permeability, which is a fundamentally required property for several construction materials [5]. Therefore, it is favorable to keep the ε_{op} of thermal insulation material for construction as low as possible. Here, it should be mentioned that achieving foamed glass with low ε_{cl} is not necessarily negative, since the resulting material can be applied as a sound insulation [6] or a catalyst carrier [7]–[9]. The distribution of gas and solid phase does not determine only whether the cells are closed or open but also their shape and size, which can reflect on the foam's properties. Wall (face) connectivity and strut (edge) connectivity along with the mean number of struts per wall can characterize the shape of the cells, however, is not commonly reported in the literature. Mean cell size (d_p), distribution, and cell symmetry are more often measured and reported characteristics [7], [10], [11].

Measuring the apparent and real density of foam (ρ_{app} and ρ_{real}) allows the determination of its ε_{tot}. ρ_{app} can be simply determined by measuring the sample's weight and dimensions while the ρ_{real} of brittle foams is determined by weighting and measuring the volume of finely crushed material with a pycnometer, which is why it is also termed powder density (ρ_{pow}). ε_{cl} and ε_{op} are normally determined with a gas pycnometer and the cell characteristics are normally evaluated from the micrographs obtained from various sources. Additionally, techniques, such as (mercury) intrusion or X-ray computed tomography, are used to obtain information about the cell size, distribution, and shape [12]–[15].

2.1.1.2 Mechanical strength

Apart from being a thermal insulator, foamed glass can also serve as a partial load carrier, reducing the need for other structural support. The compressive and flexural strength of a typical commercial foamed glass product are 0.4-6 MPa and 0.3-1 MPa, respectively [16]. The higher mechanical strength of foamed glass in comparison to polymeric foams is an advantageous property for its use in construction. Compression is the most commonly experienced mechanical stress acting on thermal insulation material in construction.

During compression, foamed glass follows a theoretical mechanism for brittle foams. The initial stage of elastic deformation can be observed only at extremely low strains and is in many cases almost non-existent [17]. Above the stage of elastic deformation, the cells begin to collapse in the stage of brittle crushing. The collapse of the cells and rearrangement of the solid results in material densification (the densification stage) leading to an additional increase in stress.

Investigations have shown that foamed glass follows similar mechanisms as described by Gibson and Ashby [18] with ε_{tot} being the most impactful foam property affecting the mechanical properties. Further, the nature of the porosity (open, closed) and distribution of the solid between the cell walls and struts significantly affect the compressive mechanism and the strength of the foam.

2.1.1.3 Embodied energy

The possibility of reducing a building's energy consumption by increasing its energy efficiency (i.e., reducing its operational energy) is well-researched and used in legislation and practice. However, the life cycle energy of a building consists of another important component that is starting to receive more attention in recent years – embodied energy. Embodied energy is the energy used for material extraction, manufacturing, transport, construction, maintenance, and demolition. Evaluating the energy associated with the mentioned life stages is normally very limited due to poor data availability, lack of agreed-upon framework, etc. However, reducing the energy costs related to embodied energy can result in a significant improvement in sustainability and the process of glass foaming is a promising candidate.

Melting of oxides that contain silica normally requires temperatures between 1200 and 1550 °C [19] and is consequently an energy expensive processing step. Implementation of a glass foaming process based on waste glass, without the glass melting step, potentially reduces the global warming potential of the production process by up to 40 % and the total use of primary energy resources by up to 50 % [20], [21]. The above comparison was done using Environmental Product Declaration data of two products with significantly different performances, i.e. less energy-intensive process results in a product with higher thermal conductivity. Such comparison by itself is not objective, since more energy-expensive and better-performing products will compensate for the invested energy difference in operational energy. However, the comparison is a good evaluation of production efficiency improvement in the case that a product with similar performance could be manufactured from a less energy-intensive process, which is an important point of this thesis.

2.1.1.4 Thermal conductivity

For the material to be practically useful as a thermal insulator, the heat transfer through it should be low, relative to other materials used in construction. Introduction of porosity into materials' structure is a common strategy for obtaining thermal insulator due to significantly lower thermal conductivity (λ) of gases in comparison to solids. Glass has a relatively low λ ($\approx$ 1000 mW $m^{-1}K^{-1}$ [4]) since it is an amorphous material, which is still approximately 40 times higher than the λ of air or CO_2 which are gases commonly present within the pores (26 or 17 mW $m^{-1}K^{-1}$, respectively). Thermal conductivity of foamed glass, therefore, decreases with increasing content of the gaseous phase (i.e. porosity), whereas typical commercial foamed glass has an effective thermal conductivity (λ_{eff}) between 36 and 80 mW $m^{-1}K^{-1}$. However, the transfer of heat does not occur only through conduction but also through convection and radiation. The λ_{eff} of a foam significantly depends on the specifics of its porous structure, which is why λ_{eff} of foamed glass will be discussed more deeply at the end of this chapter.

2.2 Glasses and Their Properties

Before further discussion about the main principles and mechanisms of direct foaming, a few concepts and properties typical of glasses should be explained.

By definition, *"glass is a nonequilibrium, non-crystalline state of matter that appears solid on a short time scale but continuously relaxed towards the liquid state"* [22]. Structurally, such materials cannot be described with a single motif that repeats throughout the whole structure as in the case of crystalline materials. Glass "structure", although now sounding as an oxymoron, can be simplified as a (random) network with one (or more) connecting element(s). Note that such network cannot be completely random since there is a restriction in a minimum distance between nuclei. A convenient way of describing such structure is called the Q^n notation, where n represents the number of neighboring Q units that are linked by common bridging oxygen [23] (Figure 2.2). Most commonly, as well as in this thesis, the Q unit is a Si-tetrahedron that consists of four (Q^0), three (Q^1), two (Q^2), one (Q^3), or zero (Q^4) non-bridging oxygens (NBOs). Ratios between the contents of Q^n elements reflect the connectivity of the network which affects the majority of the glass properties. Since the order in such network extends only to the level of several associated atoms, it is termed that glasses lack long-range order. Connectivity of the network thus originally depends on the coordination of the network ion and is further affected by the presence of other network-modifying elements. For the network to be formed, glass requires at least one network former. Glass constituents are commonly described as glass formers, modifiers and intermediates based on their ability to form and/or interact with the network. For oxide glasses, classification of different oxides into a specific group is based on properties of their bond with oxygen (strength, ionic character) and agrees fairly well with experimental observations [23].

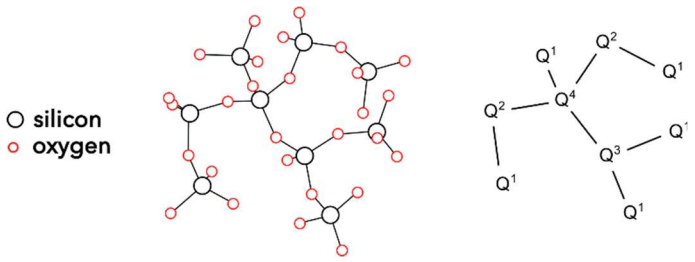

Figure 2.2: Representation of a silica network with ball-and-stick model (left) and corresponding Q^n notation (right).

Forming technique and material type do not determine whether a material is glass as long as it exhibits glass transformation behavior. Cooling a liquid below its melting temperature (T_m) normally results in crystallization accompanied by an abrupt decrease of enthalpy. The resulting structure of a crystalline solid possesses a long-range, periodic atomic arrangement. Cooling a liquid below its T_m without crystallization results in supercooled liquid where the structure continuously adjusts to the temperature without abrupt changes in enthalpy. In this range, the viscosity of the supercooled liquid depends on its temperature where with a further decrease of the temperature, the viscosity becomes so high that the structural rearrangements become incredibly time dependent. Eventually, the structure no longer changes with the temperature, and the point of this is defined as the glass transition temperature (T_g). With that, a more detailed glass definition can be introduced: "*Glass is a nonequilibrium, non-crystalline condensed state of matter that exhibits glass transition. The structure of glasses is similar to that of their parent supercooled liquids, and they spontaneously relax toward the supercooled liquid state. Their ultimate fate, in the limit of infinite time, is to crystalize.*" [22]. The continuous transition from solid to liquid or vice-

versa is one of the main reasons why glass is useful for the process of direct foaming. The gradual change of the materials' viscosity with the temperature enables more control over the process and consequently also the product properties. The T_m of glass is defined as the point where the supercooled liquid reaches the viscosity of 1 Pa s – value above which the melt is generally kept for homogenization and fining. Reaching the T_m of most commercial glass compositions generally requires temperatures above 1200 °C which is significantly higher than the temperatures used in the process of direct foaming of glass. Generally, the temperature during the direct foaming does not exceed 900 °C and the viscosity is above the Littleton Softening Point (10^8 – 10^{10} Pa s), where the viscosity is just high enough that the material can support its own weight. Staying within viscosity limits is important for the process of direct foaming since too high viscosity leads to slow expansion while too low viscosity leads to pronounced coalescence and hindered stability of the foam [24].

Crystallization is an additional effect which can importantly affect the glass viscosity or rather its rheological properties. As mentioned, glasses are amorphous solids, meaning that they do not contain significant amounts of crystalline phases. However, above the T_g and below the T_m glasses are metastable with respect to the crystalline phase. Normally, the rate of crystallization in glass is low and depends on chemical composition of glass, temperature, time and pressure. Although the rate is normally low, the crystallization or "devitrification" of glass can still lead to serious changes of several glass properties. Crystallization of glasses is described as a two-step process with formation of initial nuclei being followed by growth. Formation of nuclei of critical size is the key step which determines the crystallization process and can occur with or without the external active sites which catalyze the nucleation. Former and latter are termed heterogeneous and homogeneous crystallization. Contact between the glass phase with a second phase can result in the formation of an external active site which normally decreases the required energy for the critical cluster formation described by the classical nucleation theory. Second phase representing an active site can be a bubble (surface), container material, precipitated solid, etc. Since direct foaming process is usually performed on glass powder compacts mixed with foaming additives, heterogeneous crystallization is the prevailing mechanism, since glass powder surfaces and foaming additives will act as potential active sites. Several theoretical and experimental models deal with glass crystallization and actions required to steer the crystallization in a desired way are relatively well researched. However, these mechanisms are studied at temperatures relevant for the preparation of glass and glass-ceramics from the melt, which take place at significantly lower viscosities than glass foaming. Strategies to control the crystallization during the glass foaming are thus not well researched and remain a challenge [23].

Most technically important glasses are silicate-based with soda-lime glasses being the leading type in industrial production. Transmission of light is one of the most important properties of these glasses which is why they are used for the production of packaging glass (bottles, jars, etc.) and flat glass (windows) [25]. Recycling rate of the former in EU has grown to 78 % in 2019 (99 % in Slovenia) [26]. This example shows a large potential in improving the recycling rate of other waste glass materials, especially cathode ray tube glass (CRT).

Direct foaming of glass is possible exclusively due to its temperature versus viscosity relation, however, control over the viscosity and crystallization during the process represent a major challenge towards achieving a desired porous structure.

2.3 Water in Glass and Hydrated Glasses

Glass, especially silicate glass, is one of the most chemically inert commercial materials. This property is also the reason for its common use in packaging. Furthermore, due to its durability, glass is used in vehicles and buildings, as a container for corrosive fluids, an electrical insulator, and as an inner coating in chemical reactors. However, even the purest glass materials contain chemically bound water [27]. The content of water within the glass structure can extend from as low as a few parts per billion in the best optical fibers to several percent in natural glasses.

Glass can react with liquid water, aqueous solutions, and water vapors, whereas the reactions are generally very slow. Few possible and experimentally proven reactions are [28]:

- congruent dissolution of glass in the aqueous solution,
- exchange of alkali (earth) ions from glass for the hydrogen-bearing ions from the aqueous solution,
- diffusion of water in the glass structure,
- breaking of the silicon-oxygen network and formation of silanol functional groups.

Combination of the above-mentioned reactions very commonly creates a layer of reaction products on the glass surface, which even further decreases the diffusion kinetics and consequently the reaction rate. Despite the slow reaction kinetics and generally low concentrations of water within the glass, its effect on the glass properties is not negligible.

Focusing purely on the concentration, water has a greater effect on some glass properties than any other known oxide [23]. Only trace amounts of water are required to measurably decrease the glass transition temperature (T_g), relaxation rate, and viscosity [29]. The reason for such a disproportionate effect of water on the glass properties is related to the interactions of water with the (silicate) glass network. While it was considered for some time that the water within the glass network can exist only in the form of OH^- groups, it was Doremus [30] who suggested also the presence of molecular water, which was confirmed with infrared transmission analysis of glass treated with steam [31]. Further research has shown that the concentration of the molecular water gradually starts to dominate over the concentration of OH^- groups with increasing total water content [32]. An increase in the configurational variety for the water molecule within the Si-O-Si network of a sodium silicate glass with the increase in the total water content can be seen in Figure 2.3. At low total water content predominantly OH^- groups can be observed while with the increase in the total water content, molecular water starts interacting with sodium ions, silanols, non-bridging and bridging oxygens, further disconnecting the Si-O-Si network. Increased formation of Si units with low connectivity (i.e. Q^1 and Q^2 units with less bridging oxygens) was detected with increasing total water content [33]. Note that the initial decrease of the Si-O-Si networks' connectivity can be attributed to the formation of the OH^- groups, which can to some extent explain the disproportionate effect of water content on the properties of glass [34].

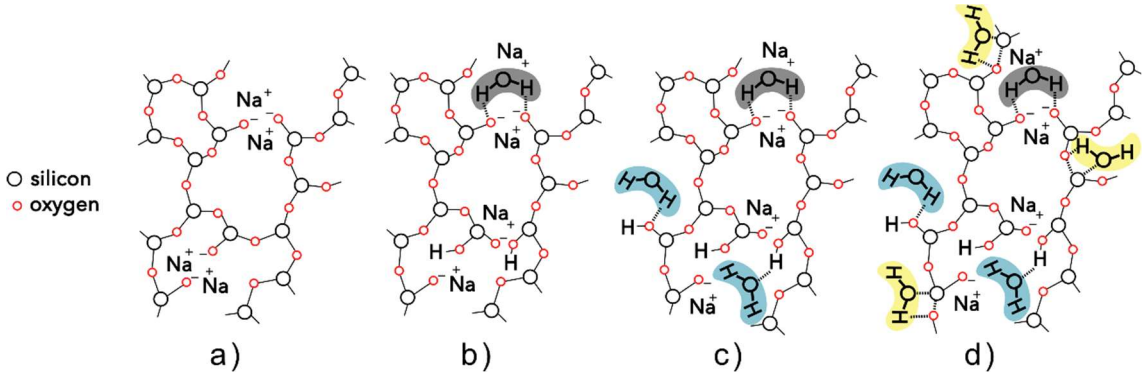

Figure 2.3: Scheme of possible water interactions within the sodium silicate glass network as a function of the total water content: a) 0 wt.%, b) < 3 wt.%, c) between 3 and 10 wt.%, d) > 10 wt.% Adapted from the ref. [35].

From only traces to a few weight percentages, water can be spontaneously present in glasses, however, introducing higher contents of water and controlling the amount of it requires further processing. Incorporation of water within the glass can be achieved during the melting or under conditions achieved in autoclaves.

Introduction of water into glass melts normally results in glass with very low concentrations of water. Here, water is present within the glass predominantly in the form of OH groups (Figure 2.3). Control over the content of water incorporated within the glass is difficult, however, it was shown that melting of a Na_2O-CaO-SiO_2-based glass in a gas-fired furnace results in higher OH content than melting in an electric furnace. This was attributed to a higher water vapor pressure in the atmosphere of a gas furnace due to the combustion products. Content of water in the same glass melt can be further varied by bubbling it through with dry or moist gas. After the cooling of such a melt at normal atmospheric pressure, obtained glass contains water only in the form of OH groups. Molecular water can be detected in glasses after melting in the case of higher pressures, e.g. glass melting in a closed vessel [29]. Such glasses, containing both OH groups and molecular water can be also termed “hydrosilicates”.

Use of higher pressures, i.e. autoclave reactors, for the incorporation of water within the glass can also be implemented at temperatures which are significantly lower than the T_m. Glasses with high contents of water can be prepared by autoclaving at temperatures as low as 120 °C, where the achievable hydration quantity depends on the amount of added water, temperature, pressure and type of glass [36]. The process of hydration with autoclave can be implemented in the presence of the liquid phase, termed as solution hydration, or without it, termed as vapor hydration.

Vapor hydration requires heating of the glass in a steam environment, where the saturated vapor pressure of water can be simply controlled with temperature. Bartholomew has shown that saturated steam method is the fastest in terms of hydration rate, however, it does not allow much control over the final water content [37]. Here, the authors already note that during the heating of such hydrated sample, foaming can occur if the surrounding pressure is too low. Phenomenon was later further researched in the studies of hydrothermal hot pressing, also discussed in this thesis under Section 2.6. It was shown that vapor hydration of silicate glass is a diffusion-controlled process, normally requiring several hours for the water to penetrate few millimeters into the material. Sodium silicate, i.e. water glass, can be produced in a similar process under increased pressure [38].

Content and species of water within the glass are normally analyzed via infrared spectroscopy [35], thermogravimetry, nuclear magnetic resonance [39], Karl-Fischer method [40] and density measurements.

2.4 Direct Foaming of Glass

With foaming, the materials' range of available properties expands significantly (Figure 2.4). Achieving a wider range of properties results in new possibilities for material utilization and shows the potential of foaming for new applications. Foaming allows a cheap synthesis of lightweight structures which can serve as structural materials, filters, membranes, carriers, support for flotation structures, packaging, and thermal insulation.

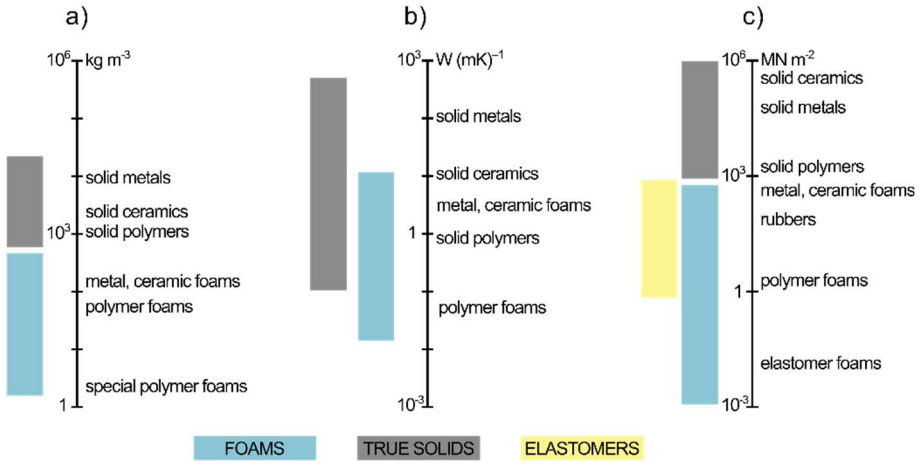

Figure 2.4: Range of properties comparison for a) density, b) thermal conductivity, and c) Young's modulus. Adapted from ref. [41].

Several traditional thermal insulators for buildings, e.g. polyurethane (PUR) and XPS, are also foamed materials. While not considered traditional [42], foamed glass is a typical example of a material with extended properties to serve as a cheap and reliable thermal insulator. Foamed glass is, therefore, an attractive material for research since it presents an elegant way to recycle obsolete, currently non-recyclable glass and possesses a unique combination of properties suitable to serve as an effective and sustainable thermal insulator.

Foaming of glass depends on the introduction of a gas phase into the glass. We can divide a few ways of achieving this into methods based on melts or powders.

Melt-based methods are usually based on the direct introduction of fluid such as CO_2 or water vapor into the molten glass, however, there are also a few exceptions where a gas-generating chemical can be utilized. The formation of foam is also a quite common phenomenon appearing on the top of the molten mass in the glass melting furnaces as a result of the bubbles rising from the melt. Bubbles are often present during the glass melting process and normally contain trapped air or decomposition products of raw materials. Even though the presence of bubbles is not always negative for scientific studies, they are almost always not desired in commercial glasses – and they need to be removed. Removal of bubbles from the glass melt is termed "fining" and is achieved with the addition of fining agents. The presence of foam in this particular case is not desired since it reduces the heat transfer from the flame to the glass melt and research efforts focus on hindering of the foam stability.

Powder-based glass foaming methods are more widely researched and can be further divided into high-pressure sintering and direct foaming. The latter is the main focus of this thesis while also being the most widely researched as well as commercially used process for the production of foamed glass. General processing via direct foaming requires heating of the glass powder mixed with the foaming additives which, upon heating, release the gas responsible for the formation of the porous structure. Peculiarities of the direct foaming

process will be further discussed after establishing which glass-related properties importantly impact the glass foaming mechanism. Synthesis of foamed glass via high-pressure sintering follows a similar principle as direct foaming, except that the process does not require the addition of gas-releasing foaming agents since the gas responsible for the formation of the porous structure is trapped within the material before the heat treatment. Trapping of the gas is achieved via pressure-assisted sintering which allows the use of different gases and various initial pressures. For this reason, high-pressure sintering can produce a well-defined model system in which one can analyze the influence of gas composition and initial pressure both on the development of porosity and on the thermal conductivity of the foamed glass [43], [44].

Few additional special methods of glass foam synthesis are known [6], [45]. Most of them are based on forming a stable porous structure based on glass powder which is later sintered into a solid form. Due to the vastly different processing and structure-parameter dependence of such special processes in comparison to direct foaming they will not be discussed further.

2.4.1 General processing and mechanism of direct foaming

Direct foaming of glass is a complex process dependent on many parameters: temperature, time, heating and cooling rates, glass stability, viscosity, surface tension, particle size distribution, foaming agents, etc. In the first step of the direct foaming process, a foaming mixture is prepared by mixing the glass powder with suitable additives, i.e. foaming agents.

Foaming mixture is then heated above the glass T_g until it reaches optimal viscosity and where, ideally, the foaming agents start to release the gas. Released gas becomes trapped within the sintered solid which starts to expand due to increasing internal pressure and viscous nature of glass above its T_g. Pore formation and growth during the direct foaming are governed by the properties of glass powder (particle size distribution, viscosity, surface tension, oxidation state, ion mobility, etc.), foaming agents (particle size distribution, reaction onset temperature, reaction rate, enthalpy, reaction products, etc.) and their interactions. Apart from the possible mentioned interactions, making the process complex, glass tends to crystallize at processing viscosity range and the system tends to achieve energetically more favorable arrangement by minimizing the surface via coalescence. The process can be divided into three stages: heating, foaming and cooling.

During the heating stage adsorbed gases and moisture are released from the surface of powder particles. Particle size distribution plays a major role during this stage, influencing the densification rate and consequently the degree of ε_{op}. Initially highly open porous powder compact starts to sinter with increasing T resulting in increasing ρ_{app}. Sample at the end of the heating stage can be characterized by a low ε_{tot}, and, more importantly, low ε_{op}. The next stage, i.e. the foaming, can start only when the beforementioned conditions are fulfilled.

Foaming stage begins at the onset of the sample expansion. Inner pressure within the sintered sample starts to increase due to the gases released from the foaming agents and low ε_{op}, preventing the gases to escape. Due to fine distribution of the foaming agent throughout the material, gas is released from a multitude of different points, enabling the formation of a porous structure. When the driving force of expansion overcomes the driving force for the sintering, surface tension, and outer pressure, the sample starts to expand. During the expansion stage, the pores can grow due to the additional release of gas, its expansion with increasing temperature, or due to coalescence. The latter is a ubiquitous phenomenon in glass foaming and its influence on the pore structure increases with increasing t_{foam} and T_{foam}. Appearance of coalescence is normal for the majority of foam systems and is governed by the processes of drainage, rupture and rearrangement [46]. Pore

walls consist of a material that seems stable but drains due to gravity. Because of the drainage the walls are becoming thinner which eventually results in wall rupture. Drainage may be a less important phenomenon in the case of glass foaming where the thinning of the walls occurs mostly due to the growth of the pores and consequential wall stretching [47]. Additional phenomenon which can promote the rupture of the walls is the presence of heterogeneities, i.e. newly formed crystalline phases.

Decrease of the temperature slows the otherwise continuously evolving porous structure, and at efficiently low temperature, the "freezing" of the structure occurs. To keep the porous structure from deviating further, the glass is cooled rapidly during this stage. Viscosity of the glass phase increases, dynamic processes are inhibited and the porous structure is retained. Such fast cooling results in appearance of stress which can lead to cracking of the pore walls and deteriorated mechanical and insulative properties. Consequently, fast cooling is normally implemented only until the temperature reaches the vicinity of T_g, from where the glass is cooled slowly to allow the relaxation.

2.4.1.1 Foaming agents

Before the glass can be foamed, glass powder is first mixed with a foaming agent which can be defined as a single chemical or a combination of several chemical compounds which release gases and enable the foaming action during the heating. Depending on the way in which they produce gas, foaming agents can be divided between the ones that decompose and the ones which react. In both cases, the process of gas evolution and consequently the foaming process depends on the interactions between the glass and foaming agents. The glass composition can thus significantly affect the decomposition or the reaction path of the foaming agents.

Decomposing foaming agents such as sulfates, nitrates or even oxides such as MnO_2 can be used for glass foaming. Note that AlN or Si_3N_4 can also be used in combination with oxidizing agents, such as Fe_2O_3, Mn_xO_y, CeO etc. [16], [48] and that decomposing oxides can be used in combination with reducing agents. More commonly used decomposing foaming agents in research are carbonates, mainly $CaCO_3$ and Na_2CO_3. It was shown that foaming is governed by the decomposition kinetics of carbonates which can be controlled to some extent via particle size, i.e. milling [49]. Particle size thus plays an even more important role when foaming with carbonates. However, even though $CaCO_3$ and Na_2CO_3 are one of the most researched foaming agents, it is difficult to achieve low density foamed glass with them (< 200 kg m^{-3}). Metal carbonates decomposition rate depends on the contact area with glass melt and increased content of carbonates or increase in the foaming temperature normally results in minimal increase in porosity and a very open structure with broken walls.

The other type of foaming agents, which are also more important industrially, are reaction-based. Here, a reducing component, such as SiC, needs a source of oxygen in order to start producing the expansion gas. The source of oxygen can be the glass itself or it can be provided by another additive. Glass being the oxygen source introduces additional complexity to the foaming process since the gas releasing reaction depends on the oxygen availability, which further depends on the redox state of glass, which is further affected by the temperature and the atmosphere. One of the main ideas of foaming with glass waste is to minimize the complexion of the process by decreasing the effect of the glass composition on the process, which can be achieved to some extent with the use of the (reducing-oxidizing) foaming couples [48], [50]. Carbon-containing foaming couples which at elevated temperatures produce a mixture of CO and CO_2 are the most researched ones. Oxygen availability affects the CO_2-producing reaction and manganese oxide is an especially interesting oxidizing agent since it exists in several valence states (Mn^{2+}, Mn^{3+} and Mn^{4+}).

Mn_2O_3, for example, can act as a sole foaming agent, while Mn_3O_4 is suitable as an oxidizing agent in combination with a carbonaceous additive. Two of the most common reactions between the carbon and Mn_3O_4 are shown below.

$$C\ (s) + \ 2Mn_3O_4(s) \rightarrow \ \ 6MnO\ (s) + CO_2\ (g) \qquad 2.1$$

$$C\ (s) + \ Mn_3O_4(s) \rightarrow \ \ 3MnO\ (s) + CO\ (g) \qquad 2.2$$

It was shown that in oxygen-free atmosphere Mn_3O_4 interacts with glass. It dissolves in the glass and releases gaseous oxygen during the reduction to Mn^{2+} state [51]. However, in the presence of carbon, Mn_3O_4 reacts with it and the reaction depends on the contact area between the particles. Redox state of the glass and the presence of H_2O can affect the reaction path; however, premature burning of carbon is the factor which affects the reaction the most. Use of carbon-based foaming agents in air atmosphere is challenging due to their reactivity with the oxygen from air and consequent burning before the closing of the pores. Partial loss of carbon-based foaming agent thus always occurs when foaming in the air atmosphere, requiring the use of its surplus in combination with strategies to inhibit the premature burning, which is one of the main goals of this thesis.

2.5 Thermal Conductivity of Foamed Glass

Transfer of heat through insulation material such as foamed glass is a combined effect of four distinct contributions. Sum of contributions from thermal conductivity through solid phase (λ_{solid}), conductivity through gas phase (λ_{gas}), convection and radiation are expressed as λ_{eff}.

In the case of a small enough pore size, the contribution from convective heat transfer can be neglected. It was shown, on foamed polymer material, that the pore size limit above which the convection becomes relevant is around 4 mm [52] and the value remains well-accepted also in the foamed glass community until today [53]. A more theoretical approach based on dimensional analysis evaluates that natural convection is negligible when the Grashof number value is below 1000.

$$Gr = \frac{g\beta\Delta T L^3 \rho^2}{\mu^2} \qquad 2.3$$

If the values for gravity acceleration (g, 9.8 m s^{-1}), volume coefficient (β, 0.0036 K^{-1}), temperature difference (ΔT, 10 K), density (ρ, 1.8 kg m^{-3}) and dynamic viscosity of gas (μ, 0.0015 Ns m^{-2}) are used in Equation 2.3, limit value for the pore size of approximately 12 mm is obtained. The majority of foamed glass materials exhibit pore sizes below the experimentally determined value as well as theoretically evaluated one (based on properties of CO_2 gas).

When the pores are sufficiently small, the convection is thus suppressed and the majority of the heat transfer occurs via λ_{solid} and λ_{gas}. Gases normally exhibit significantly lower thermal conductivity in comparison to almost any solid. Thermal conductivity of glasses is low in comparison to other solids as well, due to their amorphous structure. In comparison to metals, which contain free electrons that enable greater heat and electricity transfer, ceramics do not contain such free electrons. Vibrational coupling of neighboring atoms in glass is considerably reduced in comparison to ceramics which is why their thermal conductivity is reduced even further [54].

Amount of each phase (gas and solid) and their distribution further determines how the heat is transferred, however, it was evaluated that one third of the struts lie parallel to each axis which gives the following expression [16]:

$$\lambda = \lambda_{solid} + \lambda_{gas} = \frac{1}{3}(\rho_{rel} + 2\rho_{rel}^{3/2})\lambda_s + (1 - \rho_{rel})\lambda_g \quad 2.4$$

Note that with a decreasing value of ρ_{rel} the heat transfer through gas is becoming increasingly more important. Around 100 kg m^{-3}, conductivity through gas contributes almost 50 % to total thermal conductivity of foamed glass [55]. This shows the importance of filling the pores with a gas with low thermal conductivity or keeping the amount of open porosity low, e.g. λ of CO_2 is almost half smaller in comparison to air. Additionally, other analytical models such as Russel [56] and Schuetz-Glicksman [57] exist and are commonly used for describing the heat transfer through cellular materials, foamed glass included.

2.6 Literature Overview

Research of λ_{eff} revealed several relations to materials density and nature of porosity, from where a few useful models were developed and later compared in experimental research [58]–[61]. Products with good mechanical properties were reported in various research based on waste materials. However, it is quite common that foamed glass produced from waste materials is not lightweight (> 150 kg m^{-3}). The influence of the microstructure on the mechanical properties of foamed glass is often reported in the literature and conclusions can be correlated to other porous materials as well [6], [62]–[65]. At the same time, the experimental work regarding λ_{eff} is lacking. This could be a consequence of the difficulty of measuring λ_{eff} properly, due to the limitations in the sample size.

Based on the known structure-property correlations, desirable pore structure, yielding optimal thermal insulation properties, can be estimated. Thermal conductivity of foamed glass decreases along with decreasing density and the significance of conductivity through the gas phase takes over the conductivity through solid phase. Additionally, radiation starts to have a considerable effect with decreasing density. Low-density foam with small and closed pores, disabling convective heat transfer, filled with low conductivity gas is therefore desired in terms of thermal conductivity. However, the knowledge regarding processing-structure correlations is scarce and is in general less exact. Underlying theory regarding the geometrical constraints and topological laws of foams is well established [66], while the modelling of the foams and foamlike materials remains challenging, and requires large computational power even for relatively small systems [46].

The research in the field of foamed glass is oriented towards the use of waste materials [13], [62], [67]–[76]. This trend is beneficial for the sustainable development of material production and could potentially serve as a way of reducing the price of foamed glass, making its use more attractive. Container glass [77], flat glass [78], E-waste glass [79], and waste glass from automotive vehicles [80] are just some of the investigated wastes for the production of foamed glass. Additionally, several waste by-products of large industrial processes, such as fly ash [81], aluminum dross [82], red mud [83], slags [84], and natural materials, such as eggshells [85], pine scales [64], rice husk [86] and oyster shells [70], are researched as additives for the synthesis of foamed glass. The majority of the research of waste-based foamed glass is thus focused on the utilization of wastes from different waste sources and optimization of the process parameters in order to improve the properties of the products. However, due to the wide use of waste materials of different variety, the foaming mechanisms become increasingly complicated and the final conclusions of the investigations are usually true only for the specific systems in question.

Chapter 3

Objective and Outline of This Work

Development of sustainable materials plays an important part in the efforts towards the greener future. Here, a desire to improve one aspect often requires sacrificing the other. A similar concept applies to waste-based foamed glass. Use of increased content of waste material leads either to weakened performance or required use of energy-intensive processing steps.

The objective of this study is to establish a better understanding of a glass foaming process using hydrosilicates, with a goal of achieving high quality foamed glass from a process implemented in the air atmosphere. This study consists of three main investigations:

1. Foaming of waste glass with the addition of water glass.
2. Foaming of hydrothermally treated waste glass powder.
3. Implementation of carbonaceous foaming agent in air atmosphere with the use of water glass or hydrothermally treated waste glass.

Basic principles of foaming with the use of water glass and hydrothermally treated glass are investigated with the aim of exploiting them for the protection of carbon during the foaming in air atmosphere. First and second part of the study thus focus on the effect of hydrosilicates on the sintering behavior and released gases, while the third part also deals with the most important characteristic regarding the application – thermal conductivity.

Improving the thermal conductivity while implementing the process in the air atmosphere requires understanding of the basic processes and reactions which critically affect the foam growth. To reach this goal, the following questions need to be answered:

- How water glass affects the sintering/foaming behavior of the glass powder? How does it affect the characteristic temperature of the glass powder and/or undesired crystallization during the heating? How does the addition of water glass affect the properties of the foam?
- How does the hydrothermal treatment affect the sintering/foaming behavior of the glass powder?
- What is the role of H_2O in the case of i) water glass addition and ii) hydrothermally treated glass powder?
- What is the mechanism of expansion in the case of i) water glass addition and ii) hydrothermally treated glass powder?
- What are the pore characteristics within such foamed glass and what is the gas composition?

Achieving high quality waste-based foamed glass based on a process in air atmosphere would mean that an improved foamed glass product can be prepared with a lower embodied energy, i.e. improving one aspect without having to sacrifice the other.

Chapter 4

Experimental and Characterization Methods

4.1 Synthesis of Foamed Glass

4.1.1 Raw materials and milling

Waste cathode ray tube panel glass (CRT) powder was provided by Averhof A/S (Aarhus, Denmark), while container glass (FGF) and mixed color glass (MCF) powders were obtained from the industrial supplier from Uusioaines Oy (Finland). Mean particle size of as-received CRT, FGF and MCF glass powders was approximately 13, 23 and 26 μm, respectively. The chemical composition of the waste glass powders is shown in Table 4.1.

Table 4.1: Chemical composition of the as-received waste glass powders, expressed in wt.%.

	Na_2O	MgO	Al_2O_3	SiO_2	K_2O	CaO	Fe_2O_3	SrO	ZrO_2	BaO
CRT	7.7	0.3	2.4	61.0	7.1	0.8	0.2	7.8	1.5	9.7
FGF	13.5	1.7	1.5	72.4	0.6	9.7	0.1	0.03	0.02	0.14
MCF	13.7	1.8	1.7	71.5	0.6	9.7	0.4	0.02	0.02	0.07

Carbon (carbon black, Lehmann & Voss & Co, Hamburg, Germany), manganese (IV) oxide (MnO_2), potassium phosphate (K_3PO_4, 98 %, Alfa Aesar Karlsruhe, Germany) were used as foaming additives. Before the use MnO_2 was heat-treated at 1250 °C for 4 h and subsequently milled in order to obtain manganese (II, III) oxide (Mn_3O_4). Addition of K_3PO_4 was used to decrease the foaming temperature without significant alterations to the porous structure [61].

All foaming mixtures were prepared by dry-milling a powder mixture in a planetary ball mill with 10 mm yttria-stabilized zirconia balls at 250 rpm for a total milling time of 35 min. Foaming mixtures which contain Mn_3O_4 were milled for 30 min before adding the Mn_3O_4 and continuing the milling for an additional 5 min. Mean particle size of the obtained powder mixtures after the milling was approximately 9 μm. Different combinations of foaming additives were used for the preparation of the foaming mixtures.

Compositions and labelling suffixes presented in Table 4.2 correspond to the foaming mixture composition used for the preparation of closed porous foamed glass in [55]. The content of Mn_3O_4 is sufficient for direct oxidation of ≈ 0.15 wt.% of C according to Reaction 2.1, theoretically generating enough CO_2 for the material to expand ≈ 30 times (assuming T_{foam} of 800 °C, ideal gas behavior and initial material density of 2600 kg m^{-3}).

Table 4.2: Weight percentage of foaming additives in different foaming mixtures and corresponding labels.

Suffix	**C [wt.%]**	**Mn_3O_4 [wt.%]**	**K_3PO_4 [wt.%]**
0	0	0	1.97
Mn	0	5.89	1.85
C	0.41	0	1.96
Mn+C	0.39	5.87	1.85

The preparation procedure for the foaming mixtures was implemented under standard conditions and kept constant throughout the whole investigation process in order to obtain powders with similar particle size distributions.

4.1.2 Hydrothermal treatment of glass powder

Hydrothermally treated glass powders or hydrosilicates were prepared by hydrating as-obtained waste glass powder in an autoclave. The method of autoclaving with vapor phase was selected since it allows achieving high water contents at fast hydration rates [87]. Additionally, absence of liquid water phase at elevated temperatures eliminates the possibility of excessive leaching. The pressure within the vessel generated during such processing is theoretically equal to the saturated vapor pressure of water, which depends on the temperature.

Weighted amount of as-obtained waste glass powder was mixed with a measured amount of distilled water and sealed in a 120 ml Teflon vessel within a steel autoclave. The mixture was treated for 12 h at a constant temperature of 200 °C (theoretical pressure of 15.5 bar). Glass powders were mixed with distilled water in ratios of 9:1 or 7:3, theoretically producing hydrosilicates with water content of 10 or 30 wt.%, respectively. The amount of achievable hydrosilicate with vapor phase autoclaving is limited by the size of the vessel and decreases with the water content. Maximum achievable amount of hydrosilicate with theoretical H_2O content of 10 or 30 wt.% produced in a 120 ml vessel was 8.36 or 2.83 g, respectively. During the treatment, the material densified and the effect was more pronounced in the case of higher water content (Figure 4.1).

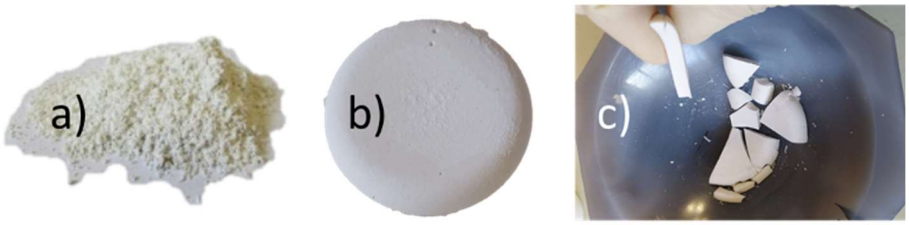

Figure 4.1: Appearance of the raw glass powders before (a) and after (b and c) the hydrothermal treatment.

Obtained hydrosilicate compacts were crushed to powder, and processed further in the same manner as the raw glass powders described in 4.1.1.

4.1.3 Addition of water glass

Foaming mixtures obtained from previously described steps (4.1.1 and 4.1.2) were either used for foaming directly or further processed by mixing them with water glass (WG). Technical grade WG with SiO_2 to Na_2O weight ratio (modulus) of 1.85:1 and with a total water content of approximately 50 wt.% was used. Addition of WG was done by weighting

the foaming mixture and manually mixing it with weighted WG in a plastic beaker. Obtained heterogeneous mixture was then transferred to an agate mortar and manually mixed until a homogeneous mixture was obtained. The time of manual mixing was kept constant (10 min) due to the high sensitivity of the WG-containing foaming mixture. The effect of mixing time is shown in A.2.2. The minimum quantity of foaming mixture used for this step was 5 g to minimize the weighting error of this preparation step due to the highly viscous nature of WG. Content of WG within the foaming mixture is expressed as a percentage of additive relative to the original foaming mixture.

After the mixing, the foaming mixtures were either foamed immediately to minimize the deviations between the batches due to the sensitivity of the mixtures, or stored for a selected amount of time to investigate the effect of the atmosphere on the foaming behavior of the foaming mixture.

4.1.4 Foaming

Before the heat-treatment, the foaming mixtures were pressed either into small cylindrical or large square compacts (Figure 4.2). Small cylindrical compacts were prepared in a steel die by uniaxial pressing at 40 MPa, using a hydraulic press, obtaining a sample with an approximate diameter, height and weight of 12 mm, 10 mm and 1 g, respectively. Large square compacts were prepared by manually compacting the foaming mixture in a square shape, obtaining a sample with approximate dimensions of 4 × 4 × 2 cm and weight of 35-40 g. Small samples were allowed to expand freely during the heat-treatment while the large samples were placed within a 10 × 10 × 4 cm stainless steel mould. The effect of small sample positioning in the furnace is shown in A.2.1. All the surfaces which could come into contact with the expanding material during the heat treatment were covered with kaolin.

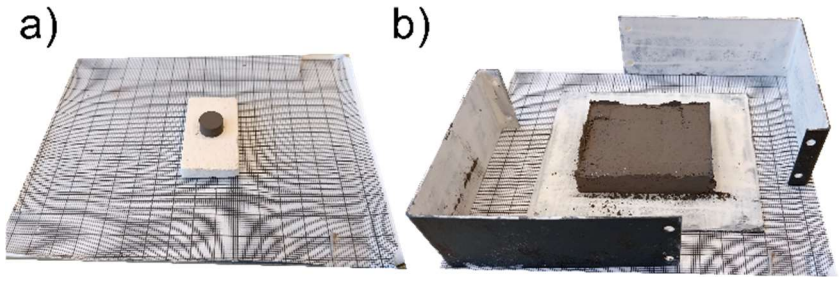

Figure 4.2: Appearance of the small, cylindrical (a) and large, square compact with the stainless steel mould (b).

Foaming mixture compacts were heat-treated in an electric chamber furnace (Bosio) from room (T_{room}) to foaming temperature (T_{foam}) of 800 °C at a heating rate of 5 °C min^{-1}. Holding time (t_{foam}) at T_{foam} was 5 and 20 min for small and large samples, respectively. After the t_{foam}, the samples were immediately placed in a pre-heated kiln and left to cool down naturally. The kiln was pre-heated to the temperature just above the theoretical glass transition temperature (T_G) of the prevailing waste glass powder in the foaming mixture. A standard kiln temperature is 550 °C. These are the standard heat-treatment conditions used to prepare each foamed glass sample unless stated otherwise.

4.2 Foaming Mixture Characterization

Foaming mixtures were investigated for their physicochemical properties and foaming behavior.

4.2.1 Physicochemical properties of the foaming mixtures

The foaming mixtures were investigated for their physicochemical properties after the initial processing (mixing and milling). Chemical composition of the foaming mixtures before the heat-treatment is expected to be well known since only mixing and milling of the glass powders and additives at given conditions normally does not result in the formation of new phases. Mixtures containing water glass and hydrothermally treated glass powders are able to form new phases during the processing and were thus further investigated with X-ray diffraction and infrared spectroscopy.

4.2.1.1 Particle size distribution – Laser granulometry

Particle size distribution of a foaming mixture significantly affects the foaming process. The particle size of foaming mixtures was monitored with the laser scattering particle size distribution analyzer (Horiba LA-920). Required amount of sample was dispersed in water with the addition of Dolapix. Measurement was carried out after 5 min of sonication and the conditions were kept standard for all powder samples.

4.2.1.2 Crystallinity – X-ray diffraction (XRD)

Diffraction techniques are more commonly used for the analysis of crystalline materials. However, the presence of crystalline phases within amorphous glass powder mixture can have a decisive effect on the foaming process, most commonly resulting in decreased expansion and more open porous structure of the obtained foamed glass sample. Malvern PANalytical Empyrean diffractometer (Netherlands) with Cu-K_a radiation source (λ = 1.54817 Å, 45 kV and 40 mA) was used for the analysis of the foaming mixtures. Standard measurement range was from 10° to 90° (2θ) with a step of 0.0263° and time per step of 500 s. Results were analyzed with HighScore Plus software, using the PDF-4 database.

4.2.1.3 Functional groups – Infrared Fourier transformed spectroscopy (FTIR)

A small amount of the foaming mixture was mixed with KBr (sample:KBr ratio of 1:12) and analyzed with IR spectroscopy (Perkin Elmer Spectrum 400 MIR, DRIFT mode).

4.2.2 Foaming behavior

4.2.2.1 Expansion behavior – Heating stage microscopy (HSM)

Approximately 25 mg of the foaming mixture was manually compacted in a steel die (ϕ = 3 mm) to mimic the compaction of the samples and placed on an alumina holder in a hot-stage microscope (EM201x, Hesse instruments). Cylindrical compact was heated at 5 °C min^{-1} to 1000 °C and its silhouette area was monitored during the heating. From this measurement, the sintering temperature (T_{sint}), foaming temperature (T_{foam}) and volumetric expansion were evaluated. Here the T_{sint} and T_{foam} were determined as the onsets of shrinkage and expansion, respectively.

4.2.2.2 Gas evolution – Thermogravimetry coupled with mass spectroscopy (TG/MS)

Approximately 30 mg of the foaming mixture was manually compacted in a steel die (ϕ = 3 mm) to mimic the compaction of the samples and placed into alumina holder. Thermogravimetric analyzer coupled with a mass spectrometer (TG/MS; NETZSCH STA 449 C/6/G Jupiter, 403 C Aëolos QMS 403) was used to follow the weight loss and gas evolution during the heating of the foaming mixtures. Standard conditions with a heating

rate of 10 °C min^{-1} and total gas flow of 100 ml min^{-1} were used. Mixture of O_2 and Ar with a ratio of 1 to 4 was used as the flow gas.

4.3 Foamed Glass Sample Characterization

After the heat treatment, foamed glass sample is obtained from the foaming mixture. All the heat-treated foaming mixtures are referred to as foamed glass, even if the heat treatment resulted in negligible foaming and consequent lack of an actual foam structure.

Obtained foamed glass samples were analyzed for their crystallinity and presence of functional groups, by crushing the samples and following the same procedure as in the case of foaming mixtures described in 4.2.1.2 (XRD) and 4.2.1.3 (FTIR).

4.3.1 Porosity

4.3.1.1 Total, open and closed porosity – Archimedes principle

Foamed glass sample porosity was calculated from the density measurements, based on the Archimedes principle. All porosity calculations are based on the initial raw glass powder densities (ρ_{pow}) determined with a helium pycnometer (Ultrapyc 1200e, Quantachrome Instruments, US).

Measurements of the smaller samples were done on the as-obtained foams after the foaming. The apparent density (ρ_{app}) was measured by the Archimedes method in water and the pycnometric density (ρ_{py}) was measured in ethanol where the samples were before submerged in ethanol under reduced pressure to eliminate the air from the open pores. Note that during foaming, a less porous layer is formed on the surface of the foamed glass samples, affecting the ρ and ε measurements.

Measurements of the larger samples were done on a cut-out piece with approximate dimensions of 2 × 2 × 2 cm. The ρ_{app} was calculated from the cut-out dimensions and weight, while the ρ_{py} was measured as in the case of the smaller samples.

The relative density (ρ_{rel}) and total- (ε_{tot}), open- (ε_{op}) and closed porosity (ε_{cl}) of the foamed glass samples were calculated according to Equations 4.1, 4.2 and 4.3.

$$\rho_{rel} = \frac{\rho_{app}}{\rho_{pow}} \qquad \varepsilon_{tot} = 1 - \rho_{rel} \tag{4.1}$$

$$\varepsilon_{cl} = \frac{1 - \frac{\rho_{app}}{\rho_{py}} - Corr^*}{\varepsilon_{tot}} \qquad \left(Corr^* = \frac{V_{pores} * \rho_{app}}{m}\right) \tag{4.2}$$

$$\varepsilon_{op} + \varepsilon_{cl} = 1 \tag{4.3}$$

Where the ρ_{pow} of the CRT panel glass was measured to be 2816 kg m^{-3}. The $Corr^*$ factor was utilized only in the case of cut-outs from the larger samples. Calculation of ε_{cl} for the larger samples was corrected for the volume of open pores on the surface of the cut-out (V_{pores}). The V_{pores} was calculated from an additional measurement where the sample was cut into eight 1 × 1 × 1 cm large pieces which were measured for their volume with a pycnometer (measuring the accessible volume of the foam). The total pycnometric volume of eight small samples is always smaller than the pycnometric volume of the larger sample. Cutting of the larger sample reveals new surfaces and new open pores, resulting in decreased pycnometric volume. Since the surface area of eight smaller pieces is exactly twice the

surface area of the initial cube, the volume of the pores on the surface of the cube (V_{pores}) can be calculated from the difference between the ρ_{py} and $\rho_{py,8}$.

Figure 4.3 shows the effect of surface porosity on the open porosity measurement for the case of an ideal foam with ordered distribution of completely closed spherical cells. It is apparent that the volume of pores on the surface has a significant effect on the measurement on the scale-size of a laboratory sample, requiring the use of a *Corr** factor.

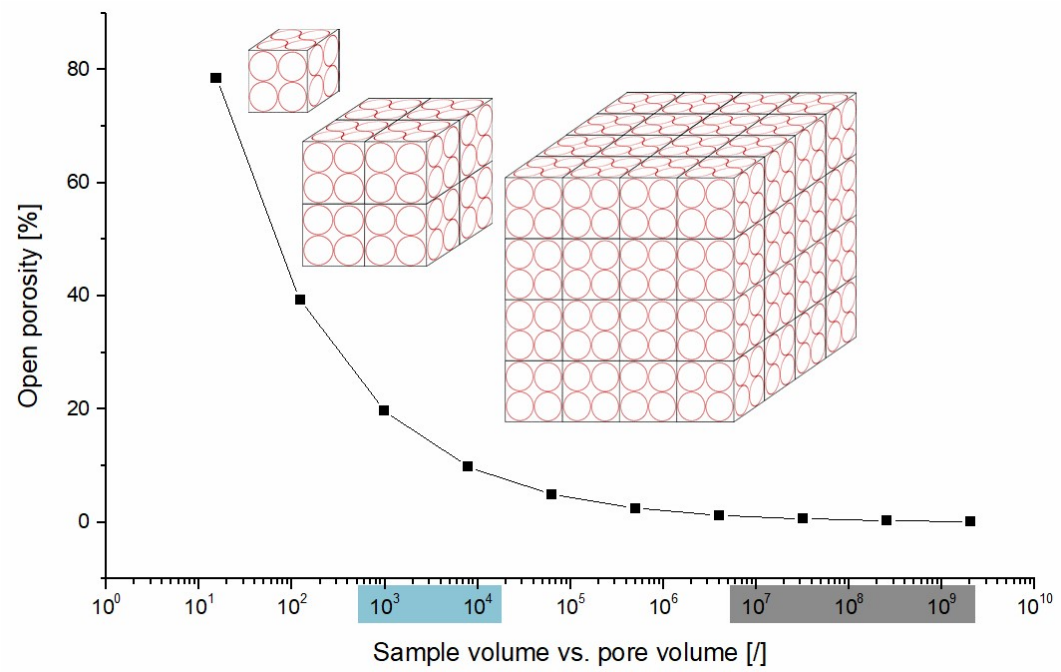

Figure 4.3: Theoretical effect of the sample size on the measurement of open porosity due to the pores on the surface. Blue and grey labels mark a common sample size from this investigation and the size required to eliminate the need for the correction of ε_{cl} measurement, respectively.

4.3.1.2 Foamed glass sample expansion

Porosity of several of the foamed glass samples reported in this study is above 90 %. Reporting density, relative density or porosity values of such samples does not give a true sense of the actual differences between the samples. For this reason, volumetric expansion (ΔV) of the samples is reported, considering the difference between the sample volumes before (V_0) and after (V_{final}) the heat-treatment. ΔV is calculated according to Equation 4.5. Final density (ρ_{final}) is equal to the apparent density (ρ_{app}) in Equation 4.4, and x is a relative mass lost during the heat treatment.

$$\Delta V = \left(\frac{V_{final} - V_0}{V_0}\right) = \frac{\frac{m_{final}}{\rho_{final}} - \frac{m_0}{\rho_0}}{\frac{m_0}{\rho_0}} = \frac{m_{final}\rho_0}{\rho_{final}m_0} - 1; \quad \frac{m_{final}}{m_0} = 1 - x \qquad 4.4$$

$$\Delta V = \left(\frac{\rho_0(1-x)}{\rho_{app}} - 1\right) \times 100\% \qquad 4.5$$

4.3.1.3 Pore size distribution – microscopy

Pore size distribution of the foamed glass samples was investigated by analyzing the images captured with scanning electron microscope (SEM, Thermo Fisher Quanta 650 ESEM) and stereomicroscope (Discovery V8 – Carl Zeiss AG). Images were taken on a cut surface of the foamed glass samples and pores were labelled manually. Images containing between 500 to 900 pores were analyzed with ImageJ software to obtain the distribution of the maximum Feret diameters, defined as the longest distance between two points on a measured object, i.e. pore [88]. Note that pore size distributions of smaller samples were evaluated from the images containing > 50 pores. Maximum Feret diameter is from here on expressed as pore size.

Classic representation of obtained data where pore number density is plotted versus the pore size fails to show the real state of the material structure. Reason being, we are interpreting 3D particle size distribution based on 2D observations. Furthermore, properties of the bulk material in interest, i.e. thermal conductivity, depend on the volumetric fractions of structural elements making the representation over 3D more sensible. For that reason, distributions were modified with the stereological conversion technique described in [89] while the average pore diameter was calculated and corrected according to [10]. A foam which contains a few extremely large pores can be visually clearly distinct from the others, which may not be true for data. Modified distributions as well as corrected average pore size allow clearer distinction between the foams.

4.3.2 Pore-gas composition

Knowing the approximate relation between the gas species within the closed pores can reveal additional information about the reactions and expansion path during the foaming. In this investigation, the composition of pore-gas was evaluated by a gas chromatograph (7890A GC System, Agilent Technologies) on a 30 m long Rt-Msieve™ 5A and Rt-QPLOT™ (Restek) columns which allows the determination of CO/CO_2 and Ultraportable Greenhouse Gas Analyser (Los Gatos Research) which allows the detection of H_2O.

A sample of pore-gas was obtained by crushing the foamed glass samples in a He-filled cell. The cell consists of a rigid cylindrical body, two crushing discs and a lid, enabling constant measurement of the inner pressure, with a rubber insert, enabling the sampling of the inner atmosphere. Foamed glass sample was placed between two crushing discs and crushing was performed manually by shaking the He-filled cell. Measurements were performed in triplicates and the background was determined by measuring the atmosphere of He-filled cell before the crushing of the foam sample. The quantity of detected CO_2 and CO gas (n_{gas}) was evaluated with the help of standard curves. The volume of the He-filled cell (V_{cell}) and crushing disks (V_{disks}) were measured and the free volume ($V_{free} = V_{cell} - V_{disks}$) within the cell was calculated.

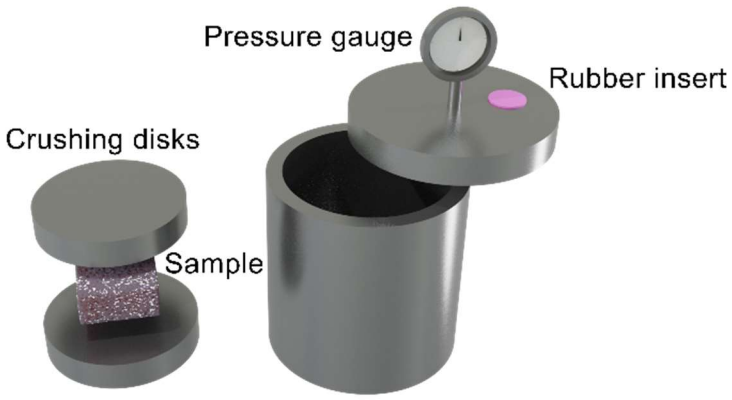

Figure 4.4: Scheme of a He-filled cell, showing the configuration of the sample and crushing disks.

The pycnometric volume of the foamed glass sample was measured before ($V_{\text{py,before}}$) and after ($V_{\text{py,after}}$) the crushing with a He-pycnometer (Ultrapyc 1200e, Quantachrome). Volume of the closed pores (V_{cp}) was evaluated from the measurement as $\mathbf{V_{cp} = V_{py,before} - V_{py,after}}$. Knowing the quantity of detected gases and the V_{cp} allows for the evaluation of the pore inner pressure ($p_{\text{inner,g}}$) as shown in Equation 4.6:

$$p_{inner,g} = \frac{n_{gas}}{V_{cp}} RT_{room} \quad \left(gas\ constant, R = 8.314\ \frac{J}{mol * K}\right) \tag{4.6}$$

Additionally, knowing the pressure before (p_{before}) and after (p_{after}) the crushing allows the second evaluation of the pore inner pressure ($p_{\text{inner,p}}$) as shown in Equation 4.7:

$$p_{inner,p} = \frac{\left(p_{after}(V_{free} - V_{py,after}) - p_{before}\left(V_{free} - V_{py,before}\right)\right)}{V_{cp}} \tag{4.7}$$

Comparison between the two pressures can reveal more about the pore gas composition. For the $p_{\text{inner,g}}$, we assume that CO and CO_2 represent the majority of the pore gas, while $p_{\text{inner,p}}$ is the actual pressure within the pores. A significantly smaller value of $p_{\text{inner,g}}$ would indicate that the pore gas contains significant amounts of other gaseous components which we were not able to detect.

4.3.3 Thermal conductivity

The thermal conductivity (λ) was measured on large foamed glass samples cut into a standard shape with approximate dimensions of 8 × 8 × 2 cm. A heat-flow meter (HFM 446 Lambda Small, Stirolab, Sežana, Slovenia) was used for this measurement in accordance with a standard (DIN EN 12667). Calibration of the instrument was done using a NIST Standard Reference Material® 1450d resulting in a typical accuracy of ±1 %. For the measurement, constant temperatures of 5 and 15 °C were used for lower and upper plate, respectively. The average temperature of the foamed glass sample during the measurement was thus 10 °C.

Chapter 5

Results and Discussion

5.1 Use of Water Glass for the Foaming of Glass

5.1.1 Introduction

Water glass (WG) is a technical name used for alkali silicates, most commonly designating sodium silicate ($(Na_2O)_x(SiO_2)_y$), normally further specified by the ratio between the SiO_2 and Na_2O (modulus) and the content of water [90]. The SiO_2:Na_2O ratio affects the size of the silicate molecules and consequentially the solubility of WG. Additionally, the content of water significantly affects the physical properties of WG, whereas it can be a solid or a liquid depending on the water content. WG is structurally described as a colloidal suspension of aqueous sodium silicate solution with silicate molecules and colloids being its main components. Water is present between/within the molecules in various configurations, i.e. in the form of a OH^- within the SiOH (silanol) functional groups or in the form of an H_2O molecule which interacts with the nonbridging oxygens of the glass network, silanol or siloxane bridges [35], [91]. It is often stated that soluble silicates consist of "free" water which can be removed by desiccating at low humidity or heating at 100°C, and "bound" water [92], [93]. Higher temperatures are required to remove "bound" water which includes water molecules trapped in the fine pores of the material and water that is part of the material structure [94]. Here, water can be present in several different configurations as a molecule or a as a part of silanol groups (discussed in 2.3).

WG is a common additive in the production [21], [95] and research [96] of foamed glass via foaming. It can be used as one of the additives [75], [97], [98] or as a sole foaming agent [99]. WG is, therefore, a well-known additive used in the foamed glass research and industry. However, the mechanism behind the foaming remains to be experimentally proven. Currently, the literature predicts that the expansion of the glass during the foaming with WG happens due to the release of the "bound" water from the WG [100]. Such explanation is possible, especially since WG releases a significant amount of water during the heating, however, no experimental evidence was found to support the mechanism.

Interestingly, water being the main expansion gas would theoretically result in foams which contain pores with unexpectedly low pressure. It is possible to detect such significantly lower pressure during the pore gas measurement (4.3.2). The reason for lower-than-expected pore pressure is low saturation pressure of water in comparison to other common expansion gases. For example, 800 °C is a common foaming temperature (T_{foam}) and for the foam to remain stable against the pressure within the pores at T_{foam} should still be higher than the outer pressure (> 1 bar). To approximate we can assume that no significant shrinkage or gas diffusion occurs during the cooling of the sample and that the pressure within the pores simply follows the ideal gas law: $pV = nRT$. Foamed

glass prepared at 800 °C and cooled to room temperature (25 °C) would theoretically contain pores with inner pressure of approximately 0.28 bar [47], [58]. However, the equilibrium vapor saturation pressure of water at room temperature is one order smaller (0.03 bar), meaning significantly lower pore pressure than theoretically expected and normally observed. Further, trapped water would either condense within the closed pores or diffuse back into the glass structure. In the case of condensate, the water can be detected during the analysis of pore gas while the structurally incorporated water can be observed with FTIR.

To investigate the process of direct foaming of glass with the addition of WG, a single foaming mixture was used. It corresponds to the foaming mixture labelled *0* in Table 4.2 with added 24 wt.% of WG and its composition is shown in Table 5.1. The foaming mixture and the foamed glass samples were prepared according to the standard processing described in 4.1.

Table 5.1: Composition of the only foaming mixture used in 5.1.

Component	CRT	K_3PO_4	WG	Mn_3O_4	C
Fraction [wt.%]	79.3	1.6	19.3	0	0

The foaming mixture used in this investigation underwent additional treatment after the initial preparation. Additional treatment performed on the foaming mixture was either drying, storing in a CO_2 atmosphere or a combination of both. Additional treatment and the labels for four corresponding foaming mixtures are shown in Table 5.2. Drying was done on 200 °C for 2 h. Note that *Fresh* foaming mixture was foamed immediately after its preparation to minimize possible reaction effects on its properties.

Table 5.2: Additional treatment performed on the foaming mixture and corresponding labels.

Additional treatment of the foaming mixture	Label
None	*Fresh*
Drying	*Dried*
Storing in CO_2 atmosphere for 24 h	*Fresh-CO_2-stored*
Drying and subsequently storing in CO_2 atmosphere for 24 h	*Dried-CO_2-stored*

The question of above-described water-dominated foaming mechanism is addressed in this investigation. Furthermore, susceptibility of a WG-containing foaming mixture to a carbonate-forming reaction is demonstrated and an alternative carbonate-dominated foaming mechanism is proposed.

5.1.2 Foaming mixture behavior during the heating

The addition of WG to the glass powder can significantly alter the powders' properties. Specifically, it is known that the presence of Na_2O [23] or water [30] in the structure affects the thermal properties of glass, practically affecting the sintering behavior of the powder. Additionally, increased partial pressure of water during the heating promotes the sintering of the glass powder as described under *Water in Glass and Hydrated Glasses* on page 8 [101]. A decrease of waste glass powders' characteristic temperatures is therefore expected when mixed with WG.

5.1.2.1 Expansion behavior

The changes of the sintering and expansion behavior of the foaming mixtures can be observed in Figure 5.1. Milled CRT glass starts to sinter at approximately 600 °C and reaches a minimum area of 71 % at approximately 700 °C. The raw glass powder therefore behaves as expected, without expansion.

After the mixing of the glass powder with WG, sintering-related shrinking can be observed only for the *Fresh-CO_2-stored* foaming mixture. The onset of sintering for the *Fresh-CO_2-stored* foaming mixture decreases for approximately 50 °C in comparison to powder of CRT panel glass (red and grey curve in Figure 5.1), while the minimum area remains at ≈70 %. The *Fresh*, *Dried* and *Dried-CO_2-stored* foaming mixtures do not exhibit significant shrinkage. Abundant evolution of the gas phase in combination with closed porosity acts as an opposing force to sintering and is expected to be one of the main reasons for the absence of shrinkage.

The *Fresh*, *Dried* and *Dried-CO_2-stored* foaming mixtures start expanding at approximately 575 °C with a similar initial rate. *Fresh* foaming mixture expands up to 800 °C (approximately 375 % of initial area) while the *Dried* and *Dried-CO_2-stored* foaming mixtures expand similarly up to 750 °C (approximately 300 % of initial area). At the expansion onset, all three foaming mixtures exhibit an initial increase followed by a slight stagnation or a decrease of area before further expansion. Such "two-stage" expansion is likely a consequence of interplay between the forces of sintering and expansion. This effect becomes more apparent in the case of *Fresh-CO_2-stored* foaming mixture. Expansion of the *Fresh-CO_2-stored* foaming mixture begins at approximately 640 °C. Here, the expansion rate is similar to other three foaming mixtures and dramatically decreases above 675 °C. *Fresh-CO_2-stored* foaming mixture reaches a maximum area of 150 % at 840 °C.

The collapse of *Fresh*, *Dried* and *Dried-CO_2-stored* foaming mixtures starts at 800 °C while the *Fresh-CO_2-stored* foaming mixture starts to collapse above 850 °C. Sharp drops can be observed in this stage due to the bursting and collapse of large pores near the surface of the foam.

Behavior of the dried foaming mixtures is very similar while the *Fresh-CO_2-stored* foaming mixture exhibits the most deviant behavior with higher T_{foam}, smaller expansion and higher temperature of collapse. Sintering and expansion behavior of the foaming mixtures in Figure 5.1 suggests that CO_2 atmosphere can significantly affect their properties. Interestingly, the effect of CO_2 atmosphere is not apparent in the case of the dried foaming mixtures since the behavior of the *Dried* and *Dried-CO_2-stored* foaming mixture is similar.

The expansion behavior of the Fresh foaming mixture is apparently affected by drying or storing in a CO_2-containing atmosphere before the heat-treatment.

The presence of H_2O within the material and/or increased H_2O partial pressure significantly affect the material properties during the heating [102], which can explain changed sintering and expansion behavior of the dried foaming mixtures. Removal of "free" water by drying decreases the foaming mixtures' ability to expand. This indicates that "free" water significantly contributes to expansion directly, as an expansion gas, or indirectly, affecting the sintering behavior of the foaming mixture [101].

Storing a fresh foaming mixture in a CO_2 atmosphere, on the other hand, results in a completely different sintering and expansion behavior. Foaming mixtures' ability to expand is decreased even further in comparison to the dried foaming mixtures and is likely related to the reactivity between the WG-CO_2.

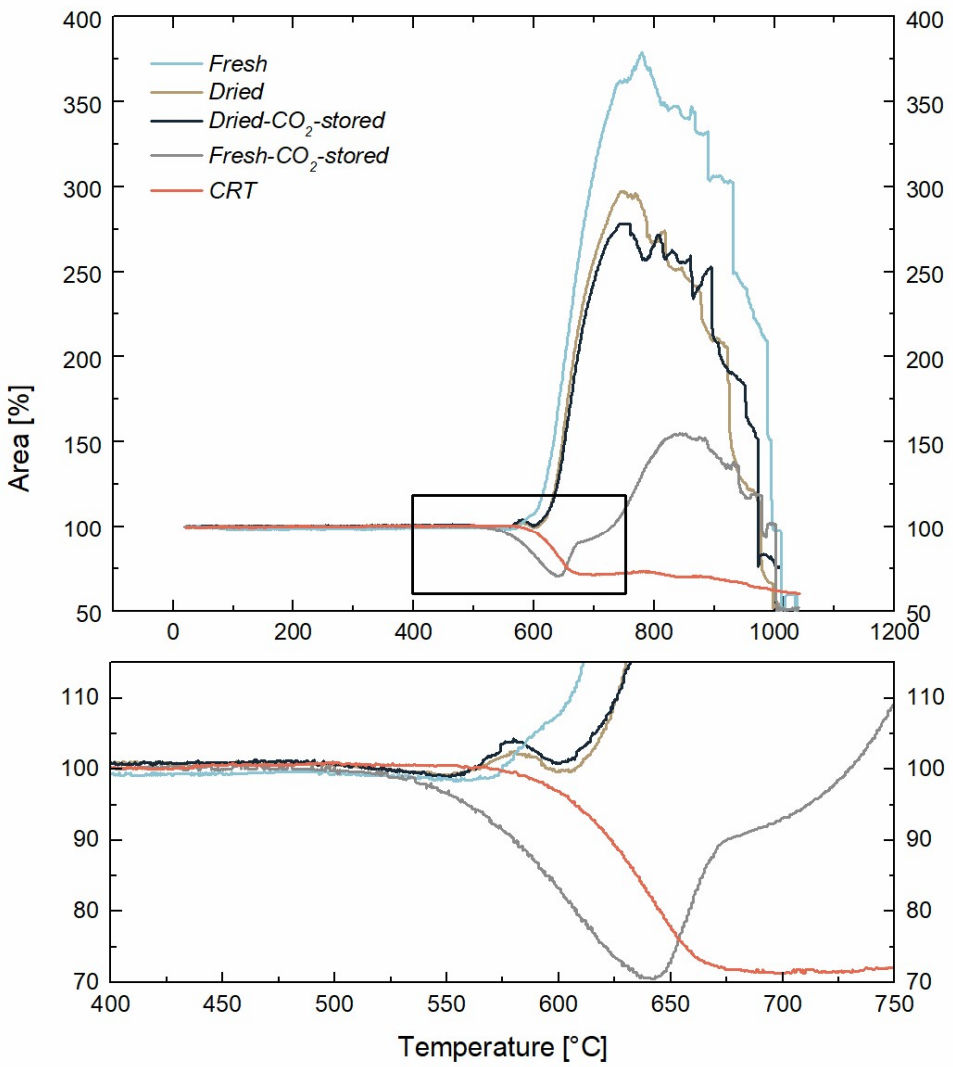

Figure 5.1: Silhouette area of the WG-containing foaming mixtures and milled CRT powder as a function of temperature (top), with a closer view of the sintering stage (bottom).

5.1.2.2 Thermal analysis and evolution of gases

Expansion behavior of the foaming mixtures greatly depends on the amount of evolved gases, their evolution rate, and the temperature at which they start to evolve. Heating of the foaming mixtures results in multiple mass loss regions accompanied by the H_2O and/or CO_2 signals.

Fresh foaming mixtures exhibit a significant low-temperature mass loss (< 400 °C), related to the evaporation of H_2O (Figure 5.2a, c and e). The *Fresh-CO_2-stored* foaming mixture exhibits smaller initial mass loss with less intense H_2O and more intense CO_2 signal compared to the *Fresh* foaming mixture, suggesting that the fresh foaming mixtures dried partially during the storage. The H_2O signal peak is located at a similar temperature (between 115 and 140 °C) for both fresh foaming mixtures (Figure 5.2c) and is in the case of the *Fresh-CO_2-stored* foaming mixture accompanied by a strong CO_2 signal (Figure 5.2e). *Fresh* foaming mixture exhibits a CO_2 signal with a maximum at approximately 300 °C, suggesting an additional CO_2 source. Similar maximum at 300 °C is not apparent for the *Fresh-CO_2-stored* foaming mixture, likely due to the overlap with more intensive first CO_2 signal. The origin of these low-temperature CO_2 signals is related either to the desorption of adsorbed CO_2 or to the decomposition of newly formed carbonate species.

More reliable conclusion about the origin of low-temperature CO_2 signals can be done after the structural analysis.

At higher temperatures (>400 °C), the *Fresh* and *Fresh-CO_2-stored* foaming mixtures exhibit a small (0.22 wt.%) and large mass loss (2.07 wt.%), respectively. The difference between *Fresh* and *Fresh-CO_2-stored* sample in this temperature range is significant, a mass loss with a difference of approximately one order showcases how differently the fresh foaming mixture starts to behave after being exposed to CO_2 atmosphere. Mass losses in this temperature region (>400 °C) are accompanied by additional CO_2 signals suggesting stronger interactions with the material than only dissolution or physical adsorption. Larger mass loss in the case of the *Fresh-CO_2-stored* foaming mixture is also accompanied by a significantly stronger gas signal in comparison to the *Fresh* foaming mixture. Presence of CO_2 signal above 650 °C in the case of the *Fresh-CO_2-stored* foaming mixture (Figure 5.2e) suggests that the pores at this temperature are still well-connected to the outer atmosphere even though the mixture already starts to expand (Figure 5.1). Vice versa, it is very likely that a pronounced gas evolution, when the material is already in the sintering stage (Figure 5.1, grey line), hinders the closing of the pores, resulting in an open porous structure. Such relation between the sintering and gas evolution results in significant loss of expansion potential and usually results in low-porosity foams, which may explain much lesser expansion of the *Fresh-CO_2-stored* foaming mixture in comparison to others.

Dried foaming mixtures exhibit a similar mass loss and gas evolution at all temperature stages, matching their similar expansion behavior (*Expansion behavior* on page 27). Drying results in a significantly smaller low-temperature mass loss (< 400 °C) in comparison to the fresh foaming mixtures. This difference is related to the evaporation of "free" H_2O (Figure 5.2b, d), which is expectedly less relevant in the case of dried foaming mixtures. The H_2O peak for the *Dried* and *Dried-CO_2-stored* foaming mixtures at approximately 300 °C is accompanied by a CO_2 signal (Figure 5.2d, f), similarly as in the case of the *Fresh* foaming mixture (Figure 5.2c). Both dried mixtures also exhibit a CO_2 peak above 600 °C accompanied by a mass loss of 0.34 and 0.38 wt.% for the *Dried* and *Dried-CO_2-stored* foaming mixture, respectively. Note that above 400 °C, *Fresh*, *Dried* and *Dried-CO_2-stored* foaming mixtures exhibit a similar mass loss and gas evolution behavior.

None of the foaming mixtures exhibit significant mass loss above 800 °C, however, several sharp CO_2 signals can be observed for the *Fresh*, *Dried* and *Dried-CO_2-stored* foaming mixtures. At this temperature, i.e. 800 °C, the mixtures are already collapsing as seen from Figure 5.1. Foam collapse is accompanied by bursting of the pores and an instant release of pore atmosphere, resulting in sharp signals as observed in Figure 5.2e and f. Such results suggest that CO_2 is one of the main constituents of the pore atmosphere, while no sharp signals above 800 °C were detected for H_2O.

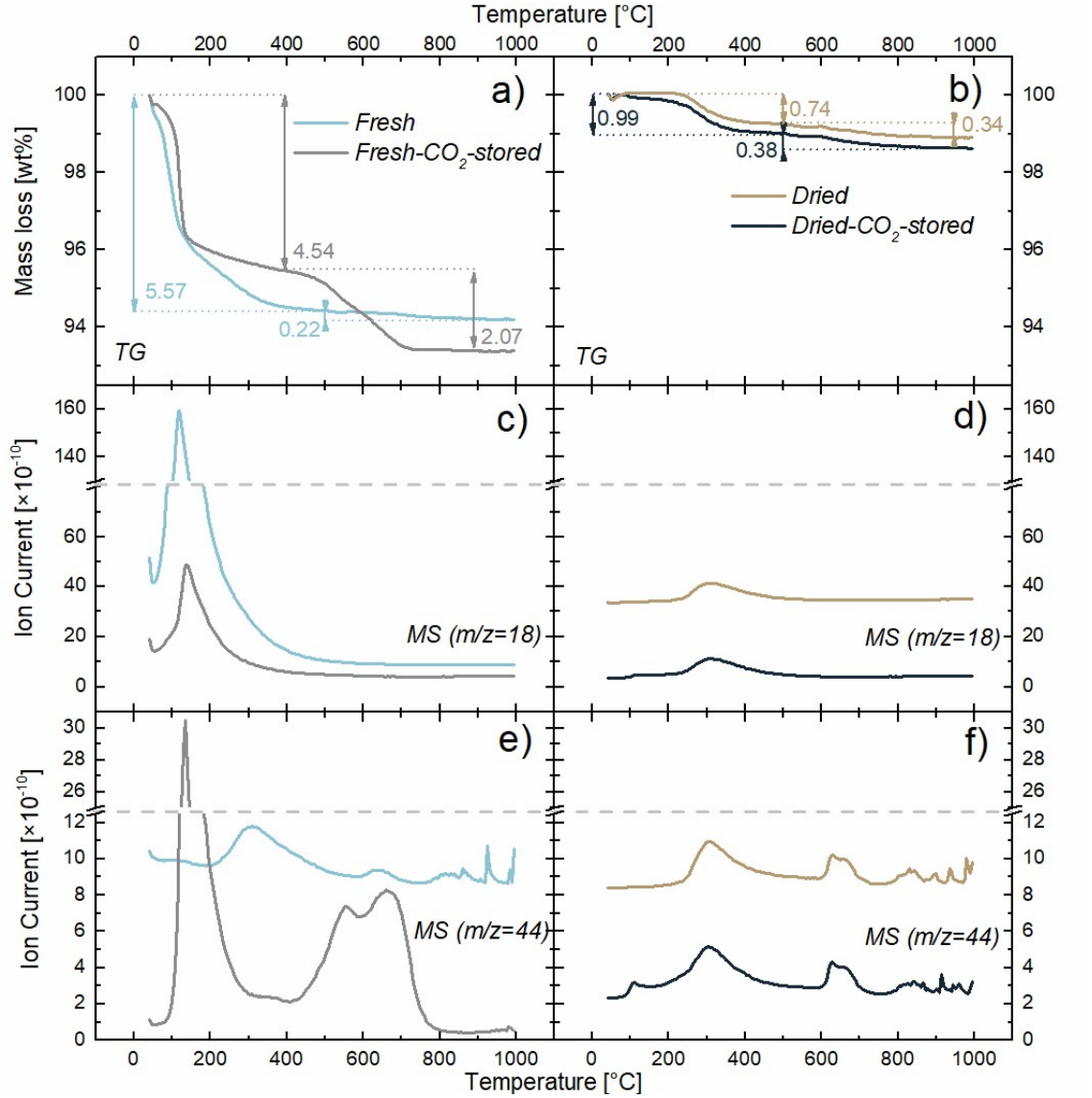

Figure 5.2: Mass loss (a, b) and evolution of H_2O (c, d) and CO_2 (e, f) during the heating of the fresh (a, c, e) and dried foaming mixtures (b, d, f). Note that the Ion Current signals are shifted for better visibility.

All of the foaming mixtures exhibit evolution of CO_2 at relatively high temperatures (> 600 °C), suggesting its incorporation with stronger interactions than only physical adsorption or dissolution in water. However, no CO_2-producing components were added to the foaming mixtures during the preparation stage. Formation of a new phase is therefore the most probable explanation especially since it is known that WG can react with CO_2 resulting in the formation of carbonates [103]. Note that it is not necessary for the foaming mixture to be in contact with a pure CO_2 atmosphere to evolve CO_2 at higher temperatures during the heat treatment, suggesting that CO_2 present in the air atmosphere is enough for the carbonate-producing reaction to occur.

Additional inspection of the gas evolution from the raw initial components (WG and CRT panel glass powder) confirms that the high-temperature evolution of CO_2 is related to the presence of WG. Furthermore, high-temperature CO_2 peak appears only after the WG was in contact with the air atmosphere (Figure 5.3). Heating of WG leads to significant mass loss below 200 °C due to the evaporation of H_2O accompanied by a signal for CO_2. It

is likely that this CO_2 peak is related to dissolved or adsorbed CO_2 which does not contribute to the expansion of the foaming mixtures. At this point WG does not exhibit any CO_2 signal above 400 °C, leaving the high-temperature CO_2 signal unexplained (Figure 5.2e and f). Furthermore, raw CRT panel glass powder does exhibit some evolution of CO_2, however, well below 600 °C. The source of CO_2 was further investigated by drying and crushing the WG by itself, mimicking the action of mixing it with the glass powder. Such dried and crushed WG expectedly exhibits significantly smaller initial mass loss, however, a new mass loss accompanied by a CO_2 signal appears just above 600 °C (brown line in Figure 5.3). This newly observed signal is very similar to the one observed in the case of the foaming mixtures and offers a likely explanation for the source of CO_2.

Reaction between sodium silicate and CO_2, often also termed efflorescence, occurs on the surface and proceeds only in the presence of water [103]. Sodium silicate films and coatings impacted by the reaction with CO_2 become brittle and lose adhesion due to the formation of carbonates containing present cations. Drying and crushing of the WG effectively increases its contact area with air, allowing the reaction with CO_2 to proceed significantly faster. A parallel can be drawn when WG is mixed with glass powder, which also increases the contact area between the air and sodium silicate, i.e. WG.

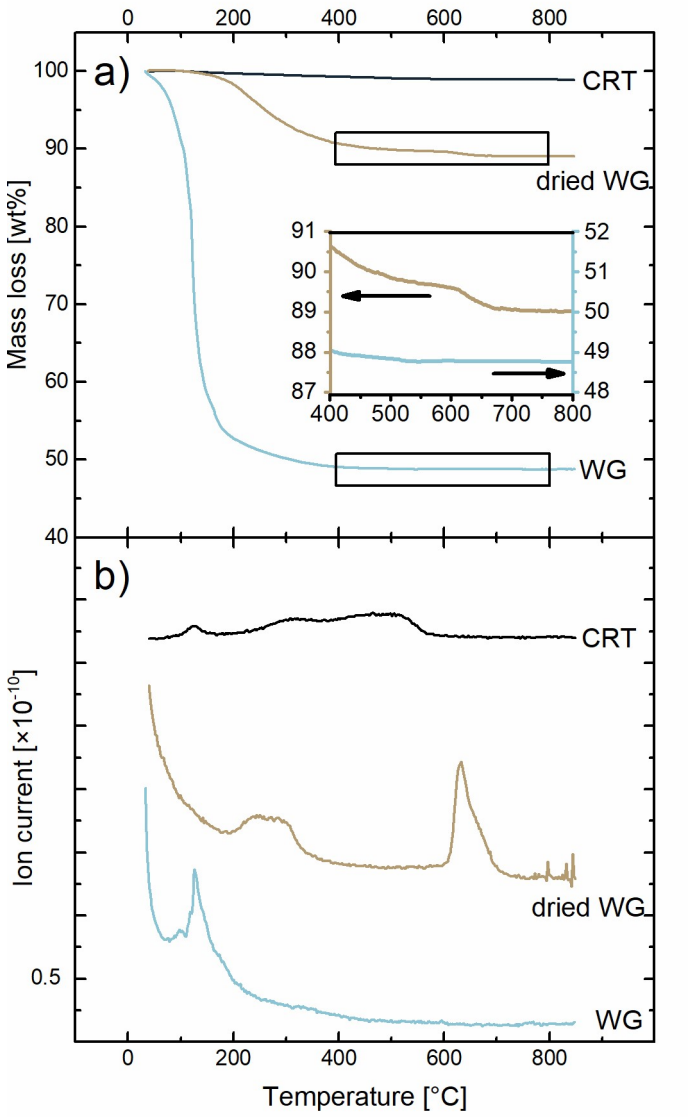

Figure 5.3: (a) Mass loss and (b) CO_2 gas evolution from CRT glass powder and WG. Note that the Ion Current signals are shifted for better clarity.

Mass loss and gas evolution results suggest that a carbonate-forming reaction occurs during the mixing of WG and glass powder and, more importantly, that the newly formed carbonates are decisive for the expansion during the foaming process. Most probable source for the carbonate formation is thus the CO_2 from the air atmosphere. Exposing the foaming mixture to pure CO_2 atmosphere (*Fresh-CO_2-stored* foaming mixture) results in a larger amount of evolved CO_2 during the heating while the expansion decreases significantly. One would expect that a larger amount of expansion gas leads to larger expansions, however, it was shown that exaggerated carbonate content leads to smaller expansions [49], [69]. Additionally, the reaction between WG and CO_2 produces also precipitated SiO_2 [103], [104] which suppresses the material's ability to sinter and results in a more open porous material. A similar behavior was reported in several investigations of the sand-WG mixtures as foundry cores [105], [106]. Exposing the dried foaming mixture to the pure CO_2 atmosphere has no significant effect on its gas evolution suggesting that the reaction between WG and CO_2 does not proceed further in the absence of moisture. This is in accordance with investigations of soluble silicates and their reactivity with CO_2 [103], [107],

[108] and can be a practical way of making the foaming mixtures less susceptible to the atmospheric effects.

5.1.2.3 Structural changes

Change in the crystallinity and functional groups of the foaming mixtures was followed to complement the expansion and gas evolution results.

Foaming mixture of glass powder and WG is susceptible to the reaction with CO_2 from the atmosphere. Initial raw materials (WG and CRT) are highly amorphous, not exhibiting any significant diffraction peaks (Figure 5.4a). Mixing of WG and CRT results in the formation of a detectable amount of crystalline phase at room temperature (blue lines in Figure 5.4b and c), which further confirms the results of TG/MS analysis indicating that a new carbonate phase is formed. Hydrous silicate and sodium carbonate crystal phases (PDFs which correspond best are 00-003-0433 and 00-008-0448, respectively) present at room temperature start to decompose during the heating and calcium silicate phase (best coinciding data from PDF 01-077-0420) is formed eventually at 900 °C. The exact determination of crystalline phases is challenging since the material is still mostly amorphous and the intensity of diffraction peaks is low, referenced PDF numbers correspond to most probable compounds which coincide best with obtained data. Higher content of crystalline phases can be observed in the case of the *Fresh-CO_2-stored* foaming mixture (Figure 5.4c). Increase in the content of crystalline phases can be observed for the *Fresh-CO_2-stored* mixture at 500 °C, which can have a significant effect on the foam stability and expansion dynamics. Higher content of crystalline phases could be the reason for a significantly different gas evolution and expansion behavior of the *Fresh-CO_2-stored* foaming mixture in comparison to others (Figure 5.1 and Figure 5.2).

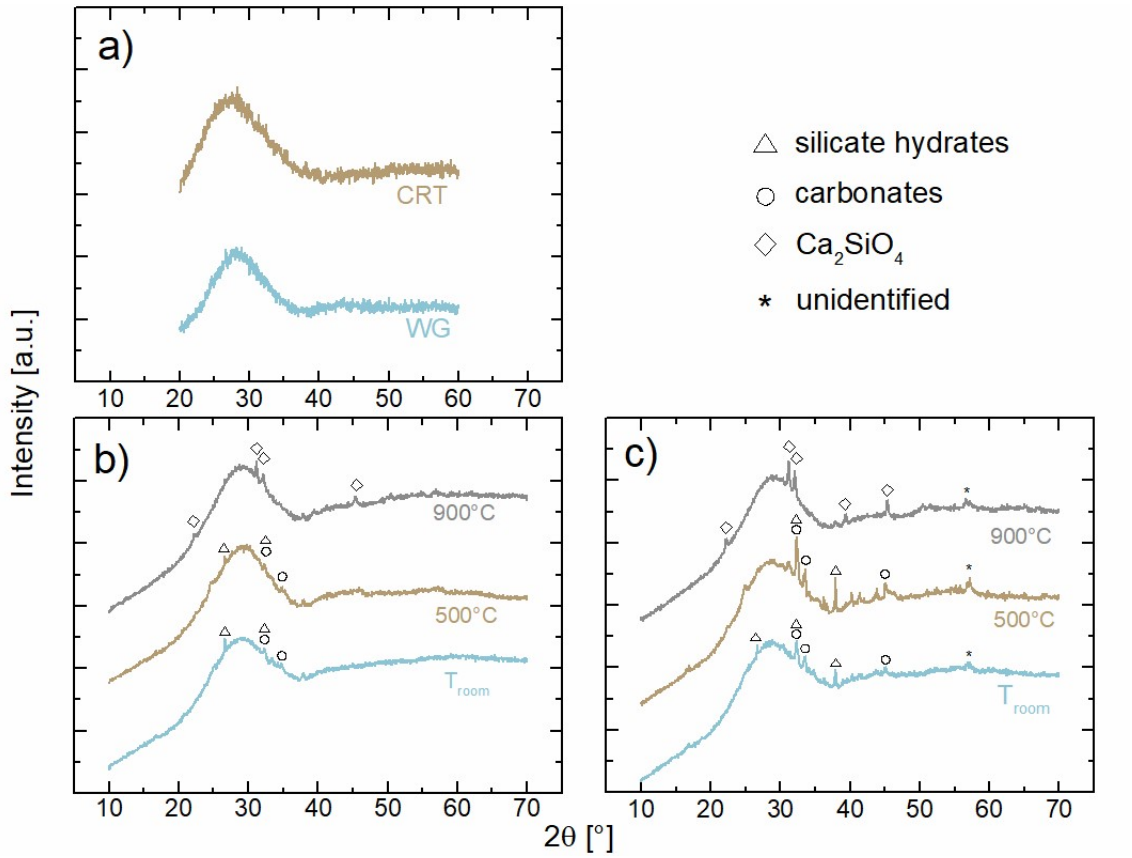

Figure 5.4: XRD patterns of a) raw input materials, b) *Fresh* and c) *Fresh-CO_2-stored* foaming mixtures as-prepared (T_{room}) and treated at 500 and 900 °C.

A similar analysis was performed using FTIR, observing the functional groups present within the foaming mixture and foamed glass samples from different stages of heat-treatment.

In Figure 5.5, the peaks with maximum at approximately 1000 and 750 cm^{-1} correspond to the vibrations of the silicate network. Intensity of silicate network peaks remains fairly constant for both foaming mixtures (Figure 5.5a and b) at different stages of heat-treatment and can serve as a reference peak for estimating the changes in the rest of the curve. The peaks at 2250-3800 cm^{-1} and at 1650 cm^{-1} indicate the presence of OH^- groups and molecular water, respectively [90]. During the heating, the majority of H_2O evaporates from the foaming mixtures below 500 °C (Figure 5.2a), resulting in a pronounced decrease of intensity for the H_2O and OH^- related signals (Figure 5.5a and b). However, the intensity of the 3600 cm^{-1} band stops decreasing at 700 °C, indicating that part of OH^- is still bound within the material above 500 °C.

The 1450 cm^{-1} peak accompanied by a less intense shoulder at 1400 cm^{-1} can be attributed to the presence of carbonates [109]. Narrow splitting of the 1450 cm^{-1} peak suggests CO_3^{2-} group is undistorted from the ideal trigonal symmetry, characteristic for crystalline carbonates. Indication for the presence of crystalline carbonates confirms the XRD results (Figure 5.4 and Figure 5.5). In the case of *Fresh-CO_2-stored* foaming mixture, some splitting of the carbonate peak can be observed, suggesting less crystalline nature or more varied interactions of CO_3^{2-} group with the matrix material. With heating, the carbonates decompose and the intensity of the carbonate peak decreases. The largest decrease in the carbonate peak intensity happens 600-700 °C, agreeing with the temperature of the maximum CO_2 gas detection from TG/MS (Figure 5.2e and f).

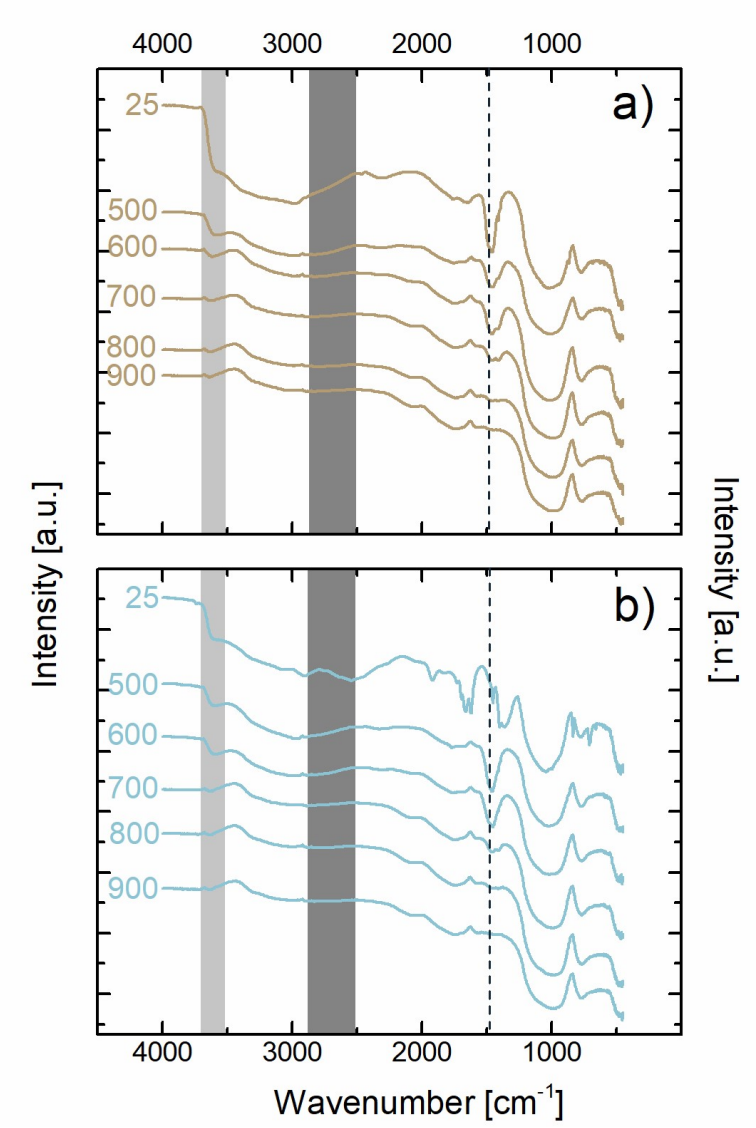

Figure 5.5: FTIR spectra of the a) *Fresh* and b) *Fresh-CO_2-stored* (labels in °C). Black and dark blue bands (3600 and 2600 cm^{-1}, respectively) denote Si(OH) stretching and bending, respectively. The dashed line at approximately 1450 cm^{-1} designates a signal for carbonates. Note that the signals are shifted for better clarity.

Structural changes observed with XRD and FTIR support previous assumptions based on the sample behavior during the heating. Both analytic techniques show that after the mixing of WG and CRT panel glass powder, crystalline carbonates are formed. Formation of a new phase explains the evolution of CO_2 at high temperatures. Prolonged exposure of the foaming mixture to the CO_2 atmosphere prior to the heat-treatment (*Fresh-CO_2-stored* foaming mixture) results in the formation of additional carbonates which hinder the expansion. Results suggest that high-temperature CO_2 evolved from newly-formed carbonates acts as the main expansion gas. Such CO_2-dominated expansion mechanism when foaming with water glass is a novelty, contradicting the commonly accepted knowledge [97], [99][1].

[1] Note that the H_2O-dominated mechanism of expansion is a commonly accepted explanation, lacking a dedicated research, and is thus not the main topic of provided references.

5.1.3 Composition of the pore gas

Formation of carbonates during the preparation of the foaming mixture and their latter decomposition during the heat-treatment results in the evolution of CO_2 which acts as the main expansion gas. If the hypothesis for this newly proposed mechanism is correct, the atmosphere within the pores should consist mostly of CO_2.

Analysis of the pore gas composition using GC confirmed the detection of significant amounts of CO_2. Additionally, foamed glass samples do not contain any traceable amounts of CO. Small amounts of O_2 and N_2 were detected. Since the foaming process is implemented in air atmosphere and the sample expansion is relatively low, air mixture (N_2/O_2) could remain trapped within the sintered body. Theoretically, based on average expansion of the samples, this would result in the pore gas containing maximum of 10-15 % of air. However, it is expected that the majority of the air atmosphere within the sample is displaced during the heating due to the evolution of CO_2 and H_2O (Figure 5.2 and Figure 5.3). Here, the most likely explanation for the presence of N_2 and O_2 is a contamination of the He-filled cell during the crushing of the samples.

Additional analysis of the He-filled cell atmosphere was done after the sample crushing, allowing the detection of H_2O (Figure 5.6). Here, a clear increase in CO_2 signal intensity can be observed at the time of the sample injection, while the signal for H_2O remains unchanged.

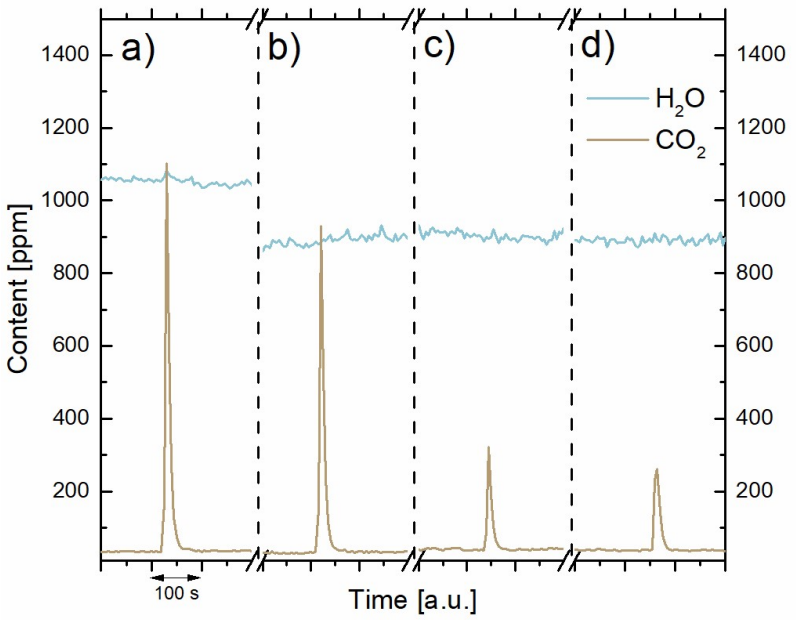

Figure 5.6: Detected signals for H_2O, CO_2, NH_3 and CH_4 gases for the sample taken from the He-filled cell after breaking the foamed glass samples prepared from *Fresh* (a and b) and *Dried* (c and d) foaming mixtures.

Analysis of the pore gas has shown an overwhelming presence of CO_2 in comparison to other theoretically relevant gases. Formation of carbonate phase occurs during the mixing of CRT panel glass powder and WG. Heating of such foaming mixture results in evolution of CO_2 at elevated temperatures and the analysis of atmosphere from the closed pores has shown that CO_2 not only escapes from the material but is also the main gas which remains trapped. This indicates that CO_2 is the main expansion gas and further confirms the proposed CO_2-dominated expansion mechanism of foaming with WG.

5.1.4 Properties of foamed glass samples

Previous results indicate that drying or storing of the foaming mixtures significantly affects their foaming behavior. Appearance of the foamed glass samples, shown in Figure 5.7, follows the previously observed trends. Foamed glass sample prepared from the *Fresh* foaming mixture can be characterized by the largest pores and size among all the samples. Consequently, *Fresh* also exhibits the largest E and lowest ρ_{app} (Table 5.3). Foamed glass sample prepared from the *Fresh-CO_2-stored* foaming mixture, also agreeing with the HSM measurement (Figure 5.1), expands the least. Exposure of the foaming mixture to the pure CO_2 atmosphere before the heat treatment results in the formation of crystalline phases which apparently hinder the sintering and expansion behavior resulting in a less porous foamed glass. Dried foaming mixtures, on the other hand, appear very similar indicating that *Dried-CO_2-stored* was not largely affected by the storage atmosphere. Interestingly, storing of the foaming mixture in air atmosphere also significantly alters its expansion behavior and the appearance of foamed glass in comparison to the fresh sample (Figure 5.7). The effect of storing, however, is more pronounced when the atmosphere is pure CO_2. The reaction between the atmosphere and foaming mixture apparently proceeds relatively quickly since there is no significant difference between the samples stored for 1 day or 1 week.

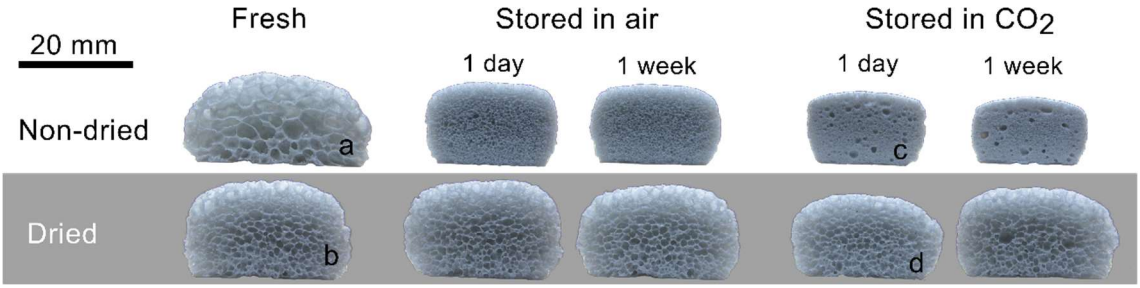

Figure 5.7: Foamed glass samples prepared from differently treated foaming mixture (labels a, b, c and d designate *Fresh*, *Dried*, *Fresh-CO_2-stored* and *Dried-CO_2-stored* samples, respectively).

Table 5.3: Expansion values (ΔV, Eq. 4.5) and ρ_{app} of the foamed glass samples. Superscripted letters designate the samples from Figure 5.7.

Label	ΔV (%)	ρ_{app} (kg m^{-3})
Fresh^a	622	257
Dried^b	337	326
Fresh-CO_2-stored^c	120	687
Dried-CO_2-stored^d	323	332

Reaction between the atmosphere and the foaming mixture affects expansion behavior of the foaming mixture, resulting in less homogeneous pore structure of the foamed glass samples, which is an important characteristic of a thermal insulation material. Manually outlined pores of the samples from Figure 5.7 and distributions are presented in Figure 5.8. It is apparent that the pore size is different if a non-dried foaming mixture is exposed to CO_2 atmosphere. Distribution of Feret diameters is similar for the *Dried* and *Dried-CO_2-stored* samples, confirming previously shown results that CO_2 atmosphere does not affect a dried WG-containing foaming mixture.

A higher partial pressure of water aids the sintering process of glass powders by decreasing the materials' characteristic temperatures [101]. A comparison between the *Fresh* and *Dried* samples suggests that this effect could also promote the coalescence of pores. The *Fresh* sample expands approximately twice as much as *Dried* which should in the case of pore expansion without the change in pore number and without coalescence theoretically lead to pores larger for a factor of $\sqrt[3]{2}$. In reality, the average pore size in the *Fresh* sample is almost twice the size of an average pore in the *Dried* sample, suggesting significant pore-merging took place during the foaming. A higher degree of coalescence typically results in a decreased number of pores and larger pores with irregular shapes [58]. On the other hand, literature sources report that during the direct foaming of glass the porosity increases up to approximately 60 % mainly due to the formation of new pores [14]. Increase of porosity at higher values becomes increasingly more dependent on the pore growth. As mentioned before, during the foaming, the solid is non-uniformly distributed between the faces and the edges of the structure. With formation of new pores and their growth, the solid is drawn into cell edges, leaving the walls increasingly thinner, eventually resulting in their rupture and merging of the pores [41]. Since the *Fresh* sample exhibits significantly higher expansion (Table 5.3) in comparison to other samples, it is expected to result in larger pores. Note that the degree of coalescence during the pore growth is dependent on several other factors, especially surface tension [61].

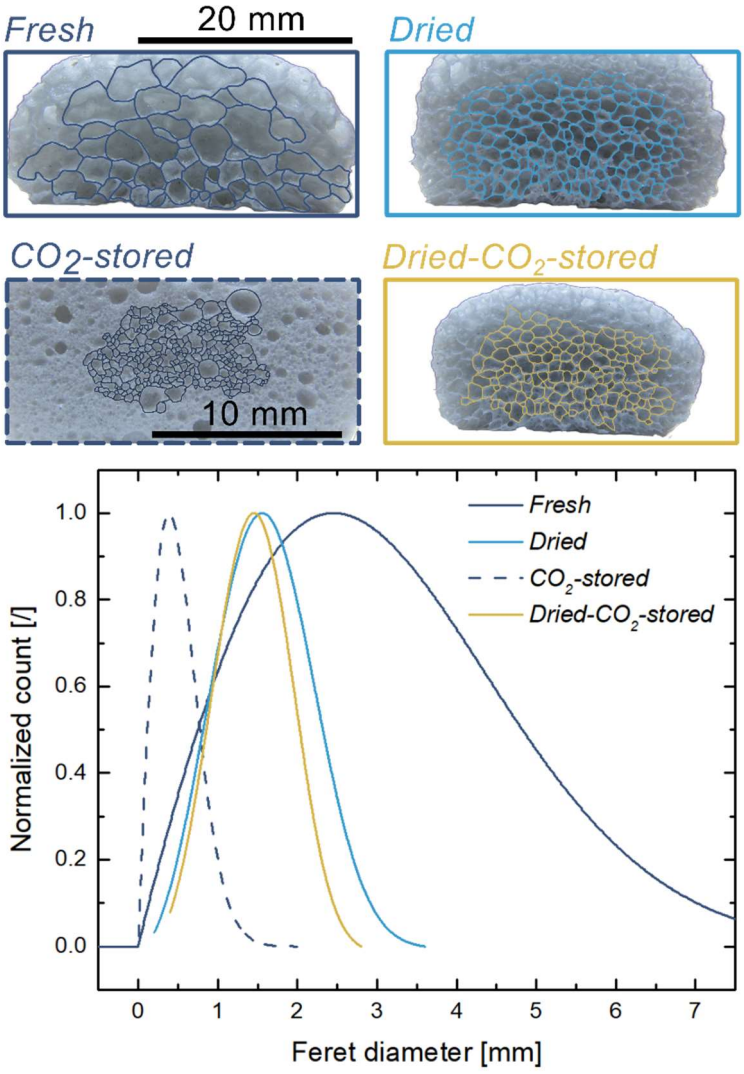

Figure 5.8: Pore size distributions and corresponding pore outlines for the analyzed foamed glass.

5.1.5 Conclusions

Foaming with the addition of WG requires special care over the atmosphere and, more importantly, the time of contact between the foaming mixture and surrounding atmosphere. Parameter of contact time is almost as important as foaming time and temperature.

Heat treatment of CRT panel glass powder and WG mixture leads to expansion and formation of a porous material. Special care over the contact time between the atmosphere and foaming mixture is required because of the reaction between the WG and carbon dioxide, resulting in the formation of crystalline carbonate phase. Newly formed phase significantly affects the expansion behavior of the foaming mixture and the predominant presence of CO_2 gas within the pores suggests decisive role of carbonates for the foam formation and expansion as shown in Figure 5.9.

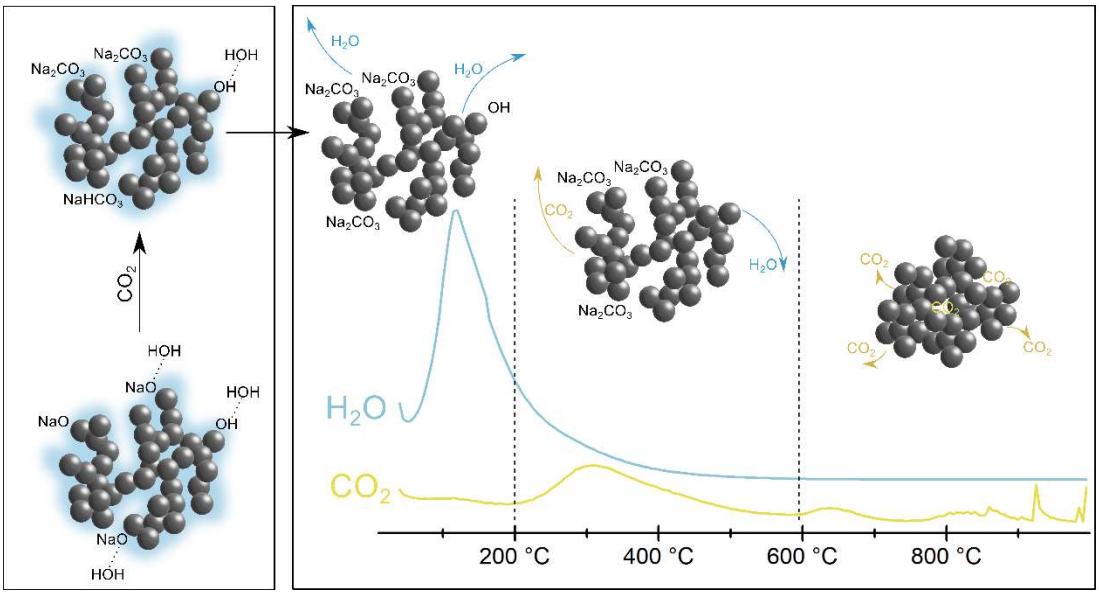

Figure 5.9: Simplified scheme on how the presence of WG on the surface of the glass particles and subsequent formation of carbonates (left) affects the foaming process (right). Heating of the foaming mixture initially results in evaporation of H_2O (< 200 °C) which can promote glass powder sintering. CO_2 starts to evolve above 200 °C, while not contributing to the expansion since the pores are still open up to approximately 600 °C. Above 600 °C, the most stable carbonates start to decompose and the gas becomes trapped within the closed pores, confirmed by the presence of sharp peaks above 800 °C.

Prolonged exposure to air atmosphere or, more pronounced, to pure carbon dioxide results in the formation of more crystalline carbonates, significantly altering the expansion behavior and characteristics of the pore structure. Drying of the mixture prevents the reaction with the atmospheric carbon dioxide, which results in foams with more consistent properties.

Results of this study contradict the generally accepted H_2O-dominated-mechanism of foaming with WG. It became apparent that foaming occurs due to the decomposition of carbonates, formation of which is primarily influenced by the exposure of the foaming mixture to carbon dioxide. With this, a new mechanism, which can significantly affect the

course of glass foaming with WG, is revealed. The influence of the atmosphere on the properties and composition of the foaming mixture is not a well explored parameter, however, it could allow additional control over the properties of foamed products in future research and/or further optimization of foaming processes which rely on the use of WG.

5.2 Direct Foaming of Hydrothermally Treated Waste Glass

5.2.1 Introduction

Direct foaming of glass can be achieved with sole addition of water glass, as shown above (*Use of Water Glass for the Foaming of Glass* on page 25) and few other literature sources [96], [99]. Furthermore, it was shown that hydrothermally treated [72] or hydrothermally hot-pressed (HHP) [76], [110]–[112] glass powders can be used in a direct foaming process to achieve foamed glass. Similarly as in the case of WG, it is commonly accepted that the foaming of hydrothermally treated glass occurs due to the water evaporation [76], [113], [114]. It is likely that the mechanism of foaming with hydrothermally treated glass is similar as in the case of WG. However, the focus here is not to further prove the previously proposed foaming mechanism but to investigate the possibility of foaming waste glasses after the hydrothermal treatment, without the use of other foaming additives.

Three waste glass compositions (FGF, MCF and CRT in Table 4.1) were treated as described under *Hydrothermal treatment of glass powder* on page 18 and will be from here on referred to as *X_H10* or *X_H30* depending on the theoretical content of water within the sample (10 or 30 wt.%, respectively), X being the label for the waste glass powder.

5.2.2 Properties of the hydrothermally treated glass powders

Hydrosilicates can be achieved by a few different routes (*Water in Glass and Hydrated Glasses* on page 8). Outcome of the processing can be incorporation of water in various configurations within the glass structure and/or formation of new (hydrous) crystalline phases. This affects the behavior of the glass powder during the heating and allows the synthesis of porous structure.

5.2.2.1 Glass powder composition

Hydrothermal treatment of the glass powders results in the formation of new crystalline phases (Figure 5.10a). It appears that crystalline phases formed in *CRT_H30* are not the same as in the case of *MCF_H30* and *FGF_H30*, which appear similar. Correspondingly, FGF and MCF waste glass powders exhibit a similar chemical composition, quite different to the one of CRT (Table 4.1). XRD signals of the *FGF_H30* and *MFC_H30* (Figure 5.10a) best coincide with the patterns for silicate alkali carbonate hydrates and zeolite (mordenite9). Formation of mordenite or other zeolite phases during the hydrothermal treatment of glass is not unusual [72], [115], [116], however, it is unusual that zeolite formation happens under saturated vapor conditions without additional precursors since raw glass does not contain significant amounts of Al_2O_3 (Table 4.1). XRD signal of the *CRT_H30* (Figure 5.10a) best coincides with Sr- and Ba-based (bi)carbonates and K- and Na-based silicates. Hydrothermal treatment to theoretical content of 10 wt.% of H_2O, on the other hand, does not result in the formation of significant amounts of crystalline phase (Figure 5.10b).

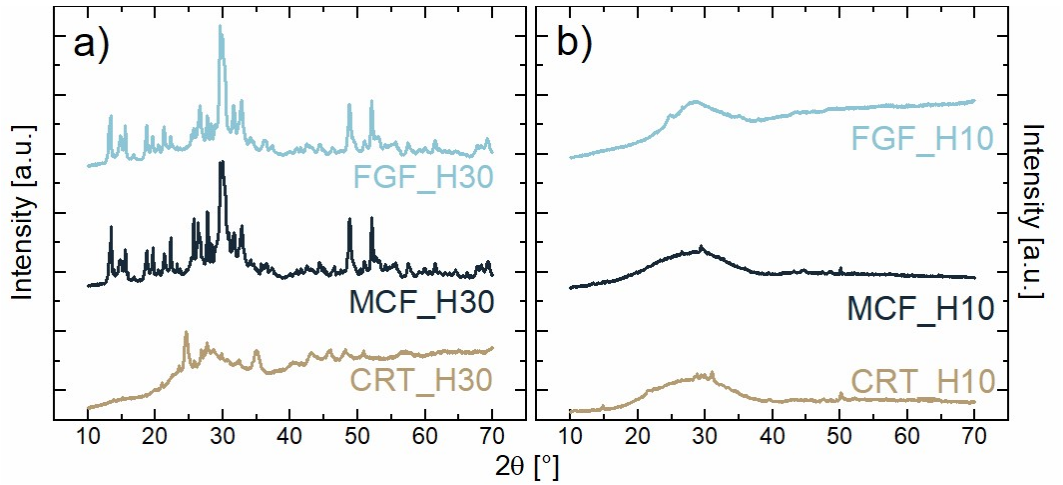

Figure 5.10: X-ray diffraction data for the hydrothermally treated glass powders with theoretical content of (a) 30 wt. % H_2O and (b) 10 wt. % H_2O.

After the heat treatment, the newly formed crystalline phases decompose or transform into amorphous material (Figure 5.10b). Newly formed crystalline phases from the X_H30 samples readily transform with temperature, since the majority of the crystalline peaks disappear from the sample with heat treatment at 800 °C (Figure 5.11a). Natural mordenite decomposes to anorthite, SiO_2, and eventually transforms to an amorphous phase above 1000 °C [117], however, in the specific case, the decomposition/transformation reactions are very likely altered due to the overwhelming presence of glass phase.

Content of crystalline phases after the heat treatment at 800 °C (Figure 5.11a) is negligible in contrast to few other literature sources, where waste glass of similar composition was treated in a similar manner [112], [118]. Note that in the case of this research, the t_{foam}, or the heat-treatment time, is fairly short and could be the reason for the lack of crystallization. On the other hand, heating to 900 °C leads to the formation of crystalline phases in FGF and MCF compositions (Figure 5.11b). CRT glass remains amorphous at 900 °C suggesting a better resistance to devitrification, i.e. glass stability, in comparison to FGF and MCF.

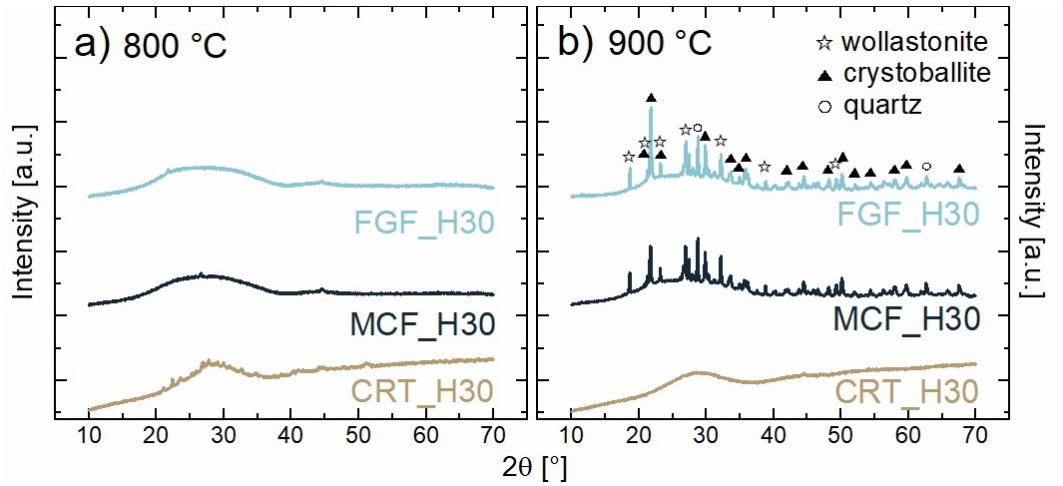

Figure 5.11: X-ray diffraction data for the hydrothermally treated glass powders with theoretical content of 30 wt. % H_2O after the heat treatment at (a) 800 °C and (b) 900 °C.

Hydrothermal treatment of the glass powders results in the formation of hydrous crystalline phases, and their presence was further confirmed with FTIR analysis (Figure 5.12). Characteristic peaks for molecular water (1640 cm^{-1}) and OH^- groups (wider bands at 3600 and 2600 cm^{-1}) can be observed in Figure 5.12a. This further proves that during the hydrothermal treatment, the water became incorporated within the structure, interacting with the glass network. Additionally, the peaks at approximately 1450 cm^{-1} indicate the presence of CO_3^{2-} groups (Figure 5.12a). All the mentioned signals disappear after the heat treatment at 800 °C (Figure 5.12b).

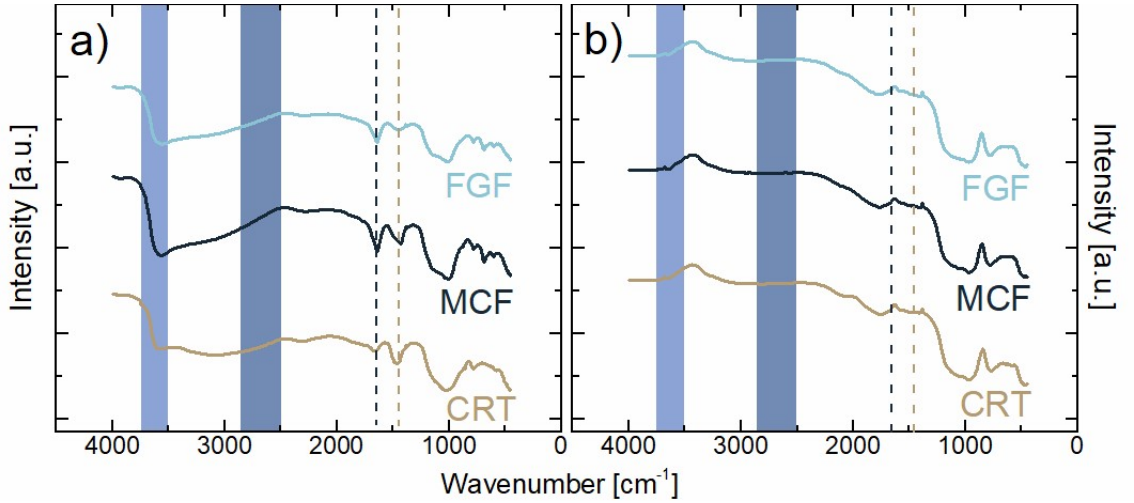

Figure 5.12: FTIR signals for the hydrothermally treated (theoretically 30 wt.% H_2O) glass powders (a) before and (b) after the heat treatment at 800 °C. Blue and dark blue bands (3600 and 2600 cm^{-1}, respectively) denote Si(OH) stretching and bending, respectively. The dashed lines at approximately 1640 and 1450 cm^{-1} designate signal for water and carbonates, respectively. Note that the lines are shifted for better clarity.

Water becomes incorporated within the glass material after the hydrothermal treatment in at least two different configurations (molecular and silanol groups). Additionally, CO_3^{2-} groups were detected, similarly as in the case of glass mixed with WG.

5.2.2.2 Expansion behavior of the hydrated glass powders

Hydrothermal treatment significantly affects the expansion behavior of CRT, MCF and FGF glass powders. Initially, the glass powders behave as expected, mainly exhibiting shrinkage during the heat treatment, which changes dramatically after the heat treatment (Figure 5.13). Characteristic temperatures from Figure 5.13 are shown in Table 5.4.

Among the raw glass powders, CRT exhibits the lowest onset temperature of sintering (T_{sint}) which is likely the reason why also *CRT_H10* and *CRT_H30* exhibit lower foaming temperatures (T_{foam}) in comparison to corresponding *MCF* and *FGF* samples (Figure 5.13a versus b and c, respectively). Additionally, *CRT_H10* and *CRT_H30* achieve higher maximum expansion values when compared to corresponding *MCF* and *FGF* samples. Expansion stage of *MCF_H10* and *FGF_H10* start at a similar temperature whereas the expansion of *FGF_H10* is smaller in comparison to *MCF_H10*. Higher content of water has an apparent effect on the behavior of all glass powders during the heat treatment since the samples which theoretically contain 30 wt.% of H_2O generally exhibit smaller shrinkage and larger expansion (Figure 5.13 and Table 5.4).

The degree to which the hydrothermal treatment affects the behavior of glass powders during heating differs between the powders. Increase of expansion is most pronounced for

the CRT glass powder, while it is comparable for the MCF and FGF. Here, the lack of crystallization in CRT glass (Figure 5.10 and Figure 5.11) could be one of the main reasons for the difference in maximum achievable expansion. Decrease of characteristic temperatures with higher content of water is in accordance with the effect of structurally bound water and increased partial pressure of water on the viscosity and sintering behavior of glass powders [30], [87], [101].

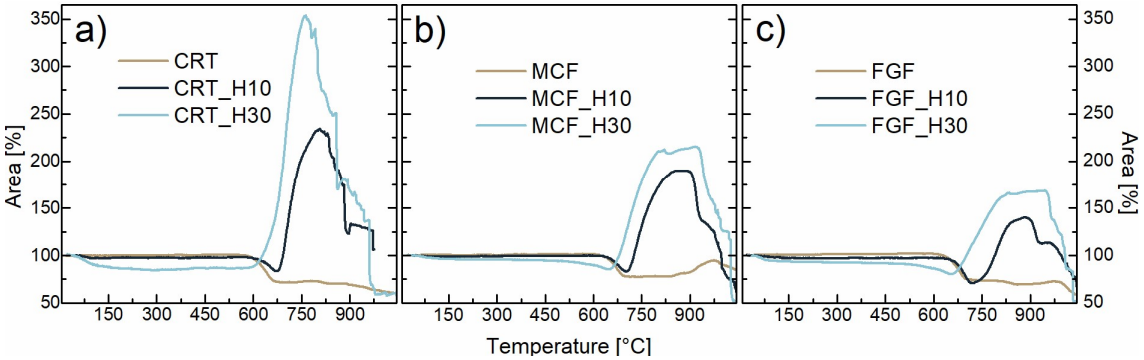

Figure 5.13: Sintering and expansion behavior of raw and hydrothermally treated (a) CRT, (b) MCF and (c) FGF glass powders.

Table 5.4: T_{sint}, T_{foam}, T_{collapse} and maximum area achieved (A_{max}) during the heating of the glass powders.

		T_{sint} [°C]	T_{foam} [°C]	T_{collapse} [°C]	A_{max}
CRT	Raw	600	/	/	100
	H10	616	675	836	235
	H30	/	595	795	355
MCF	Raw	639	/	/	100
	H10	646	705	905	140
	H30	/	655	935	168
FGF	Raw	642	/	/	100
	H10	662	725	905	190
	H30	/	660	955	215

5.2.2.3 Gas evolution from the hydrothermally treated glass powders

All hydrothermally treated glass powders exhibit a pronounced mass loss due to the evaporation of water while the evolution of CO_2 can be observed at higher temperatures.

During the first stage of the heat-treatment (below the T_{sint}), the mass loss curve of all the samples is accompanied by a strong signal for H_2O (Figure 5.14 and Figure 5.15). *CRT_H10*, *FGF_H10* and *MCF_H10* samples (theoretically containing 10 wt.% of H_2O) exhibit mass losses of 9.3, 7.9 and 6.6 wt.%, respectively (Figure 5.14). Discrepancy between the actual and theoretical water content is related to H_2O evaporation from the material prior to the analysis and is even more apparent for the *X_H30* samples where *CRT_H30*, *FGF_H30* and *MCF_H30* exhibit mass losses of 16.1, 16.5 and 15.9 wt.%, respectively (Figure 5.15). H_2O signal can be observed up to relatively high temperatures for all the glass samples (≈600 °C), resembling the TG/MS curves of the glass-water glass

mixtures (*Thermal analysis and evolution of gases* on page *28*). *MCF_H30* and *FGF_H30* exhibit less-continuous water loss in comparison to other samples which could be related to the formation of a new water-containing crystalline phase (Figure 5.10).

During the second stage of the heat-treatment (in the proximity of T_{sint} and below the T_{foam}), the signal for H_2O starts to decrease and the signal for CO_2 starts to appear for some of the samples. The rate of mass loss is lower in comparison to the first stage of the heat-treatment and slightly increases synchronously with the CO_2 signal. Detection of CO_2 at relatively high temperatures (≈600 °C) suggests the presence of carbonates, agreeing with the FTIR results (Figure 5.12). According to the appearance of the CO_2 signal and increased mass loss rate, decomposition of the carbonates for the *CRT_H10* and *CRT_H30* starts at approximately 550 °C, while for the others, the decomposition starts at higher temperature (Figure 5.14 and Figure 5.15). Higher temperature of carbonate decomposition for the MCF and FGF samples can be related to specifics of formed carbonate phases, chemical composition of glass phase [119] and/or to their sintering behavior (contact with the surrounding material).

In the last stage of the heat-treatment (above T_{foam}), no H_2O is released from the collapsing foam, while sharp CO_2 signals can be detected. A similar outcome as during the heat-treatment of the WG-containing mixtures (Figure 5.2).

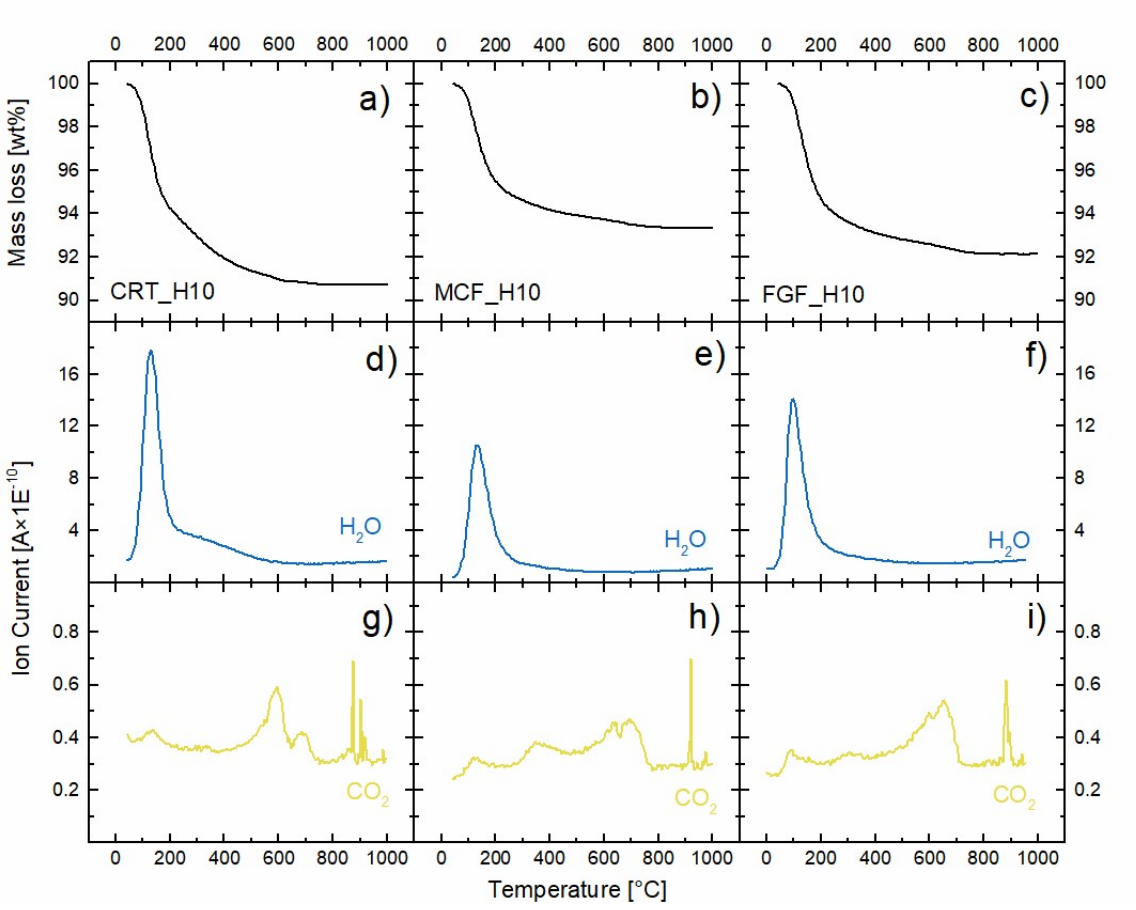

Figure 5.14: Mass loss (a, b and c), H_2O (d, e and f) and CO_2 (g, h and i) gas signals for the CRT_H10 (a, d and g), MCF_H10 (b, e and h) and FGF_H10 (c, f and i) powders during the heat treatment.

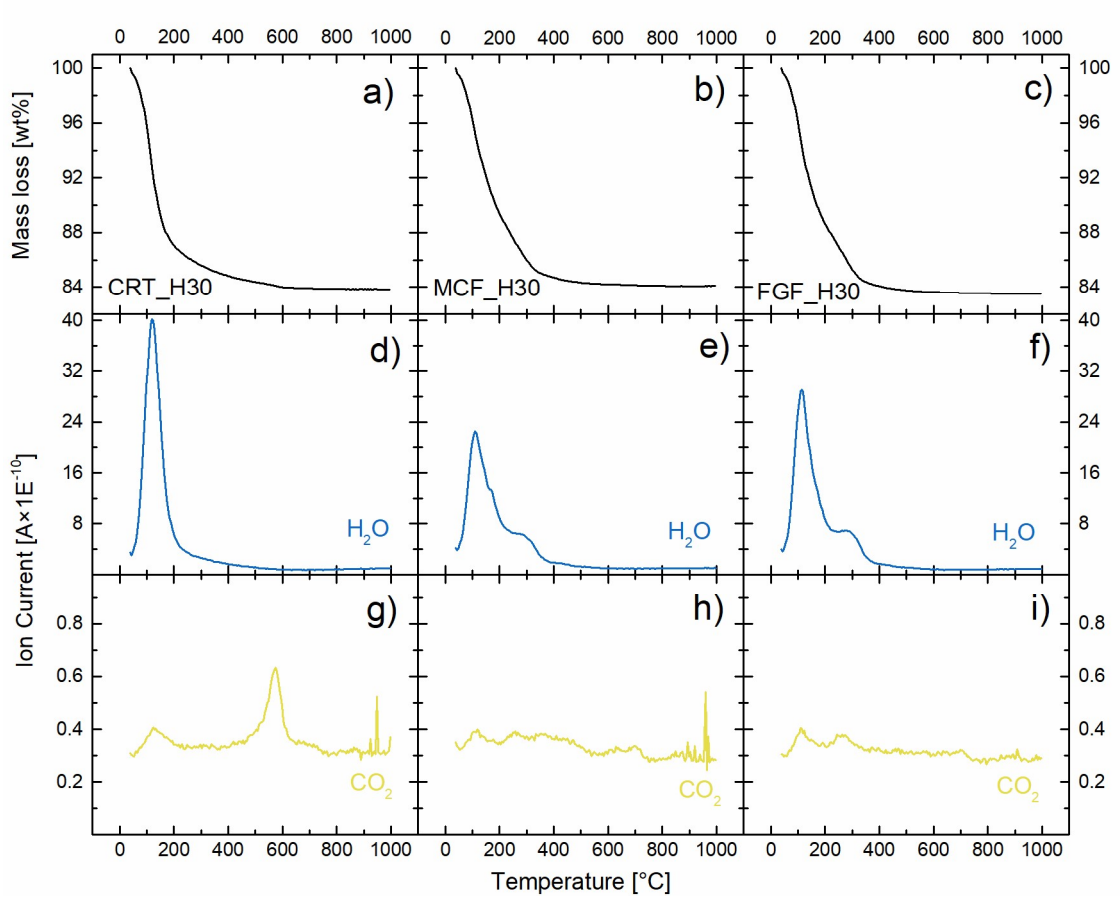

Figure 5.15: Mass loss (a, b and c), H_2O (d, e and f) and CO_2 (g, h and i) gas signals for the CRT_H30 (a, d and g), MCF_H30 (b, e and h) and FGF_H30 (c, f and i) powders during the heat treatment.

A further look into the evolution of CO_2 can improve the understanding of the expansion behavior of the hydrothermally treated glass powders (Figure 5.16). *CRT_H10* exhibits two wide peaks for CO_2 gas signal in 500 – 800 °C range, while for the *CRT_H30*, only the lower-temperature peak can be observed. This can be attributed to the effect of higher H_2O content on the shift of the sintering stage to lower temperatures, suggesting that the CO_2, which evolves at higher temperature, becomes trapped within the sintered material. The same reasoning, regarding the shift of the sintering stage to the lower temperatures, can be applied to explain the absence of CO_2 peaks in the 500–800 °C range for the *FGF_H30* and *MCF_H30* compositions. While the CO_2 peaks are present in the shaded area for *FGF_H10* and *MCF_H10*, they disappear for *FGF_H30* and *MFC_H30* (Figure 5.16).

Collapse of the foams begins above the marked shaded area in Figure 5.16 and is further confirmed by the sharp CO_2 peaks. Note that the sharp CO_2 peaks do not appear for the *FGF_H30* sample which could be due to its good stability at high temperatures, meaning that a higher temperature (not appropriate for used device) would be needed for the collapse of the foam and appearance of the peaks.

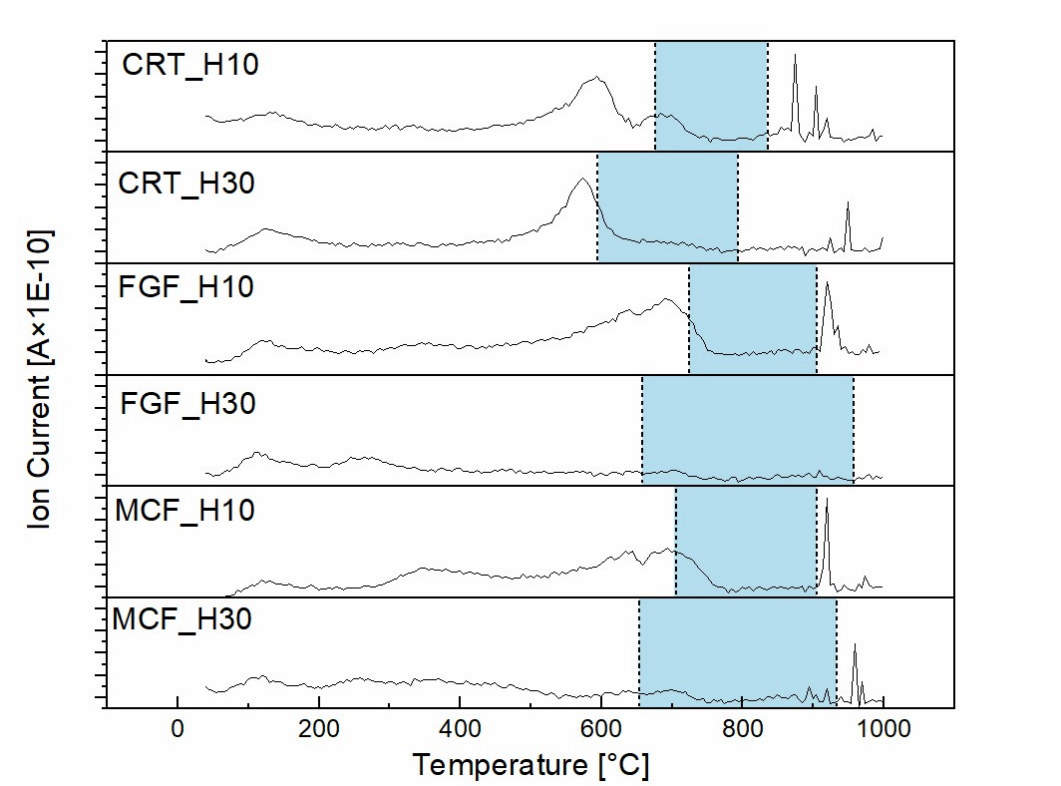

Figure 5.16: Magnified data for the CO_2 gas signal (Figure 5.14 and Figure 5.15). Shaded area labels the temperatures between T_{sint} and T_{collapse} from Table 5.4.

5.2.3 Expansion of hydrothermally treated glass

HSM analysis has shown that hydrosilicates obtained after the hydrothermal treatment of FGF, MCF and CRT glass can be expanded at elevated temperatures. Here, a maximum obtainable expansion for a 1 g sample prepared from hydrothermally treated glass is evaluated. Heating of 1 g samples follows similar trends as observed in Figure 5.13. Each hydrosilicate powder was heated to a specific temperature, its ρ_{app} was measured, results were recalculated to ΔV, and are presented in Figure 5.17. Samples prepared from the hydrothermally treated FGF and MCF powders expand for a similar amount while the one prepared from CRT expands more. Expansion value for FGF and MCF samples is still increasing at 900 °C whereas the CRT samples already start to collapse.

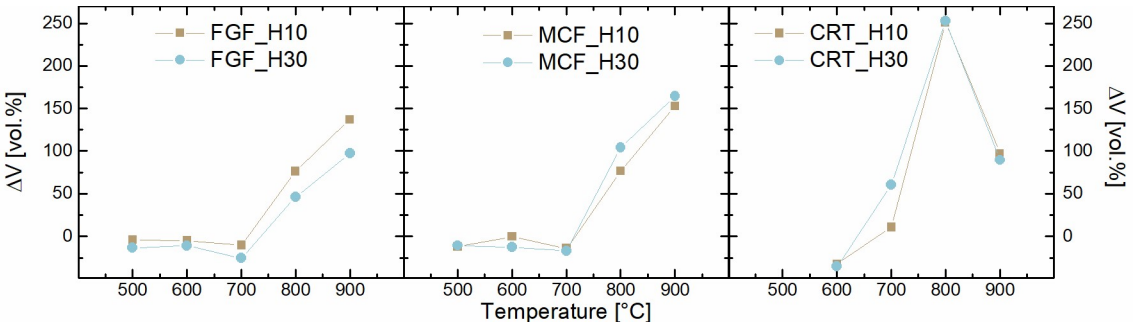

Figure 5.17: ΔV of 1g samples prepared from hydrothermally treated glass powders as a function of T_{foam}.

Cross-sections of the samples are shown in Figure 5.18. The color of the glass powders remains the same after the hydrothermal treatment and does not change during the

foaming as well. The size of the samples does not change significantly with different total H_2O content, while the pore structure is apparently affected. Foaming mixtures with higher water content appear to have larger pores as well as wider pore size distribution.

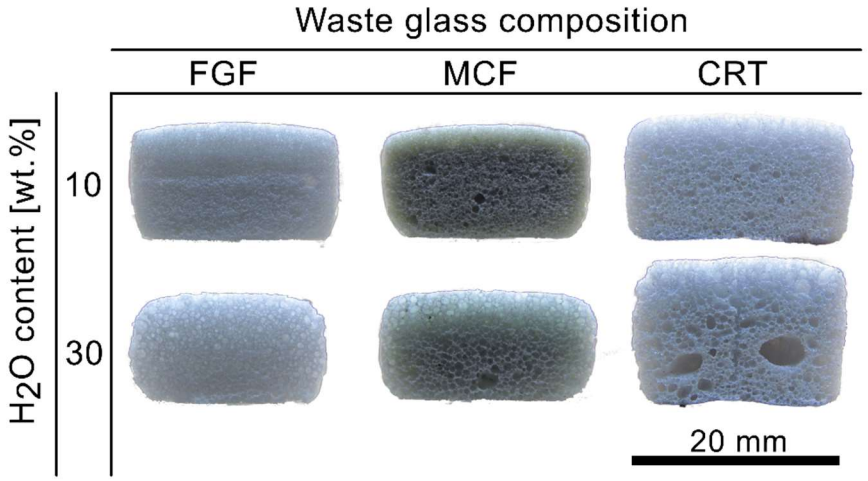

Figure 5.18: Images of the cross-sections of the foamed glass samples prepared from hydrothermally treated waste glass, foamed at the temperature of maximum expansion (900 °C for FGF and MCF, and 800 °C for CRT glass).

5.2.4 Conclusions

Hydrothermal treatment with saturated vapor transforms waste glass powders into hydrosilicates, which exhibit significantly different sintering and expansion properties in comparison to raw powders. Similarly, as in the case of WG, carbonates are detected in the structure as well as CO_2 is observed during the heating of the powders. Powders with higher content of H_2O exhibit significantly lower T_{foam} which indicates larger amounts of trapped gas within the material. Interestingly, larger amount of trapped gas did not result in larger expansion of foam samples. Maximum obtainable expansion occurred in the case of CRT glass powder.

5.3 Implementation of Carbonaceous Foaming Agent in Air Atmosphere

5.3.1 Introduction

Foamed glass exhibits potential for improvement in several aspects. Even though foamed glass possesses useful properties besides the low thermal conductivity, its usage is less common, mostly due to high production costs and consequentially higher price. High production costs are usually related to the need for adjusting the chemical composition of glass by re-melting, use of special foaming atmosphere and high processing temperatures [120]. Use of cheaper waste materials to produce more sustainable foamed glass in a direct foaming process is possible, however, the performance of such products is currently much lower [121] (Figure 5.19). Use of re-melting step [55] and special foaming atmosphere can apparently be avoided in the direct foaming process while the high foaming temperatures can only be decreased to some extent. Preparation of high-quality foamed glass using a process with a lower energy-demand would therefore decrease the production costs, improve the products' market competitiveness [122], and provide environmental benefits in terms of decreased energy consumption, CO_2 emissions, and embodied energy.

Direct foaming with a carbon and oxidizing agent couple in an oxygen-free atmosphere results in a low-density foamed glass with small and closed pores [50], [55]. Such characteristics lead to good insulative and mechanical properties. The use of oxygen-free atmosphere, which is industrially typically achieved by sub stoichiometric fuel combustion, greatly decreases the energy-efficiency of the process and increases the requirements for the furnace durability. To improve the sustainability and lower the costs of the foamed glass production, it is sensible for the process to be carried out under less demanding conditions, i.e. in air atmosphere. Furthermore, processing in air atmosphere allows the use of electric furnace which leads to additional environmental benefits, considering that the electric energy, in contrast to natural gas, can be obtained from a renewable source.

Glass foaming with carbon-based additives in air atmosphere, however, is challenging due to the reaction between the carbon and oxygen from air. Few investigations have shown that foaming with carbon can be implemented in air with the addition of WG [97], [123]. Use of WG increases the resource use of such a product, however, a recent LCA analysis has shown that a material with properties similar to the ones reported in [55] prepared in electric furnace (air atmosphere) would outperform not only commercial foamed glasses but also other conventional insulation materials with respect to environmental impacts per kg and thermal resistivity [124].

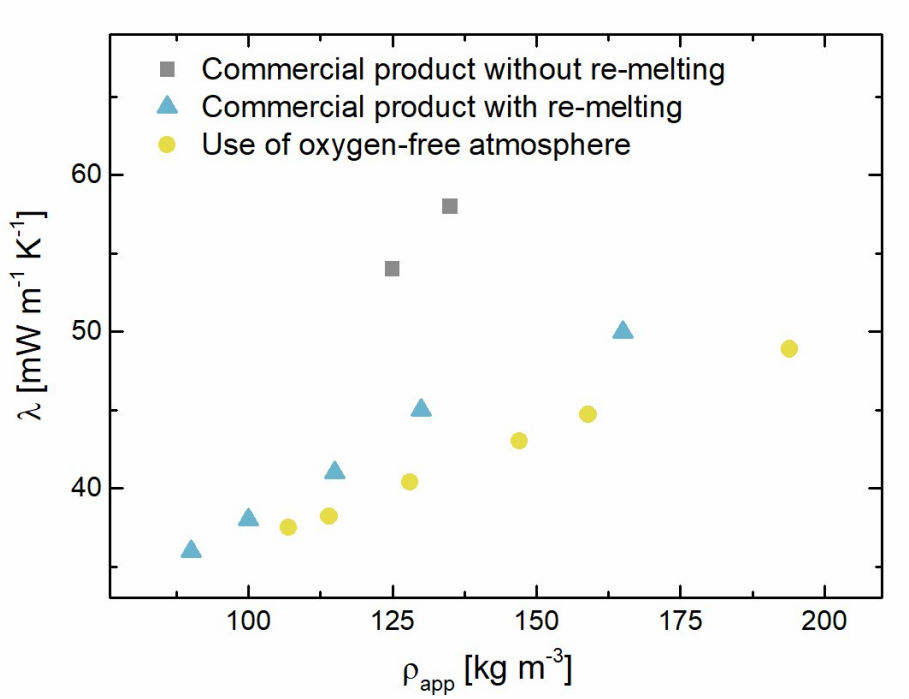

Figure 5.19: Thermal conductivity versus apparent density of the commercial products prepared with [120] and without re-melting [121], and laboratory samples prepared in an oxygen-free atmosphere [55].

Removing the need of oxygen-free atmosphere could result in a significant improvement of the process sustainability. Careful investigation of the peculiarities of the foaming with water glass or with the use of hydrous silicates suggests that they can be used to implement carbon-based direct foaming processes in the air atmosphere. Here, hydrous silicates are utilized to achieve this and obtain foamed glass with higher porosity and improved thermal insulation properties.

5.3.2 Direct foaming in the air atmosphere with the use of hydrothermally treated glass

Hydrothermally treated glass powders of FGF, MCF and CRT can be foamed in air atmosphere. However, the highest obtainable porosity of such foams is limited. Higher total content of H_2O within the powder did not result in lower density foam. Hydrated powders, prepared with saturated vapor hydration thus do not allow synthesis of foams with porosity higher than 90 vol.%. Hydrothermally treated CRT glass exhibits the most promising expansion among the tested glass compositions and was used in further experiments for that reason. Here, the applicability of hydrothermally treated glass for direct foaming in air atmosphere with the use of carbonaceous foaming agent was tested.

Hydrothermally treated CRT (theoretically containing 30 wt.% H_2O) was dried at 100 °C and milled according to the procedure described under *Raw materials and milling* on page 17. Foaming mixtures labelled *CRT_H30_0* and *CRT_H30_Mn+C* correspond to the compositions described in Table 4.2. During the heating, both foaming mixtures start to expand at approximately 650 °C and reach the maximum at approximately 800 °C (Figure 5.20, left). It is expected that these temperatures as well as area values differ from the ones observed on unaltered hydrothermally treated powders (Figure 5.13). Foaming mixture with added foaming agent achieves a slightly higher maximum area (Figure 5.20, left), indicating a positive effect of the additive on the expansion.

Larger samples were prepared from the *CRT_H30_0* and *CRT_H30_Mn+C* foaming mixtures at the temperature of maximum achieved area (800 °C). Again, the use of foaming additive had an observable effect on the expansion of the foams (ε_{tot} of 85 and 91 vol.% for *CRT_H30_0* and *CRT_H30_Mn+C*, respectively) and their structure (Figure 5.20, right).

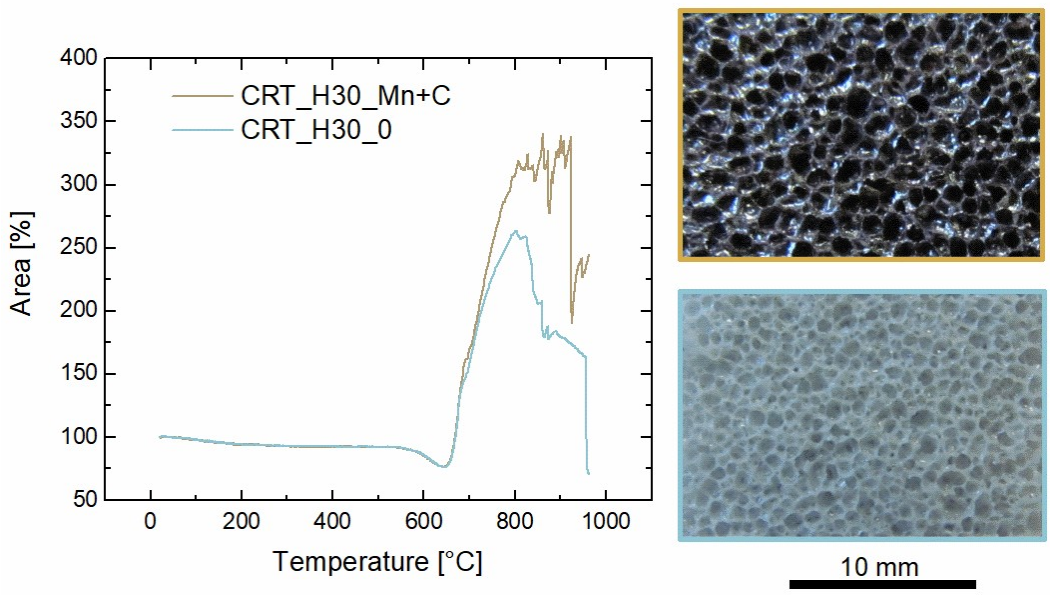

Figure 5.20: Left: sintering and expansion behavior of the hydrothermally treated glass powder with and without the carbonaceous foaming agent. Right: appearance of the corresponding foams after foaming at 800 °C.

Use of carbonaceous foaming agents for glass foaming in air atmosphere is challenging due to the premature reaction between the carbon and oxygen from air. During the heating, hydrothermally treated glass expands in air atmosphere by itself. However, with the use of carbonaceous foaming agent, the expansion is more pronounced and a foam with higher

porosity can be achieved. The result suggests that the premature burning of carbon is inhibited with the use of hydrothermally treated glass. This shows the potential for the use of hydrosilicates for the implementation of the direct foaming process with carbonaceous foaming agents in air atmosphere.

5.3.3 Direct foaming in the air atmosphere with the use of water glass

Effectivity of WG on the expansion in air atmosphere was evaluated by foaming four different foaming mixtures (Table 4.2) with a varied content of WG. If not dried, the properties of WG-containing foaming mixtures change with time (shown and discussed under *Use of Water Glass for the Foaming of Glass* on page 25). Consequently, from here on, the heat-treatment of the foaming mixtures was performed immediately after their preparation if not stated otherwise. Foaming was performed under standard conditions described under *Foaming* on page 19.

5.3.3.1 Gas evolution during the heating

The addition of WG affects the physical properties of the foaming mixture as well as the chemical reactions, which are the driving force for the expansion. It is therefore sensible to inspect the effects of WG addition on weight loss, evolved gases, crystallization and sintering/expansion behavior. Heating of the Mn+C foaming mixture (Table 4.2) in synthetic air atmosphere results in a small mass loss below 350 °C, accompanied by weak signals for H_2O and CO_2 gases (0 wt.% WG in Figure 5.21a). This result is in accordance with [125] where it is stated that CO_2 and H_2O are desorbing from the CRT glass particles during the heating. Initial mass loss and H_2O signal intensity increase significantly if the composition contains WG (curves for 12 and 24 wt.% in Figure 5.21a).

Second mass loss between 350 and 550 °C is detected simultaneously with a broad CO_2 signal and can be attributed to the undesired reaction of carbon with oxygen from the surrounding atmosphere (Figure 5.21a). It can be detected for all three foaming mixtures; however, the mass loss decreases gradually with increasing content of WG (0.68, 0.56 and 0.40 wt.% for the mixture with 0, 12 and 24 wt.% of WG, respectively). Addition of WG thus results in a smaller loss of carbon.

Further heating reveals an additional small mass loss between 600 and 840 °C, which can be seen only for the foaming mixtures that contain WG. The mass loss increases with an increasing content of WG (0.04, 0.12 and 0.31 wt.% for the foaming mixtures with added 0, 12 and 24 wt.% of WG, respectively) and is related to additional formation of CO_2. Newly formed CO_2 is confirmed by the presence of additional CO_2 signals above 600 °C. The shape of CO_2 signals is typical for a sudden release of gas, which occurs due to the opening of the pores when pore walls fracture. As already shown (5.1), carbonates formed during the preparation of the foaming mixture contribute to the evolution of CO_2 when foaming with water glass. Mass loss between 600 and 840 °C and CO_2 signals above 600 °C could therefore be related either to carbonate decomposition, reaction between carbon and Mn_3O_4, or both.

The high-temperature mass loss (> 840 °C), most noticeable for the foaming mixture with 0 wt.% of WG, can be attributed to the reduction of Mn_3O_4 to MnO, which results in the release of O_2. In the present investigation, O_2 signal could not be detected due to the background of a synthetic air atmosphere. A decreasing trend in the amount of mass loss above 840 °C can be observed, with increasing content of WG. This could mean that the addition of WG protects part of the carbon which later reacts with Mn_3O_4, resulting in a mass loss between 600 and 840 °C, and decreased mass loss above 840 °C.

The TG/MS results of the other three foaming mixtures (Figure 5.21b) with added 12 wt.% of WG also show an initial mass loss (< 350 °C) accompanied by the H_2O signal.

Mass loss between 350 and 550 °C and at high temperature (> 840 °C) remains the point of interest in this case as well. Foaming mixtures 0 and Mn, i.e. ones which do not contain carbon, do not exhibit significant mass loss between 350 and 550 °C which further confirms the mass loss and accompanying CO_2 signal are related to the undesired burning of carbon. Furthermore, carbon-free foaming mixtures exhibit significantly less intense high temperature CO_2 signals (Figure 5.21b). Foaming mixtures which contain Mn_3O_4, i.e. Mn and Mn+C, exhibit a mass loss above 840 °C attributed to the reduction of Mn_3O_4.

Here, three effects were observed which indicate that the presence of WG hinders the premature oxidation of carbon, namely:

- decreased mass loss at 350-550 °C related to CO_2 release,
- increased mass loss at 600-840 °C related to the reaction between carbon and Mn_3O_4, and
- sharp CO_2 signals above 840 °C.

This shows that the heat treatment of the mixture with added WG in the air atmosphere leads to similar reactions as in an inert atmosphere. Such result is desirable and beneficial for the foaming process since carbon is a crucial component required for the expansion and formation of low-density foamed glass.

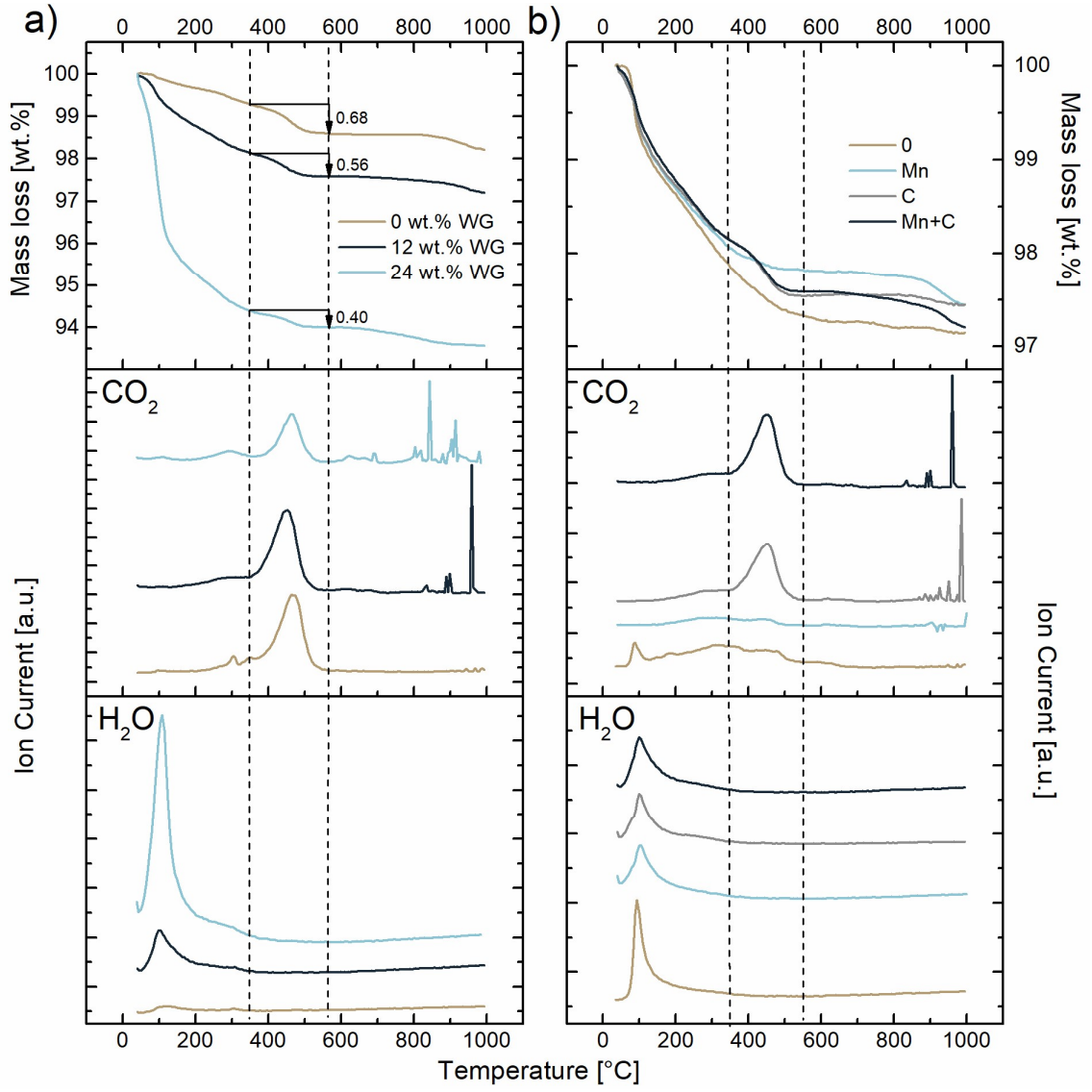

Figure 5.21: Mass loss (top), CO_2 (middle) and H_2O (bottom) signals of (a) Mn+C foaming mixture with varied content of added WG and (b) foaming mixtures with varied additives and constant content of WG (12 wt.%).

Burning of the carbon from the Mn+C foaming mixture occurs most intensively between 350 °C and 600°C, also indicated by intense CO_2 signal. Addition of WG to the foaming mixture decreases the mass loss in this temperature range, suggesting that the burning of carbon is partially inhibited. Foaming mixtures with a different content of added WG were compared for their mass loss between 350 and 600 °C (Figure 5.23). Note that the addition of WG to the composition decreases initial relative content of carbon within the foaming mixture. This is why additional dotted lines are plotted in Figure 5.23, showing a re-calculated mass loss for the 0 wt.% sample where it initially contains less carbon (initial carbon content of 12 and 24 wt.% WG samples).

The re-calculated dotted lines still show a larger mass loss, indicating that the decreased mass loss of original curves is not related solely to the smaller initial carbon content but can also be attributed to hindered burning of carbon. More precise conclusions cannot be made since the mass loss in this temperature range overlaps with the mass loss of pure CRT panel glass [125]. Despite this, a decrease of the mass loss between 350 and 550 °C is

the first indication that the addition of WG partially inhibits the reaction between the carbon and atmospheric oxygen.

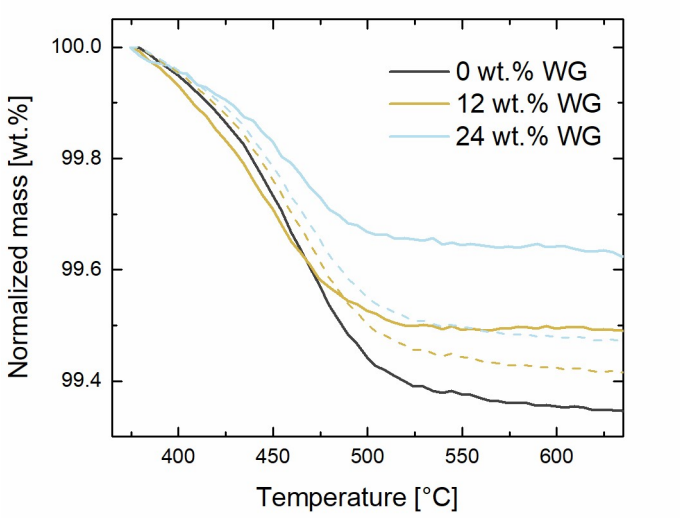

Figure 5.22: Full lines present the mass loss of the Mn+C foaming mixture normalized on the sample mass at the onset of CO_2 evolution (375 °C). Dotted lines are re-calculated values for the 0 wt.% curve with a proportionally smaller initial carbon content based on foaming mixtures with 12 and 24 wt.% WG.

5.3.3.2 Sintering and expansion behavior

The sintering behavior of the Mn+C foaming mixture with different additions of WG is presented in Figure 5.23. No change in silhouette area can be observed below 500 °C. Above 500 °C, a decrease in silhouette area indicates the start of the sintering stage. With a further increase of the temperature, the silhouette area decreases until it reaches a minimum, marked as the sintering temperature (T_{sint}). Minimum achieved area (ΔA) and the T_{sint} increase and decrease with an increasing content of WG, respectively. Without the addition of WG, $T_{sint,1}$ and ΔA_1 appear at approximately 725 °C and 84 %, respectively. Adding 12 or 24 wt.% of WG decreases T_{sint} for approximately 115 ($T_{sint,2} \approx 610$ °C) or 175 °C ($T_{sint,3} \approx 550$ °C), respectively. ΔA simultaneously increases for 10 ($\Delta A_2 \approx 90$ %) and 15 % ($\Delta A_3 \approx 95$ %). Such effect of WG addition on the sintering behavior can be explained by the presence of water bound in the structure of WG. The presence of water in the glass structure and increased partial pressure of water both decrease the viscosity of glass, and, consequently, facilitate the sintering process [87], [101].

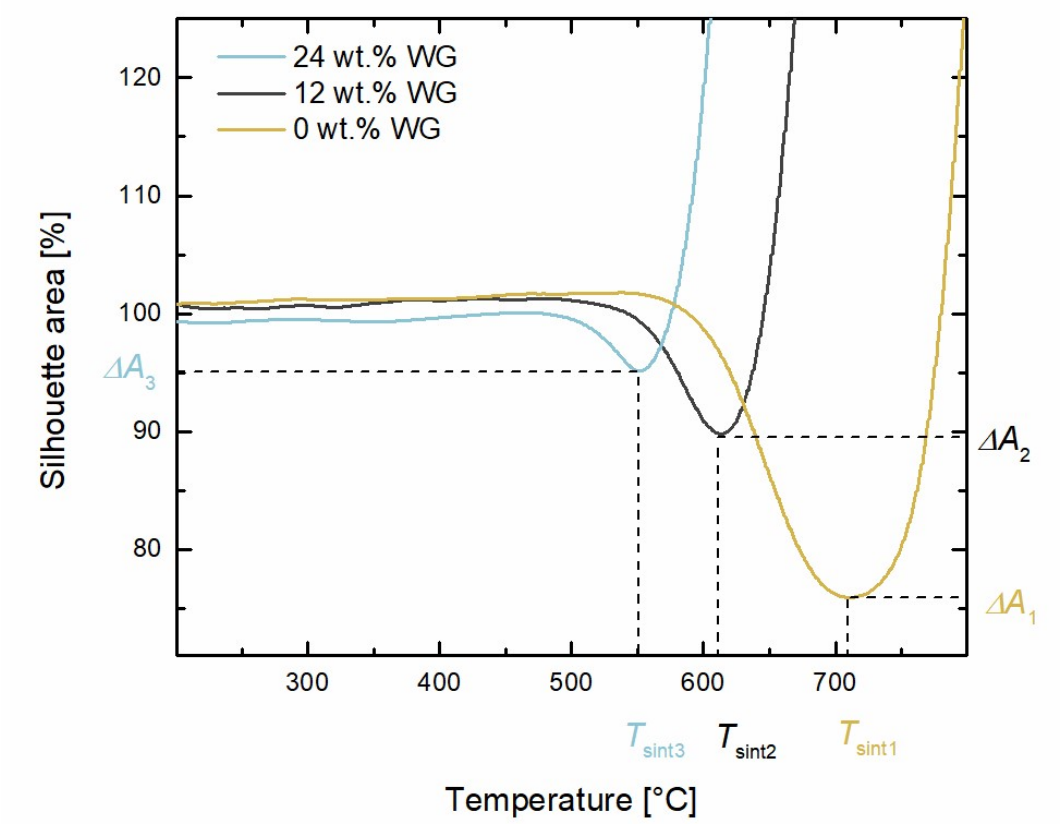

Figure 5.23: Sintering behavior of the Mn+C foaming mixture containing 0, 12 and 24 wt.% of WG.

Expansion behavior of the foaming mixtures containing different combinations of foaming agents is presented in Figure 5.24. The heat-treatment in Figure 5.24 was performed only up to the temperature of foam collapse (800 °C) to examine the shrinkage behavior after the heat-treatment. Temperature of foam collapse was determined from the expansion behavior of the CRT foaming mixtures in Figure 5.1.

Silhouette area of the Mn+C foaming mixture starts increasing rapidly when the temperature passes $T_{\mathrm{sint},2}$ (≈610 °C), determined from Figure 5.23. Silhouette area of the Mn+C foaming mixture reaches the maximum value of approximately 550 % at 790 °C and final value of 480 %. If the shape of the sample does not deviate significantly during the expansion, the final silhouette area of 480 % would theoretically result in volumetric expansion of 1000 % or a ten-fold increase of the initial volume.

The other three foaming mixtures (*Mn*, *C* and *0*) start expanding at a slightly higher temperature (≈650 °C) with a very similar rate. Their maximum and final silhouette areas are significantly lower in comparison to Mn+C foaming mixture. Additionally, maximum and final silhouette area of the Mn, C and 0 foaming mixtures are in the range between 230-300 %. Comparable values for the three different foaming mixtures suggest a common source contributing to the expansion of the material, i.e. water glass.

Results show a similar expansion behavior of the Mn, C and 0 foaming mixtures and suggest an additional gas-releasing reaction contributing to the expansion of the Mn+C foaming mixture. This contribution is the key for achieving a product with a low density, which is one of the most important parameters among the requirements for good thermal insulation properties of foamed glass [58], [126]. Additionally, these results already suggest that the use of WG can allow the implementation of direct foaming with a carbonaceous foaming agent in air atmosphere.

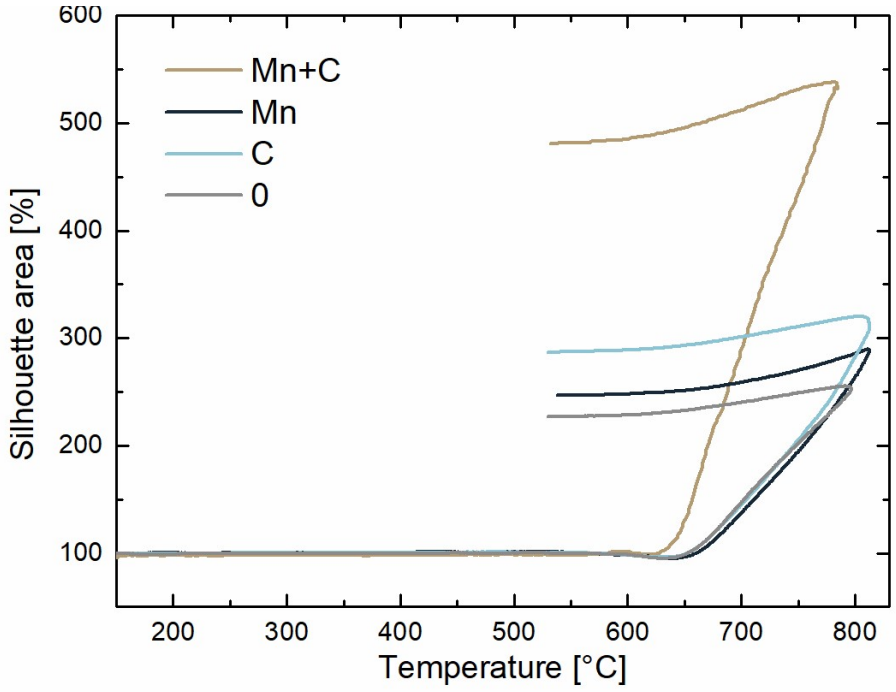

Figure 5.24: Expansion behavior of the *Mn+C*, *Mn*, *C* and *0* foaming mixtures with added 12 wt.% of WG.

TG/MS and HSM analysis revealed that the addition of WG protects the carbon and enables considerable expansion of the foamed glass in the air atmosphere. At least two mechanisms could explain how WG protects the carbon during the direct foaming in air atmosphere. The first mechanism is related to increased local presence of H_2O vapors, which gradually evaporates during the heat-treatment and can be detected even above 400 °C. H_2O release during the heating dilutes and displaces the air which is initially present between the glass particles. A less oxidative atmosphere is created within the sample and carbon burning is inhibited. The second mechanism relates to the sintering behavior of the mixture. T_{sint} decreases with the content of added WG, consequently shifting the pore closing process to lower temperatures preventing the escape of formed gases at lower temperature and preventing the contact between carbon and outer atmosphere.

5.3.3.3 Foaming and properties of small samples

To further determine how the addition of WG affects the process of direct foaming in air atmosphere, *0*, *Mn*, *C* and *Mn+C* foaming mixtures with varied content of WG were prepared (0-24 wt.%). Temperature for the preparation of the mixtures was constant (800 °C), determined as optimal foaming temperature for the *Mn+C* foaming mixture with 12 wt.% of added WG.

Foamed glass samples were tested for their crystallinity with XRD even though CRT panel glass normally exhibits high glass stability and therefore does not crystallize easily [24]. Additives affect the crystallization during the heating which can lead to undesired lesser expansion and open pore structure [127]. All the foamed glass samples exhibit a broad peak over a wide range of 2θ, indicating a lack of long-range order, characteristic for glass (Figure 5.25). Diffraction peaks have low intensity and resemble the results from the foamed glass samples prepared without the addition of WG [55], [125].

The addition of WG can affect the crystalline content of the foaming mixture, as already established in *Structural changes* on page 33, especially after prolonged contact with CO_2

atmosphere. Effect of WG content on the change in the sample crystallinity can also be seen in Figure 5.25a, even though the samples were foamed immediately after the preparation of the foaming mixture.

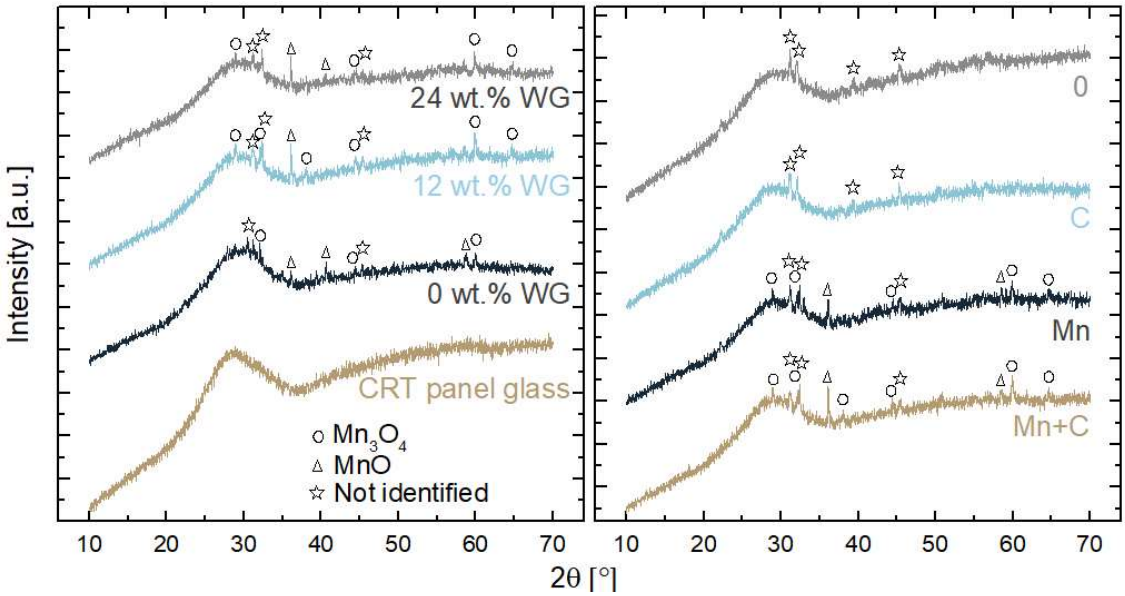

Figure 5.25: Left: XRD patterns of the CRT panel glass and foamed glass samples prepared from the Mn+C foaming mixture with different contents of added WG. Right: XRD patterns of the foamed glass samples prepared from different foaming mixtures with added 12 wt.% of WG.

Apparent density (ρ_{app}) and open porosity (ε_{op}) of the foamed glass samples are shown in Table 5.5. Direct foaming without the addition of WG, expectedly, results in non-expanded sample with high density. Carbon burns out of the sample before the sintering and gas evolution at higher temperatures is no longer possible. The content of open porosity increases and ρ_{app} decreases with increasing content of WG for all the foaming mixtures. Mn+C foaming mixture results in the foamed glass samples with the lowest density while the other three foaming mixtures result in foamed glass samples with a similar density. Result shows that sole addition of carbon or Mn_3O_4 does not contribute significantly to the decrease of ρ_{app}. Use of both additives leads to significantly lower ρ_{app}. This indicates that the reaction between carbon and Mn_3O_4 occurs during the foaming, which further implies that carbon is present within the sintered sample due to the protective role of added WG. The results are in accordance with TG/MS analysis which suggested that more carbon was protected with higher content of WG.

Table 5.5: ρ_{app} and ε_{op} of the small foamed glass samples prepared from different foaming mixtures with a varied content of WG.

Content of water (vol.%)	Foaming mixture	*0*	*C*	*Mn*	*Mn+C*
0	ρ_{app} [kg m^{-3}]	2124	2114	1552	1682
	ε_{op} [%]	0	0	0	0
4	ρ_{app} [kg m^{-3}]	1058	1006	922	647
	ε_{op} [%]	4	0	0	3
8	ρ_{app} [kg m^{-3}]	743	631	655	346
	ε_{op} [%]	3	1	0	10
12	ρ_{app} [kg m^{-3}]	640	456	546	203

	ε_{op} [%]	3	3	0	28
16	ρ_{app} [kg m^{-3}]	542	401	439	173
	ε_{op} [%]	6	4	1	14
20	ρ_{app} [kg m^{-3}]	383	325	351	165
	ε_{op} [%]	2	2	17	7
24	ρ_{app} [kg m^{-3}]	272	283	274	166
	ε_{op} [%]	79	3	75	14

Sample properties shown in Table 5.5 were recalculated according to Equation 4.5 and are presented in Figure 5.26. Expansion data allow better comparison and visualization of the similarities and differences between the expansion of the foaming mixtures. The expansion of the samples prepared from the foaming mixture *0* can be assumed as the baseline value for all the foaming mixtures, directly related to the presence of WG. Direct contribution of WG to the foaming is discussed in the *Use of Water Glass for the Foaming of Glass* on page 25, showing that the majority of the expansion can be attributed to the decomposition of carbonates and subsequent evolution of CO_2. However, few sources assume that evaporation of strongly bound water at elevated temperatures can contribute to the expansion [99], which is why H_2O evaporation is still labelled as a (less) possible reaction in Figure 5.26. Values above this baseline should be related to the formation of additional gases during the reactions between other foaming additives. The samples prepared from the *Mn* or *C* foaming mixtures achieve values slightly above the WG-baseline due to the decomposition of Mn_3O_4 or water-gas shift reaction, respectively. However, all the described reactions apparently result in a minimal evolution of gas since they only slightly contribute to the expansion of the *Mn* and *C* foaming mixtures. Furthermore, expansion values of *Mn* and *C* are similar to foaming mixture *0*. Such result suggests a single main source of expansion in *0*, *Mn* and *C* foaming mixtures. A much larger expansion or additional expansion occurs in the *Mn+C* foaming mixture. Most probable reason for this is additional gas evolution from the reaction between carbon and Mn_3O_4. Such comparison between the expansion values of foamed glass samples further suggests that the addition of WG indeed protects the carbon from the premature reaction with the oxygen from the air atmosphere. This enables the reaction between the carbon and Mn_3O_4 to occur and results in more expanded foams.

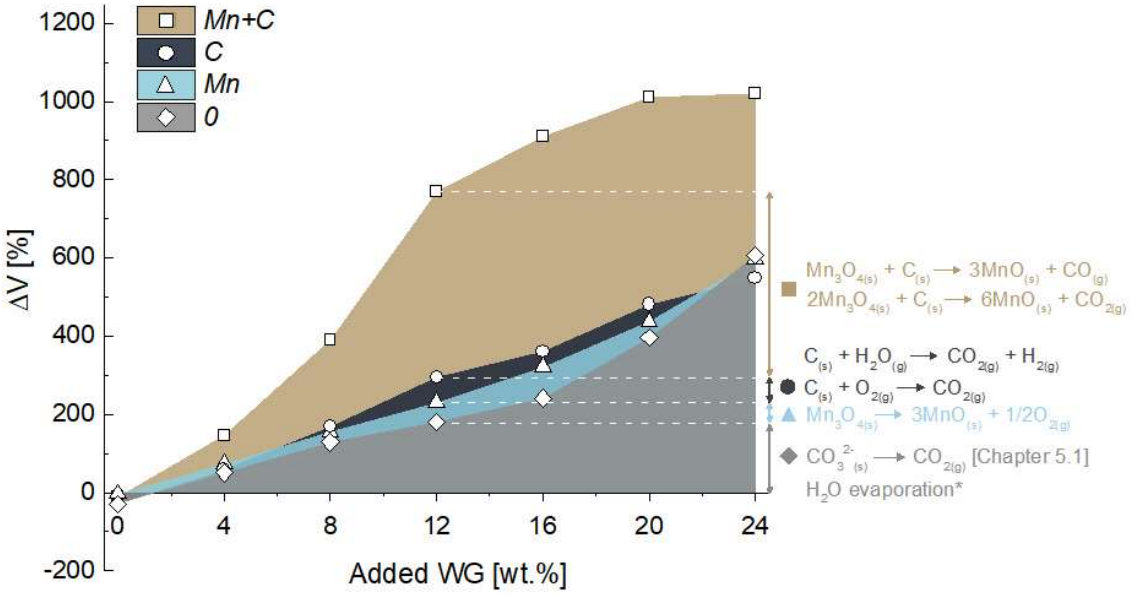

Figure 5.26: Volumetric expansion of the foamed glass samples (Equation 4.4) prepared from different foaming mixtures. On the right side: horizontal arrows represent relative contribution of corresponding reactions to the expansion of the foaming mixtures with 12 wt.% of WG (reactions from [51]).

Effect of WG addition on the protection of carbon can be observed not only from the size but also from the color of the small foamed glass samples. Images of their cross-sections are shown in Figure 5.27. The size of the foamed glass samples increases along with the content of added WG, which is in accordance with the results shown above.

Foamed glass samples prepared from the foaming mixture *0* are white while the ones prepared from *C* change the color from white to black with increasing content of WG. Such change of color suggests that carbon remains within the sample during the heat-treatment and is an additional indication of the protective role of WG. The carbon in the sample prepared from the foaming mixture *C* can remain unreacted on the pore walls or participates in the gas-releasing redox reactions with multivalent ions [128] in the glass or H_2O [129] released from WG. Carbon not reacting or reacting with the ions from the glass contributes to the darker color of the sample [130]. A similar observation of color-change with the addition of WG was reported in a study of foaming with WG and glycerol [97].

Foamed glass samples prepared from the *Mn* foaming mixture exhibit a violet to pink color transition with increasing content of WG. The color of these samples indicates the incorporation of Mn^{2+}/Mn^{3+} ions into the glass structure [128, Ch. 9].

Foamed glass samples prepared from the *Mn+C* foaming mixture change their color from dark violet to grey with increasing addition of WG. Color at low WG content is related to the same effect as in the case of the samples prepared from the *Mn* foaming mixture. Higher WG contents, however, result in more residual carbon within the sample as observed from the samples prepared from the *C* foaming mixture. This allows the reaction between carbon and Mn_3O_4 to occur, resulting in the reduction of the manganese species, and affects the color of the foamed glass samples [128, Ch. 9]. The reduction of the Mn_3O_4 is in accordance with the XRD results (Figure 5.25).

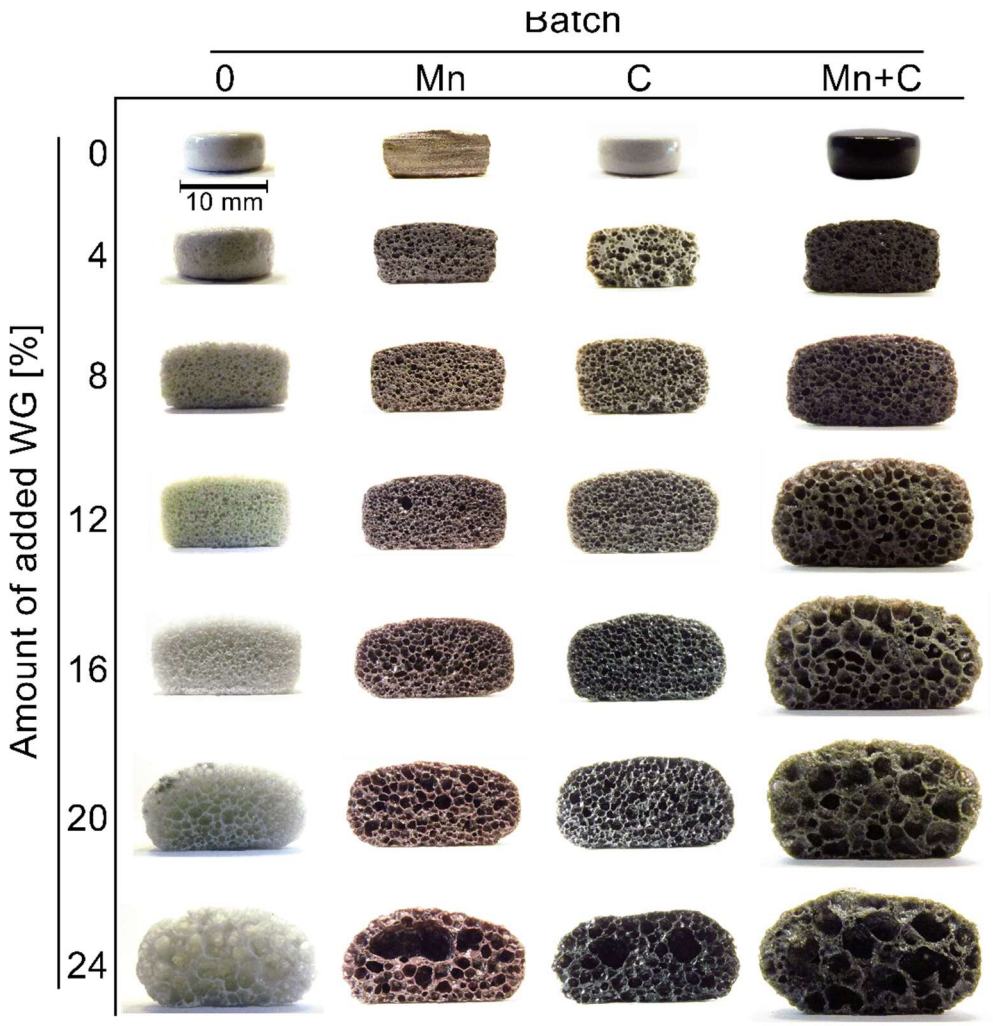

Figure 5.27: Images of cut foamed glass samples prepared from different foaming mixtures (top) containing different amounts of added WG (left). Note that the three samples with the highest density are not cut.

5.3.3.4 Foaming and properties of large samples

Larger samples were prepared from the *Mn+C_12* and *Mn+C_24* foaming mixtures according to the procedure described under *Foaming* on page 19. T_{foam} was varied to obtain the samples of different density. Expectedly, lower T_{foam} is required for the *Mn+C_24* foaming mixture to achieve a foamed glass sample of similar ρ_{app} as with *Mn+C_12*. Larger samples are held at the T_{foam} longer in comparison to smaller samples which can result in an excessive coalescence of pores. Excessive growth of larger pores on the account of smaller ones is apparent from the comparison shown in Figure 5.28. Non-homogeneous distribution of solid and gas phase is apparent in the larger sample (Figure 5.28, top right side) where several larger pores surrounded by smaller ones can be observed.

Pore size distribution becomes wider and shifts to higher values for the larger sample which can be generally observed in porous materials where coalescence occurred [13], [14]. Apart from the coalescence, excessively nonhomogeneous pore growth can also occur due to the changed surface-to-volume ratio of the larger sample. As mentioned in 5.3.3.2, displacement of air by evaporated water and local creation of less oxidative atmosphere within the sample can protect the carbon from the premature oxidation. It is likely that water partial pressure within the sample increases with increasing distance from the sample

surface. This would result in more leftover carbon as well as in a more pronounced effect discussed in [101], i.e. lower glass viscosity. Consequently, more carbon remains available for the CO_2-producing reaction with Mn_3O_4 which promotes the pore growth even further.

Significant increase of the volume-dominant pore size from approximately 2 to above 4 mm can be problematic due to the activation of the convective heat transfer [52] which can significantly contribute to higher λ_{eff} [4]. Additionally, excessive growth can lead to a more open porous structure and exchange of inner atmosphere with the surrounding air, again increasing the λ_{eff}. Evaluated ε_{op} of the large sample (Figure 5.28, top right) is above 90 %. Effects of increased foaming time and sample size can therefore negatively influence the structure and properties of the material, requiring further optimization of the processing parameters.

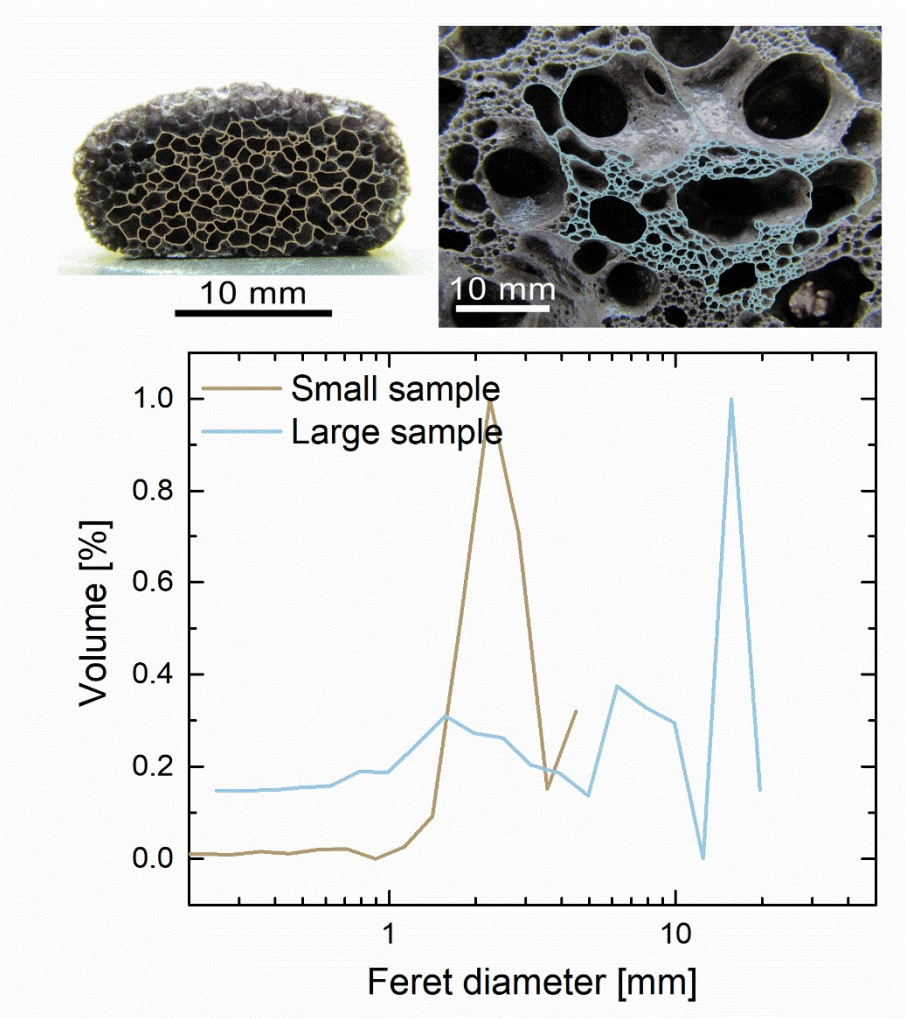

Figure 5.28: Image of the outlined pores from the small and large sample (top left and right, respectively) and pore size distribution.

To avoid excessive coalescence and preserve a similar pore structure during the preparation of the larger samples, foaming mixtures were either heat-treated at lower T_{foam} or dried before the heat treatment. Drying of the foaming mixture before the foaming of the large sample reduces the total content of water by freeing less strongly bound water, mitigating the pronounced effect of the sample size and resulting coalescence [33].

Lowering of the T_{foam} to 770 °C or drying of the foaming mixture beforehand results in a significantly different pore structure and size (Figure 5.29) in comparison to the large

sample in Figure 5.28. Density of both larger samples prepared with adjusted parameters increases, however, their average pore size remains well under 4 mm, which can be beneficial for the λ_{eff}.

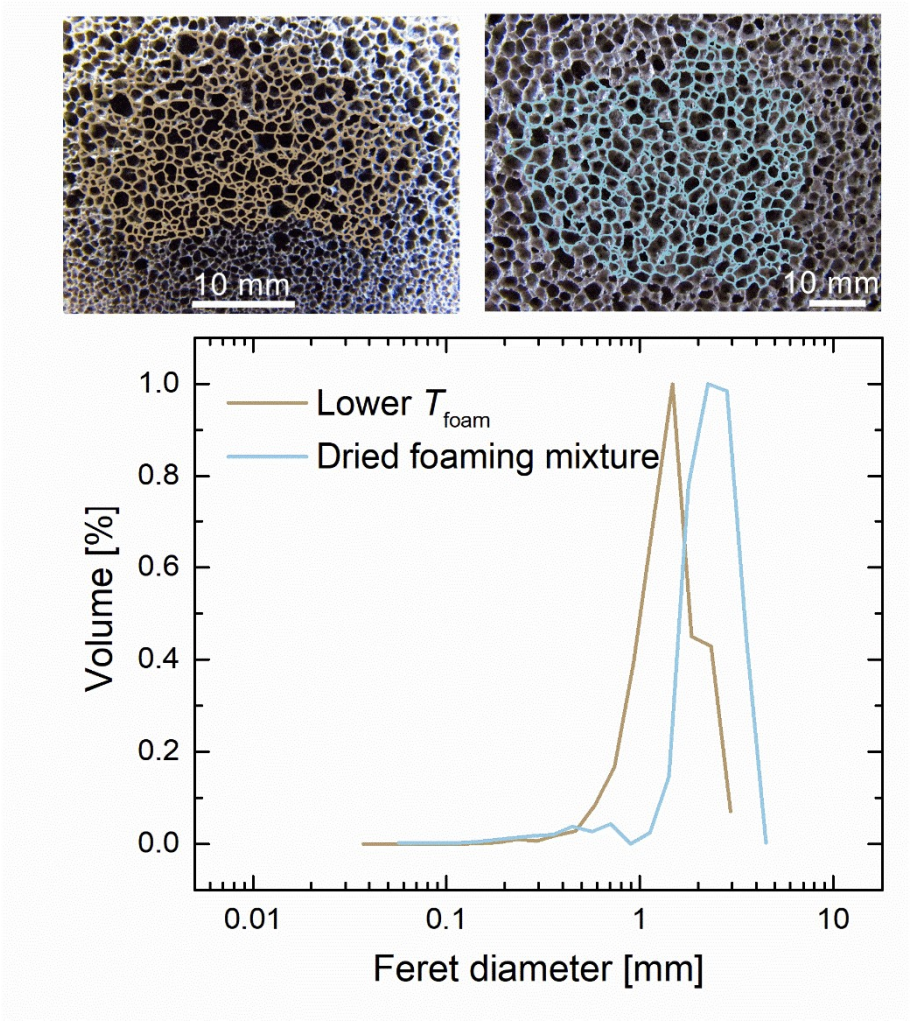

Figure 5.29: Image of the outlined pores from the large samples prepared at lower temperature (T_{foam} = 770 °C, top left) or by drying the foaming mixture beforehand (T_{foam} = 800 °C, top right).

Foaming mixtures of *Mn+C_12* and *Mn+C_24* were used and synthesis parameters (T_{foam} and drying of the foaming mixtures) were further varied to achieve samples with a variety of different densities. Their properties are reported in Table 5.6. The ρ_{app} of the samples decreases with higher T_{foam} and higher WG content.

As discussed in *Use of Water Glass for the Foaming of Glass* on page 25, the foaming mixture is sensitive to the air atmosphere and needs to be quickly processed further, otherwise its properties will begin to change. This effect is apparent for these samples as well, if further processing of the foaming mixtures was delayed onto the next day, maximum achievable porosity decreases significantly (immediately processed versus stored samples in Table 5.6). The reason is related to the formation of crystalline products from the reaction between the WG and CO_2, which hinder the expansion capability of the foam.

Table 5.6: ρ_{app}, λ_{eff}, ε_{tot} and ε_{op} for the large foamed glass samples prepared at given conditions. Bottom series of samples were processed the next day while the top series were processed immediately.

T_{foam} [°C]	Added WG [wt.%]	Drying	ρ_{app}	ε_{tot}	ε_{op}	$\varepsilon_{op,corr}$	λ_{eff}
800	12	N	130	95.4	>90		54.8
730	24	N	177	93.7	26	8	44.9
755	24	N	145	94.8	52	13	41.6
770	12	N	180	93.6	54	29	41.2
800	12	Y	146	94.8	51	20	39.5
790	12	Y	286	89.8	26		62.8
800	12	Y	236	91.6	35		53.7
800	12	Y	168	94.0	34		44.2
800	12	Y	228	91.9	27		52.5
810	12	Y	214	92.4	23		51.5

Thermal conductivity of discussed samples generally decreases with decreasing density, with almost linear correlation in the analyzed density range (Figure 5.30). The relation between the λ_{eff} and ρ_{app} is similar to the one reported in [55]. Distribution of the λ_{eff} values can be well described with the Schuetz-Glicksman analytical model [57], if the thermal conductivity of the gas and solid phase are 17 (CO_2) and 925 mW m^{-1} K^{-1} (CRT glass), respectively, and the K value is set to be around 0.5. Sample with the lowest ρ_{app} (130 kg m^{-3}) apparently deviates from this trend, exhibiting much higher λ_{eff} (54.8 mW $m^{-1}K^{-1}$) which is a consequence of large pores (large sample in Figure 5.28).

The lowest λ_{eff} of 39.5 mW m^{-1} K^{-1} was obtained at ρ_{app} of 145 kg m^{-3}. Such low λ_{eff} values indicate that the pores are in major part filled with low heat-conducting gas and that the content of open porosity is low. Furthermore, small pore size (< 4mm) is preventing significant contribution from convective heat transfer, and ρ_{app} above 145 kg m^{-3} is preventing significant contribution from the radiative heat transfer [55]. Further decrease of the ρ_{app} would likely result in λ_{eff} starting to deviate from the general trend due to the increased contribution from the radiative heat transfer.

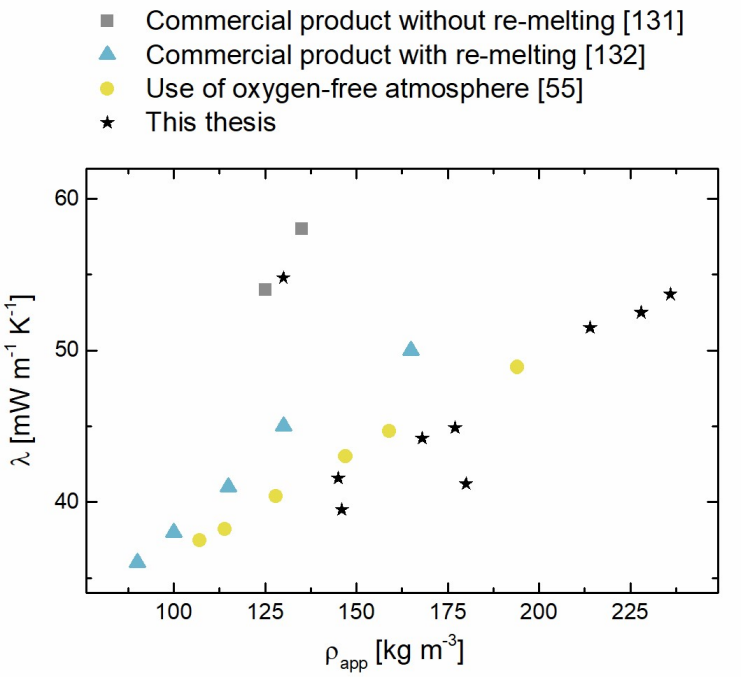

Figure 5.30: λ_{eff} versus ρ_{app} of relevant industrial products ([131], [132]) and research results (Table 5.6).

5.3.4 Impact of the process implementation in the air atmosphere

Results indicate that the thermal conductivity of the foamed glass prepared in this research is comparable to the one in reference [55], and the best commercial products [120]. Investigated processing can thus provide an effective way for the recycling of waste CRT panel glass [79]. Effective transfer of the process to the air atmosphere is expected to lead to better fuel efficiency and furnace durability in comparison to foaming in oxygen-free atmosphere, improving also the energy efficiency of the production. Furthermore, a positive impact of the air atmosphere on the global warming potential is apparent from the comparison between the environmental product declarations of common commercial products prepared in different processes ([20] and [21]). Implementation of the process in the air atmosphere allows for the use of an electrically-powered furnace instead of a gas-combustion furnace, where the energy can be obtained from renewable sources. In terms of climate change potential, the best product prepared via investigated processing (39.5 mW mK at 146 kg m^{-3}) would leave a 25 % smaller footprint in comparison to a commercial foamed glass of similar performance. Furthermore, in the case of use of renewable energy sources, i.e. wind, this decrease would be even larger (70 %) [124].

Transfer of the process to the air atmosphere with the use of water glass thus significantly decreases the embodied energy of the foamed glass without hindering its performance as a thermal insulation material. All these factors positively affect the environmental impact of the potential product which is in agreement with current trends in policy-making and construction industry [133], [134]. Additionally, the process's high energy efficiency and use of waste glass can lead to a decrease in price for the potential product, which could be an important factor when considering foamed glass' higher cost compared to other thermal insulation materials [3]. Consequently, industrial use of the investigated process would positively contribute to the sustainability and energy efficiency of the foamed glass sector.

5.3.5 Conclusions

Glass foaming in air atmosphere with the use of carbonaceous foaming agent is normally difficult to perform due to the premature burning of carbon. Hydrosilicates can be used to protect the carbon from the premature reaction with the oxygen, allowing it to perform its role at higher temperatures.

Use of hydrothermally treated glass in combination with carbonaceous foaming agent results in increased expansion values. The highest achievable ε_{tot} with the use of hydrothermally treated glass powder in combination with carbon and Mn_3O_4 was 91 %. Such value is promising and processing is worth of further research, however, it is well below required ε_{tot} required to achieve low λ_{eff} values of the best commercial foamed glass products.

Use of WG allows simpler processing and can result in foams with ε_{tot} around 95 %. WG protects the carbon by decreasing the T_{sint} of the foaming mixture and by displacing the air during the heating stage of the process due to the constant release of H_2O. The expansion of the foaming mixture is related directly to the presence of WG and the redox reaction between carbon and Mn_3O_4. Redox reaction increasingly contributes to the expansion of the foaming mixture with higher content of WG, confirming the role of WG in protecting the carbon. Investigated processing allows the synthesis of foamed glass with ρ_{app} and λ_{eff} as low as 145 kg m^{-3} and 39.5 mW m^{-1} K^{-1}, respectively. These values are comparable or superior to the foamed glass prepared in inert atmosphere, or to the foamed glass prepared from more pristine raw materials. Thus, with the addition of WG, foamed glass with a low λ_{eff} can be produced entirely from the waste glass. Such processing has a lower impact on the environment and results in a material comparable to the best commercial products. Furthermore, investigated mechanisms of foaming with WG in combination with carbonaceous foaming agent can provide guidance for future research on the sustainable production of foamed glass.

Chapter 6

Final Conclusions

Production of the building insulation is commonly associated with processes which either obtain the materials from petrochemicals or from natural resources, both requiring high energy inputs to achieve the final product. Use of recycled materials for this purpose can significantly contribute towards more sustainable future of the building industry. This thesis dealt with the use of waste glass for the production of foamed glass. I studied the use of CRT glass together with a foaming couple of carbon and Mn_3O_4 with an emphasis on implementing the process in the air atmosphere. Selected means, through which the process implementation can be achieved, were hydration of the glass powder and use of WG.

In the first step, I investigated the peculiarities of foaming with the addition of WG, where I stumbled upon an interesting result regarding the basic mechanism of the process. Analysis of the gas within the closed pores of the foams has revealed an overwhelming presence of CO_2 which was surprising, as it contradicts the commonly accepted H_2O-dominated mechanism. Based on this, I proposed a likely explanation that the foaming mechanism is based on the formation of carbonates and their subsequent decomposition during the heating. This idea was further supported by the results from the structure analysis and TG/MS. Structure analysis of the foaming mixture has revealed the presence of crystalline phases and carbonates after the mixing with WG while the TG/MS revealed significant evolution of CO_2 at elevated temperatures. Interestingly, allowing the carbonate-producing reaction to proceed further does not result in more pronounced expansion but the opposite. It is almost certain that the reasons for lesser expansion in this case are additional crystallization and excessive gas evolution during the heating, both of which hinder the closing of the pores. Results indicate the susceptibility of the WG-containing powder mixture for the reaction with the atmosphere and showcase the importance of processing consistency when working with WG.

In the second step, I examined the foaming of three hydrothermally treated waste glass powders. Similarly, as in the case of foaming with the addition of WG, the formation of crystalline phases and carbonates plays an important part during the foaming of hydrothermally treated glass powders. Evolution of CO_2 at elevated temperatures further suggests that the expansion of the powders occurs due to the decomposition of newly formed carbonates. Hydration of the powders to higher contents of H_2O does not necessarily result in larger expansion. Maximum expansion of 250 vol.% was achieved for the CRT glass powders foamed at 800 °C.

In the last step, I used previously examined hydrosilicates for foaming in air atmosphere with the use of carbon and Mn_3O_4 as a foaming couple. Hydrothermally treated CRT glass expands slightly more when used in combination with the foaming couple even though the TG/MS analysis suggests that significant amounts of CO_2 remain trapped in the foam in the case of powders containing 30 wt.% of H_2O. Such inferior expansion ability does not allow the synthesis of foams with porosity around 95 %, which are the goal of this thesis.

Use of WG, on the other hand, allows the synthesis of high porosity foams which exhibit homogenous pore structure. Comparison between the expansion capability of the foaming mixtures with missing additives showed the importance of foaming couple for the expansion. With that, I have shown that WG contributes to the foaming directly, by forming the carbonates, and indirectly, by protecting the carbon and enabling the reaction of the foaming couple. Heating stage microscope and TG/MS results suggest that there are at least two possible mechanisms through which WG protects the carbon. The first one is related to pronounced evaporation of H_2O from within the sample, diluting and displacing the air atmosphere which is initially present in the pores between the particles. The second one is related to the sintering behavior of the mixture, where higher addition of WG decreased the T_{sint} of the powder. In the end, higher addition of WG resulted in decreased mass loss related to the premature burning of carbon, darker appearance of the foamed glass samples and larger expansion. The lowest λ_{eff} of 39.5 mW m^{-1} K^{-1} was achieved with the use of 12 wt.% of WG, foamed at 800 °C. Although achieving lower density would require additional optimization, the properties of foamed glass samples in this thesis are comparable to the best commercial products.

As mentioned before, performance is not the only aspect of materials development. Recent EU directives emphasize sustainable development and resource independence, which are likely to become even more important factors in materials development in the future. The production of waste-based foamed glass has been on a similar track for some time. However, there remains room for improvement, such as the use of less energy-demanding processes, as shown in this dissertation. The sharp increase in the use of energy sources such as solar and wind suggests that we may finally be becoming less inclined to use fossil fuels, leading to an increased tendency to use electric- instead of combustion furnaces. Whereas the use of air instead of a reduced atmosphere as in a combustion furnace is one of the main goals of this dissertation. With the increased use of electric furnaces, the need for processes that can be carried out in an air atmosphere will increase. In addition, it is in line with sustainable development that the production of foamed glass uses locally available materials. Here, a significant difference in waste materials availability between the regions should be considered, which requires an additional investment in the development and optimization of the processes. Since the chemical composition of the matrix material can significantly affect the foaming process is sensible that research will continue towards finding a processing path which is less composition dependent. In my opinion, the future research in the field of foamed glass will therefore be directed towards the use of a diverse spectrum of waste materials, with an emphasis on locally available waste, and testing different combinations of foaming additives, with the aim of achieving a controlled release of expansion gas that does not strongly depend on the chemical composition of the surrounding matrix material. The use of carbon-containing additives has proven to be very successful in the preparation of high-quality foamed glass. There is a possibility that carbon as an additive will continue to be used in the air-atmosphere process in the future, and the knowledge gained from this dissertation could contribute to further research and understanding of foaming.

The main conclusion from this thesis is that the use of hydrosilicates in glass foaming process requires an additional care and consistency from the processing point of view, however, it allows the use of carbonaceous foaming agents in the air atmosphere. Such processing enables the production of quality foamed glass based almost entirely on waste glass with significantly reduced embodied energy. Furthermore, investigation on foaming with hydrothermally treated glass and revealing the peculiarities of WG foaming mechanism can offer a valuable guidance for the future development and optimization of a sustainable glass foaming process.

Appendix A

Additional Information for the Experimental and Characterization Methods

A.1 Particle Size Distribution Before Milling

As-received powders were measured at standard conditions with Horiba LA940 apparatus as described in the *Experimental and Characterization Methods* chapter on page 20. CRT panel glass powder exhibits unimodal particle size distribution while FGF and MCF glass powders exhibit bimodal particle size distribution. Additionally, particle size distribution of the CRT panel glass powder is narrower in comparison to FGF and MCF glass powders.

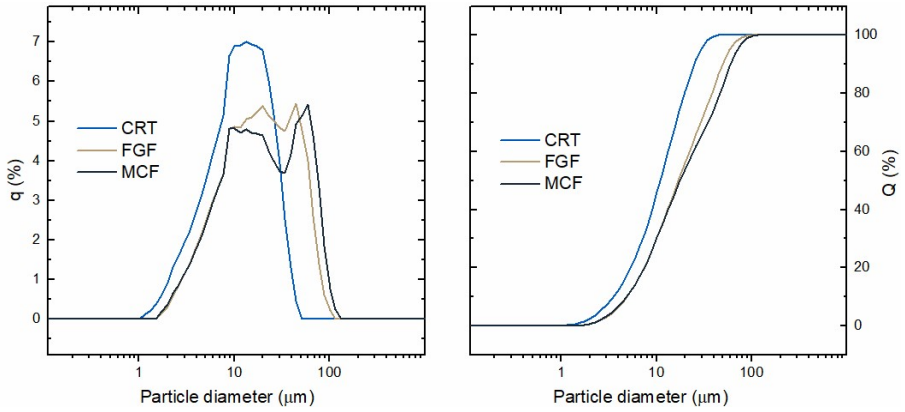

Figure 6.1: Frequency (left) and cumulative (right) particle size distribution of the as-obtained raw glass powders.

A.2 Repeatability of Sample Preparation

Repeatability for the preparation of the smaller samples was investigated for the composition of waste CRT glass which contains all the foaming additives, i.e. foaming mixture *Mn+C* described in Table 4.2.

A.2.1 Effect of position

Size of the used furnace allows for the preparation of several small (ϕ 12 mm, 1 g) samples. Samples were prepared with standard foaming procedure; their ρ_{app} was measured after and the results are shown in Figure 6.2. Effect of the sample position on its expansion was

evaluated with this experiment. The placement of the samples on a kaolin-coated surface is shown on the inset of Figure 6.2 with the temperature calibration zone being located in the middle, i.e. sample no. 5. The porosity of the foamed glass samples does not vary significantly with their position (± 0.7 %), where the last three positions contribute the most to this deviation (deviation of 0.2 % between the first 6 positions).

The deviation between the samples with respect to their position in the furnace does not vary significantly, implying that 9 small samples can be prepared simultaneously without being affected by the positioning.

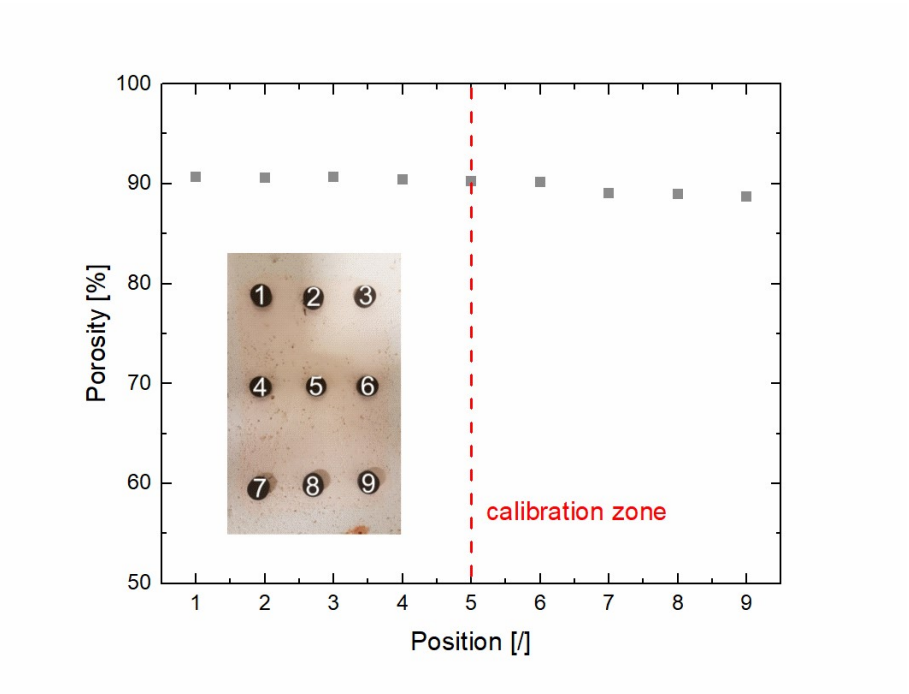

Figure 6.2: Porosity of the foamed glass samples as a function of their position. Their configuration is shown in the onset image, with position no. 5 being in the center of the calibration zone.

A.2.2 Effect of mixing time

Addition of water glass (WG) to the foaming mixture increases its sensitivity to the atmosphere. It is thus important to investigate the repeatability of the mixture preparation and the effect of preparation deviations on the properties of obtained foamed glass samples. To investigate the effect of time on the foaming behavior, i.e. reaction between air and WG, the time of manual mixing was varied slightly. All other parameters of foaming mixture preparation and foaming were kept constant. Figure 6.3 shows the porosity of the foaming mixtures as a function of the manual mixing time in air atmosphere. Note that for this experiment, only the first six positions were utilized to avoid additional deviations (Figure 6.2). Porosity between the samples mixed for different times deviates for approximately ±1.1 %. However, a trend of decreasing porosity with increasing time can be observed suggesting that severely prolonged time of manual mixing could significantly affect the foaming and should therefore be considered as an important parameter.

Exposing the foaming mixtures to the air atmosphere for different times can lead to observable differences between the foamed glass samples. Consequently, the time of manual mixing of WG and glass powder was fixed (5 min) during the preparation of all the foaming mixtures. Additionally, the samples were heat-treated immediately after their preparation, if not stated that the WG-containing foaming mixture was additionally treated.

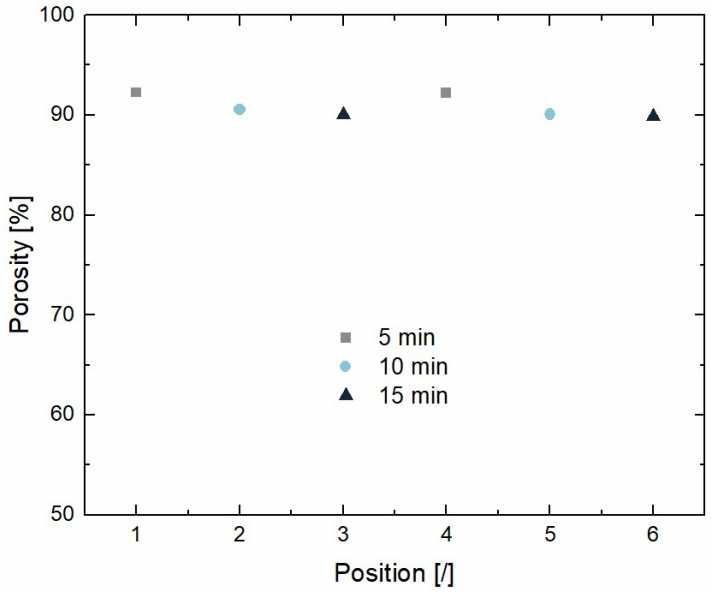

Figure 6.3: Porosity of the foamed glass samples as a function of their mixing time and position in the furnace.

References

[1] M. Faraday, Philosophical transactions., *Philos. Trans. R. Soc. London*, vol. 120, pp. 1–57, 1829.

[2] L. Aditya, T. M. I. Mahlia, B. Rismanchi, H. M. Ng, M. H. Hasan, H. S. C. Metselaar, O. Muraza, H. B. Aditiya, A review on insulation materials for energy conservation in buildings, *Renew. Sustain. Energy Rev.*, vol. 73, no. March, pp. 1352–1365, 2017.

[3] D. Kumar, M. Alam, P. X. W. Zou, J. G. Sanjayan, R. A. Memon, Comparative analysis of building insulation material properties and performance, *Renew. Sustain. Energy Rev.*, vol. 131, no. July, p. 110038, 2020.

[4] J. König, V. Nemanič, M. Žumer, R. R. Petersen, M. B. Østergaard, Y. Yue, D. Suvorov, Evaluation of the contributions to the effective thermal conductivity of an open-porous-type foamed glass, *Constr. Build. Mater.*, vol. 214, pp. 337–343, 2019.

[5] EN 13167 Thermal insulation products for buildings - Factory made cellular glass (CG) products - Specification, European Comittee for Standardization (CEN). 2012.

[6] G. Kyaw Oo D'Amore, M. Caniato, A. Travan, G. Turco, L. Marsich, A. Ferluga, C. Schmid, Innovative thermal and acoustic insulation foam from recycled waste glass powder, *J. Clean. Prod.*, vol. 165, pp. 1306–1315, 2017.

[7] A. Lejeune, A. Cabrol, R. Lebullenger, A. Denicourt-Nowicki, A. Roucoux, A. Szymczyk, A. Couvert, P. F. Biard, Development of a Sustainable Heterogeneous Catalyst Based on an Open-Cell Glass Foam Support: Application in Gas-Phase Ozone Decomposition, *ACS Sustain. Chem. Eng.*, vol. 8, no. 7, pp. 2854–2864, 2020.

[8] A. Lejeune, A. Cabrol, R. Lebullenger, A. Denicourt-Nowicki, A. Roucoux, A. Couvert, P. F. Biard, Novel and Sustainable Catalytic Ruthenium-Doped Glass Foam for Thermocatalytic Oxidation of Volatile Organic Compounds: An Experimental and Modeling Study, *Ind. Eng. Chem. Res.*, vol. 59, no. 33, pp. 14758–14766, 2020.

[9] A. Cabrol, A. Lejeune, R. Lebullenger, A. Denicourt-Nowicki, A. Roucoux, A. Couvert, P. F. Biard, Simulation and optimization of the removal of toluene in air by ozonation with a catalytic open-cell foam, *Chem. Eng. Res. Des.*, vol. 168, pp. 453–464, 2021.

[10] J. Pinto, E. Solórzano, M. A. Rodriguez-Perez, J. A. De Saja, Characterization of the cellular structure based on user-interactive image analysis procedures, *J. Cell. Plast.*, vol. 49, no. 6, pp. 555–575, 2013.

[11] Y. N. Qu, J. Xu, Z. G. Su, N. Ma, X. Y. Zhang, X. Q. Xi, J. L. Yang, Lightweight and high-strength glass foams prepared by a novel green spheres hollowing technique, *Ceram. Int.*, vol. 42, no. 2, pp. 2370–2377, 2016.

[12] F. Mear, P. Yot, M. Cambon, R. Caplain, M. Ribes, Characterisation of porous glasses prepared from Cathode Ray Tube (CRT), *Powder Technol.*, vol. 162, no. 1, pp. 59–63, 2006.

[13] V. Ducman, L. Korat, A. Legat, B. Mirtič, X-ray micro-tomography investigation of the foaming process in the system of waste glass-silica mud-MnO2, *Mater. Charact.*, vol. 86, pp. 316–321, 2013.

[14] M. B. Østergaard, M. Zhang, X. Shen, R. R. Petersen, J. König, P. D. Lee, Y. Yue, B. Cai, High-speed synchrotron X-ray imaging of glass foaming and thermal conductivity simulation, *Acta Mater.*, vol. 189, pp. 85–92, 2020.

[15] C. Arriagada, I. Navarrete, M. Lopez, Understanding the effect of porosity on the mechanical and thermal performance of glass foam lightweight aggregates and the influence of production factors, *Constr. Build. Mater.*, vol. 228, p. 116746, 2019.

[16] M. Scheffler, P. Colombo, Glass Foams, in *Cellular Ceramics*, M. Scheffler and P. Colombo, Eds. Weinheim: Wiley - VCH Verlag GmbH & Co. KGaA, 2005, pp. 158–176.

[17] F. Méar, P. Yot, R. Viennois, M. Ribes, Mechanical behaviour and thermal and electrical properties of foam glass, *Ceram. Int.*, vol. 33, no. 4, pp. 543–550, 2007.

[18] L. J. G. and M. F. Ashby, *Cellular Solids - Structure and Properties*. Cambridge University Press, 1999.

[19] A. K. Varshneya, J. C. Mauro, *Fundamentals of inorganic glass making*. 2019.

[20] Environmental Product Declaration Foamglas.

[21] Environmental Product Declaration Glapor.

[22] E. D. Zanotto, J. C. Mauro, The glassy state of matter: Its definition and ultimate fate, *J. Non. Cryst. Solids*, vol. 471, no. June, pp. 490–495, 2017.

[23] J. E. Shelby, *Introduction to Glass Science and Technology - 2nd edition*, Second. Cambridge CB4 0WF, UK: The Royal Society of Chemistry, 2005.

[24] R. R. Petersen, J. König, Y. Yue, The viscosity window of the silicate glass foam production, *J. Non. Cryst. Solids*, vol. 456, pp. 49–54, 2017.

[25] H. Pfaender, *Schott Guide to Glass*, Second edi. Springer Science & Business Media, 2012.

[26] J.-P. Judson, Europe's glass value chain confirms steady progress at 79% glass collection for recycling, 2022. [Online]. Available: https://closetheglassloop.eu/.

[27] R. K. Iler, *The Chemistry of Silica*. JOHN WILEY & SONS, 1979.

[28] R. H. Doremus, *Glass Science*, Second edi. New York: JOHN WILEY & SONS, 1994.

[29] S. Zietka, J. Deubener, H. Behrens, R. Müller, Glass transition and viscosity of hydrated silica glasses, *Phys. Chem. Glas. Eur. J. Glas. Sci. Technol. Part B*, vol. 48, no. 6, pp. 380–387, 2007.

[30] M. Tomozawa, Water in glass, *J. Non. Cryst. Solids*, vol. 73, no. 1–3, pp. 197–204, 1985.

[31] F. M. ERNSBERGER, Molecular Water in Glass, *J. Am. Ceram. Soc.*, vol. 60, no. 1–2, pp. 91–92, 1977.

[32] J. Acocella, M. Tomozawa, E. B. Watson, The nature of dissolved water in sodium silicate glasses and its effect on various properties, *J. Non. Cryst. Solids*, vol. 65,

no. 2–3, pp. 355–372, 1984.

[33] T. Uchino, T. Sakka, Y. Ogata, M. Iwasaki, Machanism of hydration of sodium silicate glass in a steam environment: 29Si NMR and ab initio molecular orbital studies, *J. Phys. Chem.*, vol. 96, no. 18, pp. 7308–7315, 1992.

[34] H. Mei, Y. Yang, A. C. T. van Duin, S. B. Sinnott, J. C. Mauro, L. Liu, Z. Fu, Effects of water on the mechanical properties of silica glass using molecular dynamics, *Acta Mater.*, vol. 178, pp. 36–44, 2019.

[35] T. Uchino, T. Sakka, M. Iwasaki, Interpretation of Hydrated States of Sodium Silicate Glasses by Infrared and Raman Analysis, *J. Am. Ceram. Soc.*, vol. 74, no. 2, pp. 306–313, 1991.

[36] R. F. Bartholomew, P. A. Tick, S. D. Stookey, Water/glass reactions at elevated temperatures and pressures, *J. Non. Cryst. Solids*, vol. 38–39, no. PART 2, pp. 637–642, 1980.

[37] R. F. Bartholomew, High-water containing glasses, *J. Non. Cryst. Solids*, vol. 56, pp. 331–342, 1983.

[38] H. H. Weldes, K. R. Lange, Properties of soluble silicates, *Ind. Eng. Chem.*, vol. 61, no. 4, pp. 29–44, 1969.

[39] E. Robert, A. Whittington, F. Fayon, M. Pichavant, D. Massiot, Structural characterization of water-bearing silicate and aluminosilicate glasses by high-resolution solid-state NMR, *Chem. Geol.*, vol. 174, no. 1–3, pp. 291–305, 2001.

[40] R. Balzer, H. Behrens, T. Waurischk, S. Reinsch, R. Müller, P. Kiefer, J. Deubener, M. Fechtelkord, Water in Alkali Aluminosilicate Glasses, *Front. Mater.*, vol. 7, no. May, 2020.

[41] L. J. Gibson, M. F. Ashby, *Cellular solids*. 1997.

[42] F. Asdrubali, F. D'Alessandro, S. Schiavoni, A review of unconventional sustainable building insulation materials, *Sustain. Mater. Technol.*, vol. 4, no. 2015, pp. 1–17, 2015.

[43] M. B. Østergaard, R. R. Petersen, J. König, M. Bockowski, Y. Yue, Impact of gas composition on thermal conductivity of glass foams prepared via high-pressure sintering, *J. Non-Crystalline Solids X*, vol. 1, p. 100014, 2019.

[44] M. B. Østergaard, R. R. Petersen, J. König, M. Bockowski, Y. Yue, Foam glass obtained through high-pressure sintering, *J. Am. Ceram. Soc.*, vol. 101, no. 9, pp. 3917–3923, 2018.

[45] W. Huo, S. Yan, J. M. Wu, J. Liu, Y. Chen, Y. Qu, X. Tang, J. Yang, A novel fabrication method for glass foams with small pore size and controllable pore structure, *J. Am. Ceram. Soc.*, vol. 100, no. 12, pp. 5502–5511, 2017.

[46] R. I. Saye, J. A. Sethian, Multiscale modeling of membrane rearrangement, drainage, and rupture in evolving foams, *Science (80-.).*, vol. 340, no. 6133, pp. 720–724, 2013.

[47] R. R. Petersen, Foam Glass for Construction Materials: Foaming Mechanism and Thermal Conductivity, p. 75, 2015.

[48] J. García-Ten, A. Saburit, M. J. Orts, E. Bernardo, P. Colombo, Glass foams from oxidation/reduction reactions using SiC, Si <inf>3</inf>N <inf>4</inf> and AlN powders, *Glas. Technol. Eur. J. Glas. Sci. Technol. Part A*, vol. 52, no. 4, pp. 103–

110, 2011.

[49] J. König, R. R. Petersen, Y. Yue, Influence of the glass-calcium carbonate mixture's characteristics on the foaming process and the properties of the foam glass, *J. Eur. Ceram. Soc.*, vol. 34, no. 6, pp. 1591–1598, 2014.

[50] J. König, R. R. Petersen, N. Iversen, Y. Yue, Application of foaming agent–oxidizing agent couples to foamed-glass formation, *J. Non. Cryst. Solids*, no. July, p. 120469, 2020.

[51] R. R. Petersen, J. König, N. Iversen, M. B. Østergaard, Y. Yue, The foaming mechanism of glass foams prepared from Mn3O4, carbon and CRT panel glass, *Ceram. Int.*, vol. 47, no. 2, pp. 2839–2847, 2021.

[52] R. E. Skochdopole, The thermal conductivity of foamed plastics, *Chem. Eng. Prog.*, vol. 57, no. 10, pp. 55–59, 1961.

[53] P. Cimavilla-Román, J. Villafañe-Calvo, A. López-Gil, J. König, M. Á. Rodríguez-Perez, Modelling of the mechanisms of heat transfer in recycled glass foams, *Constr. Build. Mater.*, vol. 274, 2021.

[54] L. J. Gibson, M. F. Ashby, *Cellular solid Structure and properties - Second edition*, Second edi. Cambridge University Press, 1997.

[55] J. König, A. Lopez-Gil, P. Cimavilla-Roman, M. A. Rodriguez-Perez, R. R. Petersen, M. B. Østergaard, N. Iversen, Y. Yue, M. Spreitzer, Synthesis and properties of open- and closed-porous foamed glass with a low density, *Constr. Build. Mater.*, vol. 247, 2020.

[56] H. W. Russell, Principles of Heat Flow in Porous Insulators, *J. Am. Ceram. Soc.*, vol. 18, no. 1–12, pp. 1–5, 1935.

[57] M. A. Schuetz, L. R. Glicksman, A basic study of heat transfer through foam insulation, *J. Cell. Plast.*, vol. 20, no. 2, pp. 114–121, 1984.

[58] R. R. Petersen, J. König, Y. Yue, The mechanism of foaming and thermal conductivity of glasses foamed with MnO<inf>2</inf>, *J. Non. Cryst. Solids*, vol. 425, pp. 74–82, 2015.

[59] E. Solórzano, M. A. Rodriguez-Perez, J. Lazaro, J. A. De Saja, Influence of solid phase conductivity and cellular structure on the heat transfer mechanisms of cellular materials: Diverse case studies, *Adv. Eng. Mater.*, vol. 11, no. 10, pp. 818–824, 2009.

[60] A. S. Llaudis, M. J. O. Tari, F. J. G. Ten, E. Bernardo, P. Colombo, Foaming of flat glass cullet using Si3N4 and MnO2 powders, *Ceram. Int.*, vol. 35, no. 5, pp. 1953–1959, 2009.

[61] M. B. Østergaard, R. R. Petersen, J. König, Y. Yue, Effect of alkali phosphate content on foaming of CRT panel glass using Mn3O4and carbon as foaming agents, *J. Non. Cryst. Solids*, vol. 482, no. December 2017, pp. 217–222, 2018.

[62] E. Bernardo, R. Cedro, M. Florean, S. Hreglich, Reutilization and stabilization of wastes by the production of glass foams, *Ceram. Int.*, vol. 33, no. 6, pp. 963–968, 2007.

[63] E. Bernardo, F. Albertini, Glass foams from dismantled cathode ray tubes, *Ceram. Int.*, vol. 32, no. 6, pp. 603–608, 2006.

[64] N. P. Stochero, J. O. R. de Souza Chami, M. T. Souza, E. G. de Moraes, A. P. N. de Oliveira, Green Glass Foams from Wastes Designed for Thermal Insulation,

Waste and Biomass Valorization, vol. 12, no. 3, pp. 1609–1620, 2021.

[65] Y. Attila, M. Güden, A. Taşdemirci, Foam glass processing using a polishing glass powder residue, *Ceram. Int.*, vol. 39, no. 5, pp. 5869–5877, 2013.

[66] J. Stavans, The evolution of cellular structures, *Reports Prog. Phys.*, vol. 56, no. 6, pp. 733–789, 1993.

[67] N. Stiti, A. Ayadi, Y. Lerabi, F. Benhaoua, R. Benzerga, L. Legendre, Preparation and characterization of foam glass based waste, *Asian J. Chem.*, vol. 23, no. 8, pp. 3384–3386, 2011.

[68] R. Lebullenger, S. Chenu, J. Rocherullé, O. Merdrignac-Conanec, F. Cheviré, F. Tessier, A. Bouzaza, S. Brosillon, Glass foams for environmental applications, *J. Non. Cryst. Solids*, vol. 356, no. 44–49, pp. 2562–2568, 2010.

[69] M. T. Souza, B. G. O. Maia, L. B. Teixeira, K. G. de Oliveira, A. H. B. Teixeira, A. P. Novaes de Oliveira, Glass foams produced from glass bottles and eggshell wastes, *Process Saf. Environ. Prot.*, vol. 111, pp. 60–64, 2017.

[70] L. B. Teixeira, V. K. Fernandes, B. G. O. Maia, S. Arcaro, A. P. N. de Oliveira, Vitrocrystalline foams produced from glass and oyster shell wastes, *Ceram. Int.*, vol. 43, no. 9, pp. 6730–6737, 2017.

[71] C. Mugoni, M. Montorsi, C. Siligardi, F. Andreola, I. Lancellotti, E. Bernardo, L. Barbieri, Design of glass foams with low environmental impact, *Ceram. Int.*, vol. 41, no. 3, pp. 3400–3408, 2015.

[72] T. Takei, H. Ota, Q. Dong, A. Miura, Y. Yonesaki, N. Kumada, H. Takahashi, Preparation of porous material from waste bottle glass by hydrothermal treatment, *Ceram. Int.*, vol. 38, no. 3, pp. 2153–2157, 2012.

[73] M. Yu, L. Liu, J. Li, An overall Solution to Cathode-Ray Tube (CRT) Glass Recycling, *Procedia Environ. Sci.*, vol. 31, pp. 887–896, 2016.

[74] H. R. Fernandes, D. D. Ferreira, F. Andreola, I. Lancellotti, L. Barbieri, J. M. F. Ferreira, Environmental friendly management of CRT glass by foaming with waste egg shells, calcite or dolomite, *Ceram. Int.*, vol. 40, no. 8 PART B, pp. 13371–13379, 2014.

[75] L. Lakov, K. Toncheva, A. Staneva, T. Simeonova, Z. Ilcheva, Composition , Synthesis and Properties of Insulation Foam Glass Obtained From Packing Glass Waste, *J. Chem. Technol. Metall.*, vol. 48, no. 2, pp. 125–129, 2013.

[76] M. Suzuki, T. Tanaka, N. Yamasaki, Use of hydrothermal reactions for slag/glass recycling to fabricate porous materials, *Curr. Opin. Chem. Eng.*, vol. 3, pp. 7–12, 2014.

[77] S. Smiljanić, U. Hribar, M. Spreitzer, J. König, Influence of additives on the crystallization and thermal conductivity of container glass cullet for foamed glass preparation, *Ceram. Int.*, vol. 47, no. 23, pp. 32867–32873, 2021.

[78] J. König, R. R. Petersen, N. Iversen, Y. Yue, Suppressing the effect of cullet composition on the formation and properties of foamed glass, *Ceram. Int.*, vol. 44, no. 10, pp. 11143–11150, 2018.

[79] Z. Yao, T.-C. Ling, P. K. Sarker, W. Su, J. Liu, W. Wu, J. Tang, Recycling difficult-to-treat e-waste cathode-ray-tube glass as constructionand building materials A critical review.pdf, *Renew. Sustain. Energy Rev.*, vol. 81, pp. 595–604, 2018.

[80] A. Siddika, A. Hajimohammadi, V. Sahajwalla, Stabilisation of pores in glass foam by using a modified curing-sintering process: sustainable recycling of automotive vehicles' waste glass, *Resour. Conserv. Recycl.*, vol. 179, no. January, p. 106145, 2022.

[81] H. R. Fernandes, D. U. Tulyaganov, J. M. F. Ferreira, Preparation and characterization of foams from sheet glass and fly ash using carbonates as foaming agents, *Ceram. Int.*, vol. 35, no. 1, pp. 229–235, 2009.

[82] M. Sassi, A. Simon, Waste-to-reuse foam glasses produced from soda-lime-silicate glass, cathode ray tube glass, and aluminium dross, *Inorganics*, vol. 10, no. 1, 2022.

[83] Y. Guo, Y. Zhang, H. Huang, K. Meng, K. Hu, P. Hu, X. Wang, Z. Zhang, X. Meng, Novel glass ceramic foams materials based on red mud, *Ceram. Int.*, vol. 40, no. 5, pp. 6677–6683, 2014.

[84] H. Zhou, K. Feng, Y. Liu, L. Cai, Preparation and characterization of foamed glass-ceramics based on waste glass and slow-cooled high-titanium blast furnace slag using borax as a flux agent, *J. Non. Cryst. Solids*, vol. 590, no. May, p. 121703, 2022.

[85] H. R. Fernandes, F. Andreola, L. Barbieri, I. Lancellotti, J. M. Pascual, J. M. F. Ferreira, The use of egg shells to produce Cathode Ray Tube (CRT) glass foams, *Ceram. Int.*, vol. 39, pp. 9071–9078, 2013.

[86] F. A. da Silva Fernandes, S. Arcaro, E. F. Tochtrop Junior, J. C. Valdés Serra, C. P. Bergmann, Glass foams produced from soda-lime glass waste and rice husk ash applied as partial substitutes for concrete aggregates, *Process Saf. Environ. Prot.*, vol. 128, pp. 77–84, 2019.

[87] R. F. Bartholomew, *Water in Glass*, vol. 22. ACADEMIC PRESS, INC., 1982.

[88] H. G. Merkus, *Particle Size Measurements: Fundamentals, Practice, Quality.* Springer Netherlands, 2009.

[89] D. L. Sahagian, A. A. Proussevitch, 3D particle size distributions from 2D observations: Stereology for natural applications, *J. Volcanol. Geotherm. Res.*, vol. 84, no. 3–4, pp. 173–196, 1998.

[90] H. Roggendorf, M. Fischer, R. Roth, R. Godehardt, Influence of Temperature and Water Vapour Pressure on Drying Kinetics and Colloidal Microstructure of Dried Sodium Water Glass, *Adv. Chem. Eng. Sci.*, vol. 05, no. 01, pp. 72–82, 2015.

[91] H. Mohsin, S. Maron, I. Maurin, E. Burov, G. Tricot, L. Devys, E. Gouillart, T. Gacoin, Thermal behavior of waterglass: foaming and xerogel-to-glass evolution, *J. Non. Cryst. Solids*, vol. 566, no. April, 2021.

[92] K. B. Langille, D. Nguyen, J. O. Bernt, D. E. Veinot, M. K. Murthy, Mechanism of dehydration and intumescence of soluble silicates - Part I Effect of silica to metal oxide molar ratio, *J. Mater. Sci.*, vol. 26, no. 3, pp. 695–703, 1991.

[93] K. B. Langille, D. Nguyen, J. O. Bernt, D. E. Veinot, M. K. Murthy, Mechanism of dehydration and intumescence of soluble silicates. Part II: Effect of the cation., *J. Mater. Sci.*, vol. 26, no. 3, pp. 704–710, 1991.

[94] I. Shapiro, I. M. Kolthoff, Studies on Aging of Precipitates and Coprecipitation. XLIII. Thermal Aging of Precipitated Silica (Silica Gel), *J. Am. Chem. Soc.*, vol. 72, no. 2, pp. 776–782, 1950.

[95] R. Tschiersch, S. Monika, A. Kuhne, J. Driesner, EP2523912A1, 2010.

[96] V. Ducman, M. Kovačevič, The Foaming of Waste Glass, *Key Eng. Mater.*, vol. 132–136, pp. 2264–2267, 1997.

[97] N. S. Karandashova, B. M. Goltsman, E. A. Yatsenko, Analysis of Influence of Foaming Mixture Components on Structure and Properties of Foam Glass, *IOP Conf. Ser. Mater. Sci. Eng.*, vol. 262, no. 1, 2017.

[98] E. A. Yatsenko, B. M. Goltsman, L. A. Yatsenko, Investigation of the raw materials' composition and ratio influence on the structure and properties of the foamed slag glass, *Mater. Sci. Forum*, vol. 843, pp. 183–188, 2016.

[99] D. Hesky, C. G. Aneziris, U. Groß, A. Horn, Water and waterglass mixtures for foam glass production, *Ceram. Int.*, vol. 41, no. 10, pp. 12604–12613, 2015.

[100] K. K. Éidukyavichus, V. R. Matselkene, V. V. Balkyavichus, A. A. Shpokauskas, A. A. Laukaitis, L. Y. Kunskaite, Use of cullet of different chemical compositions in foam glass production, *Glas. Ceram. (English Transl. Steklo i Keramika)*, vol. 61, no. 3–4, pp. 77–80, 2004.

[101] I. Cutler, B., Effect of Water Vapor on the Sintering of Glass Powder Compacts, *J. Am. Ceram. Soc.*, vol. 52, no. 1, pp. 11–13, 1969.

[102] F. O. Méar, R. Podor, J. Lautru, S. Genty, R. Lebullenger, Effect of the process atmosphere on glass foam synthesis: A high-temperature environmental scanning electron microscopy (HT-ESEM) study, *Ceram. Int.*, vol. 47, no. 18, pp. 26042–26049, 2021.

[103] D. E. Veinot, K. B. Langille, D. T. Nguyen, J. O. Bernt, Efflorescence of soluble silicate coatings, *J. Non. Cryst. Solids*, vol. 127, no. 2, pp. 221–226, 1991.

[104] A. Horvat, J. Golob, R. Gabrovšek, Carbonation of sodium disilicate during spray-drying, *Chem. Biochem. Eng. Q.*, vol. 15, no. 4, pp. 149–152, 2001.

[105] R. G. Liptai, An experimental study of the effects of additives on the collapsibility of carbon dioxode-sodium silicate bonded foundry cores, 1960.

[106] M. Stachowicz, K. Granat, D. Nowak, K. Haimann, Effect of hardening methods of moulding sands with water glass on structure of bonding bridges, *Arch. Foundry Eng.*, vol. 10, no. 3, pp. 123–128, 2010.

[107] M. Cerruti, C. Morterra, Carbonate formation on bioactive glasses, *Langmuir*, vol. 20, no. 15, pp. 6382–6388, 2004.

[108] C. J. GOODBRAKE, J. F. YOUNG, R. L. BERGER, Reaction of Beta-Dicalcium Silicate and Tricalcium Silicate with Carbon Dioxide and Water Vapor, *J. Am. Ceram. Soc.*, vol. 62, no. 3–4, pp. 168–171, 1979.

[109] R. A. Brooker, S. C. Kohn, J. R. Holloway, P. F. McMillan, Structural controls on the solubility of CO2 in silicate melts Part II: IR characteristic of carbonate groups in silicate glasses, *Chem. Geol.*, vol. 174, no. 1–3, pp. 241–254, 2001.

[110] T. Yoshikawa, S. Sato, T. Tanaka, Fabrication of low temperature foaming glass materials using hydrothermal treatment, *ISIJ Int.*, vol. 48, no. 2, pp. 130–133, 2008.

[111] Z. Matamoros-Veloza, J. C. Rendón-Angeles, K. Yanagisawa, E. E. Mejia-Martínez, J. R. Parga, Low temperature preparation of porous materials from TV panel glass compacted via hydrothermal hot pressing, *Ceram. Int.*, vol. 41, no. 10, pp. 12700–12709, 2015.

[112] Z. Matamoros-Veloza, J. C. Rendón-Angeles, K. Yanagisawa, M. A. Cisneros-

Guerrero, M. M. Cisneros-Guerrero, L. Aguirre, Preparation of foamed glasses from CRT TV glass by means of hydrothermal hot-pressing technique, *J. Eur. Ceram. Soc.*, vol. 28, no. 4, pp. 739–745, 2008.

[113] Z. Matamoros-Veloza, K. Yanagisawa, J. C. Rendón-Angeles, S. Oishi, The effect of hydrothermal hot-pressing parameters on the fabrication of porous ceramics using waste glass, *J. Phys. Condens. Matter*, vol. 16, no. 14, 2004.

[114] Z. Matamoros-Veloza, K. Yanangisawa, J. C. Rendón-Angeles, S. Oishi, M. A. Cisneros-Guerrero, Preparation of porous glass-ceramics under different hydrothermal hot pressing conditions, *Solid State Ionics*, vol. 172, no. 1-4 SPEC. ISS., pp. 597–600, 2004.

[115] Z. Yao, D. Wu, J. Liu, W. Wu, H. Zhao, J. Tang, Recycling of typical difficult-to-treat e-waste: Synthesize zeolites from waste cathode-ray-tube funnel glass, *J. Hazard. Mater.*, vol. 324, pp. 673–680, 2017.

[116] D. B. Hawkins, Kinetics of glass dissolution and zeolite formation under hydrothermal conditions., *Clays Clay Miner.*, vol. 29, no. 5, pp. 331–340, 1981.

[117] F. Pechar, D. Rykl, Thermal decomposition of natural mordenite, *Indian Acad. Sci.*, vol. 41, no. February 1985, pp. 339–344, 1987.

[118] K. Yanagisawa, N. Bao, M. Kariya, A. Onda, K. Kajiyoshi, Z. Matamoras-Veloza, J. C. Rendón-Angeles, Development of a recycling technique of used glass by conversion to porous materials, *WIT Trans. Ecol. Environ.*, vol. 92, pp. 95–100, 2006.

[119] R. V. Siriwardane, J. A. Poston, C. Robinson, T. Simonyi, Effect of additives on decomposition of sodium carbonate: Precombustion CO2 capture sorbent regeneration, *Energy and Fuels*, vol. 25, no. 3, pp. 1284–1293, 2011.

[120] Owens Corning Foamglas@. [Online]. Available: https://www.foamglas.com/en-us/products/. [Accessed: 26-Feb-2020].

[121] Glapor Schaumglasprodukte. [Online]. Available: https://www.glapor.de/en/produkte/cellular-glass-boards/. [Accessed: 26-Feb-2020].

[122] C. C. Pavel, D. T. Blagoeva, Competitive landscape of the EU ' s insulation materials industry for energy-efficient buildings, 2018.

[123] U. Hribar, M. Spreitzer, J. König, Applicability of water glass for the transfer of the glass-foaming process from controlled to air atmosphere, *J. Clean. Prod.*, vol. 282, 2021.

[124] C. Rodriguez, J. König, F. Freire, Prospective life-cycle assessment of a novel building system with improved foam glass incorporating high recycled content, *Sustain. Prod. Consum.*

[125] J. König, R. R. Petersen, Y. Yue, D. Suvorov, Gas-releasing reactions in foam-glass formation using carbon and MnxOyas the foaming agents, *Ceram. Int.*, vol. 43, no. 5, pp. 4638–4646, 2017.

[126] M. B. Østergaard, B. Cai, R. R. Petersen, J. König, P. D. Lee, Y. Yue, Impact of pore structure on the thermal conductivity of glass foams, *Mater. Lett.*, vol. 250, pp. 72–74, 2019.

[127] A. A. Proussevitch, D. L. Sahagian, V. A. Kutolin, Stability of foams in silicate

melts, *J. Volcanol. Geotherm. Res.*, vol. 59, no. 1–2, pp. 161–178, 1993.

[128] J. D. Musgraves, J. Hu, L. Calvez, *Springer Handbook of Glass*. 2019.

[129] J. Gadsby, C. N. Hinshelwood, K. W. Sykes, The Kinetics of the Reactions of the Steam-Carbon System., in *Proceedings of the Royal Society A: Mathematical, Physical and Engineering Sciences*, 1946, p. 21.

[130] J. König, R. R. Petersen, Y. Yue, Fabrication of highly insulating foam glass made from CRT panel glass, *Ceram. Int.*, vol. 41, no. 8, pp. 9793–9800, 2015.

[131] GLAPOR webpage. [Online]. Available: https://www.glapor.de/en/. Accessed 20.01.2023.

[132] FOAMGLAS webpage. [Online]. Available: https://www.foamglas.com/en-us/. Accessed 20.01.2023.

[133] A. Allouhi, Y. El Fouih, T. Kousksou, A. Jamil, Y. Zeraouli, Y. Mourad, Energy consumption and efficiency in buildings: Current status and future trends, *J. Clean. Prod.*, vol. 109, pp. 118–130, 2015.

[134] K. A. Marcellus-Zamora, P. M. Gallagher, S. Spatari, Can Public Construction and Demolition Data Describe Trends in Building Material Recycling? Observations From Philadelphia, *Front. Built Environ.*, vol. 6, no. August, pp. 1–7, 2020.

Bibliography

Publications Related to the Thesis

Original Scientific Articles

1. U. Hribar, M. B. Østergaard, N. Iversen, M. Spreitzer, J. König. "The mechanism of glass foaming with water glass." Journal of Non-Crystalline Solids, vol. 600, 122025, 2023.
2. U. Hribar, M. Spreitzer, J. König. "Applicability of water glass for the transfer of the glass-foaming process from controlled to air atmosphere." Journal of Cleaner Production, vol. 282, 125428, 2021.
3. S. Smiljanić, U. Hribar, M. Spreitzer J. König. "Influence of additives on the crystallization and thermal conductivity of container glass cullet for foamed glass preparation." Ceramics International, vol. 47(23), 32867-32873, 2021.

Contribution of thesis author to the publications related this thesis:
Uroš Hribar conducted the research and investigation process, prepared the foamed glass samples, conducted the majority of data collection (excluding the thermal conductivity measurements and gas chromatography measurements), analyzed the data, and wrote the publications numbered 1 and 2.
For the publication 3 Uroš Hribar performed the thermal conductivity measurements with HotDisk and reviewed the original draft (written by Sonja Smiljanić).

Popular Article

U. Hribar, M. Spreitzer, J. König, "Razvoj sinteze trajnostnega izolacijskega materiala." Novice IJS, vol. 197, 11-14, 2021.

Published Scientific Conference Contribution Abstracts

U. Hribar, M. Spreitzer, J. König. Foaming of CRT waste glass in air atmosphere with the use of carbon black. 26th International Congress on Glass : 3-8 July 2022, Berlin DE, p. 374.
J. König, U. Hribar, S. Smiljanić. Development of foamed glass with improved thermal insulation properties and sustainability. 26th International Congress on Glass : 3-8 July 2022, Berlin DE, p. 385.
U. Hribar, M. Spreitzer, J. König. The mechanism of glass-foaming with water glass. K. Nagode (ed.), et al. Throughout knowledge towards a green new world : 13th Jožef Stefan International Postgraduate School Students' Conference and 15th Young Researchers' Day of Chemistry, material science, biochemistry and environment, (CMBE day), 27th-28th May 2021, Ljubljana, p. 71.
U. Hribar, M. Spreitzer, J. König. Pore evolution in water-containing glass. P. Jovičević-Klug (ed.) et al. Book of abstracts: first online conference: 12th Jožef Stefan

International Postgraduate School Students' Conference and 14th Young Researchers' Day of Chemistry, material science, biochemistry and environment, (CMBE day), 15th of May 2020, p. 48.

U. Hribar, M. Spreitzer, J. König. Improvement of foamed glass production with the use of hydrated sodium silicate. M. Godec (ed.), et al., Program ad book of abstracts., 27th International Conference on Materials and Technology, 16th-18th October 2019, Portorož, Slovenia. Ljubljana: Inštitut za kovinske materiale in tehnologije, p. 62.

U. Hribar, M. Spreitzer, J. König. Improvement of foamed glass production with the use of hydrated sodium silicate. M. Topole (ed.) et al. Book of abstracts: science of the future how to stay up-to-date with your research! 11th Jožef Stefan International Postgraduate School Students' Conference and 13th Young Researchers' Day of Chemistry, material science, biochemistry and environment, (CMBE day), 15th-16th May 2019, Planica, p. 67.

Other Publications

Original Scientific Articles

U. Hribar, M. Spreitzer, T. Rojac, J. König. Destabilization of the ferroelectric order in $Na_{0.5}Bi_{0.5}TiO_3$ – 6 wt.% $BaTiO_3$ ceramics through doping. Journal of the European Ceramic Society, vol 42 (8), 3446-3453, 2022.

Scientific Conference Contribution Abstracts Without Publication

U. Hribar, S. Stevanoska, M. Spreitzer, J. König, S. Džeroski. Modelling the relation between processing parameters and material properties in foamed glass production with machine learning: ML4M 2022, Young researcher's workshop on Machine learning for materials, 9th-13th May 2022, SISSA Miramare Campus Trieste, Italy.

U. Hribar, M. Spreitzer, J. König. The mechanisms of glass-foaming with water glass. Vitrogeowastes 2021, 24th-26th May 2021, Baeza, Spain.

Biography

Uroš Hribar obtained his Chemical Engineering bachelor's degree from the Faculty of Chemistry and Chemical Technology, University of Ljubljana, in 2015. He continued with the studies at the University of Ljubljana and received his Chemical Engineering master's degree in 2018. The same year, he enrolled in the third-level study program of Nanosciences and Nanotechnologies at the Jožef Stefan International Postgraduate School in Ljubljana and started working as a Young Researcher at the Advanced Materials Department (K9).